

Forside

Eksamensinformationer

NGEA06012E - Geology-Geoscience Thesis 60 ECTS,
Department of Geosciences and Natural Resource
Management - Kontrakt:121716 (Jacob Mathias Jensen)

Besvarelsen afleveres af

Jacob Mathias Jensen
kbq585@alumni.ku.dk

Administration

Eksamensteam, tel 35 33 64 57
eksamen@science.ku.dk

Bedømmere

Karsten Høgh Jensen
Eksaminator
khj@ign.ku.dk
☎ +4535322484

Torben Obel Sonnenborg
Eksaminator
tso@geus.dk

Besvarelsesinformationer

Titel: Investigation of possible karstification and transient groundwater modelling of Grenaa catchment

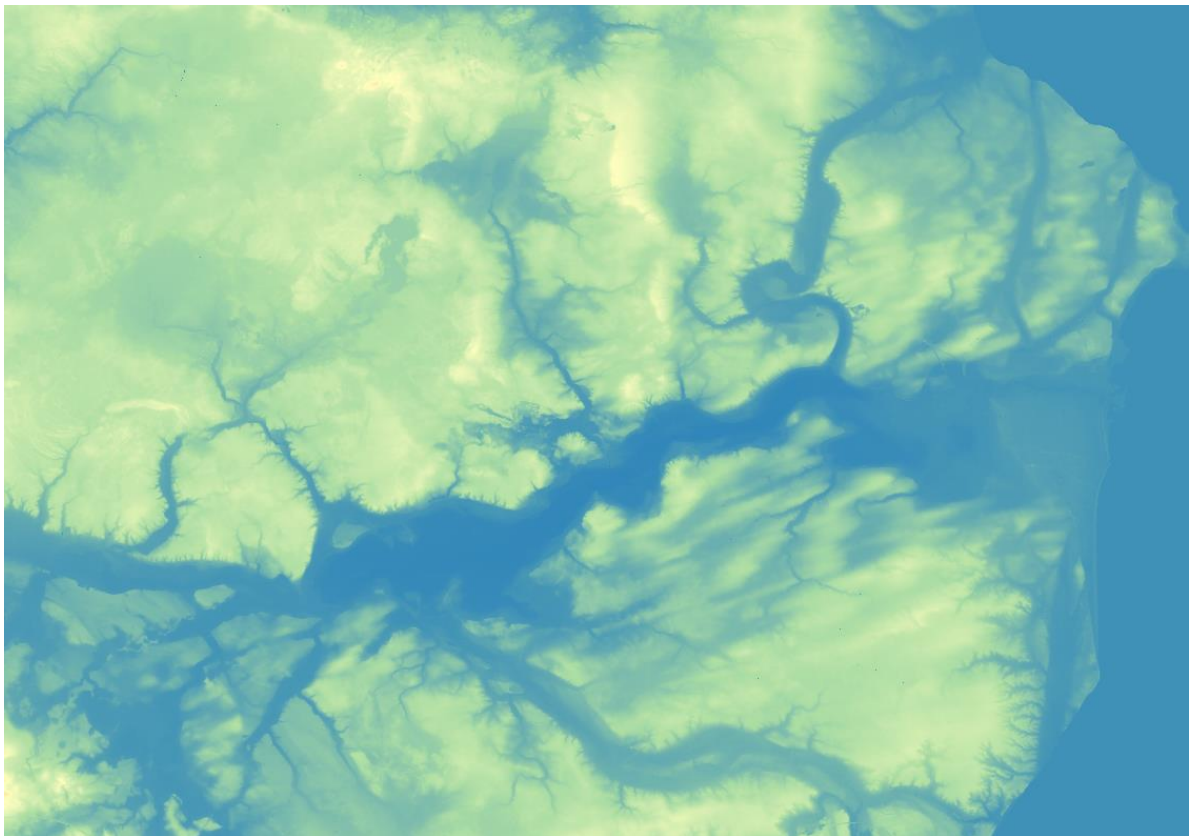
Titel, engelsk: Investigation of possible karstification and transient groundwater modelling of Grenaa catchment

Tro og love-erklæring: Ja

Indeholder besvarelsen fortroligt materiale: Nej

UNIVERSITY OF COPENHAGEN

DEPARTMENT OF GEOSCIENCES AND NATURAL RESOURCE MANAGEMENT



Master thesis

Jacob Mathias Jensen (KBQ585)

Investigation of possible karstification and transient groundwater modelling of Grenaa catchment

Supervisor: Karsten Høgh Jensen & Torben O. Sonnenborg

Submitted on: 20th May 2021

Name of department: Department of Geosciences and Natural Resource Management

Author(s): Jacob Mathias Jensen (KBQ585)

Title and subtitle: Investigation of possible karstification and groundwater modelling of Grenaa catchment

Topic description: Part of the Grenaa catchment consists of the heavily drained Kolindsund lake. Kolindsund was a lake that was connected to the sea up to the late 19th century. This drainage has altered the natural groundwater flow in the catchment. Together with increasing precipitation and rising sea level due to climate change, the natural hydrological system is changing. This could impact decision making on the future usage of the area because of rising groundwater levels. To understand what will happen with the surface near groundwater in the catchment further hydrological modelling using MIKE-SHE must be carried out. This is to better simulate changes to the climate or area in the future.

Objectives:

- Investigating possible karstification in the area
- Develop different models to better simulate the groundwater in the area
- Investigate the waterflow of Enslev pumpstation spring

Supervisor: Karsten Høgh Jensen
Torben O. Sonneborg

Submitted on: 20th May 2021.

Abstract

The catchment of Grenaa river is located at Djursland in Denmark. This catchment has through history undergone large changes. 1000 years ago, it was a fjord, 300 years ago it was a lake and today it is artificial drained farmland. These low lying areas of Kolindsund and the city of Grenaa located in Grenaa rivers estuary makes it special receptive to climate change. To make good decisions on how to mitigate this precise river and groundwater modelling must be done. Previous models have had large problems with modelling the correct head throughout the area. And there was tales of and some evidence of karst in the area. This paper reports on signs of karst, analysis of a large spring at Enslev pumpstation and three different methods of modelling the groundwater using a transient model build in MIKE SHE and MIKE Hydro. The three different models consist of a homogenic model based on the DK model, a Heterogenic chalk model based on the DK model, and a model where the chalk is divided into three layers based on the measured resistivity of the layer.

The analysis of the area found 136 dolines throughout the area. It is not known whether these dolines are from dead ice or dissolution of the chalk. The average thickness of the quaternary layers suggest it is from dead ice.

The analysis of Enslev pumpstation spring showed that around 46% of the water is return water that comes from the outer drain channel.

The three groundwater models ended with average RMSE as followed: The homogenic model with a mean RMSE of 2. The heterogenic model with a mean RMSE of 1.87. And the model with the new geology based on petrophysical properties with a mean RMSE of 1.6.

The much lower RMSE for the model with the new geology based on petrophysical properties compared to the two others shows that dividing the chalk based on petrophysical properties yields a much lower RMSE compared to the traditional modelling of the chalk.

Table of contents

ABSTRACT	3
ACKNOWLEDGEMENT	8
INTRODUCTION	9
THEORY	10
Darcy	10
Karst	11
Chemistry	13
Karstic flow	15
TEM	15
GEOLOGICAL SETTINGS	16
Pre quaternary	16
Quaternary	16
Post and late glacial deposits	16
Rivers	17
Draining	18
SIGNS OF KARST IN THE AREA	18
Springs	18
Sinkholes	19
Size	23
Depth to chalk	23
Possible kettles	24
SYSTEMATIC WALKTHROUGH FOR SPECIFIC YIELD AND DRAWDOWN	24
ENSLEV PUMPSTATION SPRING	26
Positions of measurements	29
Flow	30

NEW GEOLOGICAL MODEL	34
SKYTEM investigation	35
Data.....	38
Interpretation.....	39
The final geological model	43
FLOW LOGS	44
Flowlogs to tem	44
61.219	45
61.221	47
61.149	49
Flow logs to model	50
71.394 and 71.443	50
81.310 and 71.393	52
Flow logs areas	53
MODEL CUTOUT	53
Boundary conditions.....	54
Model setup	55
Land use	55
Climate	55
Temperature	55
Precipitation.....	56
Reference evapotranspiration	56
Unsaturated zone	56
River	56
Pumps	56
Geological model.....	56
Sensitivity analysis.....	57
Covariance matrix	58
DISTRIBUTED HYDRAULIC CONDUCTIVITY FOR THE CHALK LAYERS MODEL.	59

DISTRIBUTED HYDRAULIC CONDUCTIVITY FOR THE CHALK LAYERS MODEL RESULTS.....	59
Mean head.....	60
Well timelines.....	61
Enslev pumpstation.....	62
Skærvad stream.....	63
Mapped mean error.....	64
Statistic.....	67
UNIFORM DK MODEL.....	68
UNIFORM DK MODEL RESULTS.....	69
Mean head.....	69
Well timelines.....	70
Enslev pumpstation.....	71
Skærvad stream.....	72
Map statistic.....	72
Statistic.....	75
NEW GEOLOGICAL MODEL.....	76
Sensitivity analysis.....	77
Correlation matrix.....	77
NEW GEOLOGICAL MODEL RESULTS.....	78
Mean hydraulic head.....	79
Well timelines.....	80
Enslev Pumpstation.....	81
Skærvad stream.....	82
Map statistic.....	82
Statistic.....	86
DISCUSSION.....	87

Dolines	87
Enslev pumpstation spring	87
Flow logs	88
Geological model based on resistivity patterns in the chalk.	88
Weakness of the new geological model.....	89
Kolindsund	89
Fornæs klint and coast.....	90
Streams	91
Problems with wells	91
TEM France	91
Enslev Pumpstation.....	91
Skærvad stream	92
Comparing of results	92
Quaternary layers	93
Chalk layers	94
All statistics	95
CONCLUSION.....	96
REFERENCES	99
APPENDICES	100
Appendix A	101
Appendix B	102
Appendix C	104
Appendix D.....	105
Appendix E	106
Appendix F	107
Appendix G.....	108

Acknowledgement

I would like to express my sincere gratitude to my advisors Professor Karsten Høgh Jensen & Adjunct Professor Torben O. Sonnenborg for support and guidance throughout the process of this thesis.

I would also like to thank Bertel Nilsson and Eva Sebök for helping with the process of this thesis.

Thanks to Khan Academy for helping me throughout my studies and helping refresh my knowledge while writing this thesis.

A thanks to Geoscene3d for making a student license available. And a special thanks to DHI for let me use a student license to MIKE.

Introduction

The focus area is situated at the eastern part of Djursland in Denmark. The area has a special interest due to the large catchment of Grenaa river, its estuary, and the drained lake in Kolindsund. Kolindsund is of special interest for the area. At the stone age the area north of Kolindsund were an island. Somewhere between the stone age and the Viking age were Kolindsund no longer connected to Randers fjord and were then a fjord. Up to this time the water in Kolindsund were saltwater. After the Viking age the mouth of Kolindsund were sedimented over and Kolindsund became a lake connected to Kattegat by Grenaa river.

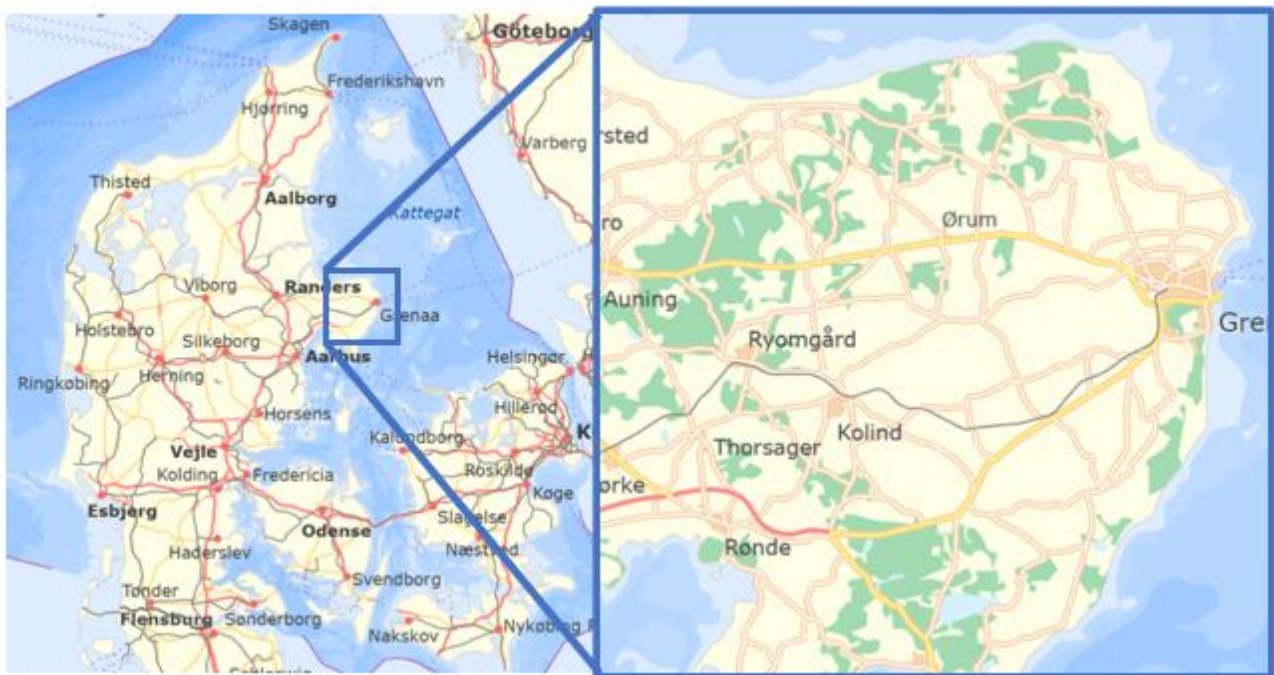


Figure 1: The figure shows where the focus area is in Denmark.

In 1872 was worked started to make the channels used to drain the lake. The lake was later successfully drained to be used for agricultural use due to the extremely fertile agricultural land created by the lake and marine sediments.

Today the interest of the area is mainly for agricultural use but the uses of drainage in Kolindsund could draw in saltwater that could make conventional farming impossible. In recent years, the interest of use has started to change. The focus in the public around climate change has started the work on identifying ways to mitigate different problems that can occur in the future.

But also the different environmental and recreational organizations has raised awareness about how the area could be used different. This could be stopping drainage of Kolindsund so that it once again would become a shallow lake. It has then been proposed that this lake could be a sanctuary for birdlife and outdoor recreation like canoeing and bird watching.

When Kolindsund first where drained there were encountered a problem with the amount of water that needed to be drained. This problem occurred again when Enslev pumpstation were established. To build the pumpstation the surroundings needed to be drained. The amount of water needed to be drained impacted the quality of the drinking water in the nearby village of Enslev. At this time, a large spring at the bottom of drain channel were already known. This spring will be investigated to find out if the water is purely groundwater that could be a sign of karstic flow.

This paper will investigate different methods to model groundwater flow in the focus area. The paper will also investigate the possibility of karst development in the catchment and different key points of interest. This will be done to raise the precision of the modelling in the area so that this knowledge could be used to mitigate climate change or repurpose the area of Kolindsund.

Theory

Darcy

To mathematical describe groundwater flow the Darcy law has been derived from experiments in the laboratory. It is the simplest law to describe groundwater flow. It states that the flow has a linear relationship with the hydraulic gradient. Darcy's law is:

$$Q = -K A \frac{\partial h}{L}$$

The different components in Darcy's are: Q is the discharge, K is the hydraulic conductivity, A is an area that describe the geological architecture and $\frac{\partial h}{L}$ is the hydraulic gradient (Fitts, 2013).

The simplicity of Darcy's law only describe flow in one direction. To describe groundwater flow in three dimensions three different equations of Darcy's law must be combined. The three are in the X, Y and Z directions. They can be described by the following equations:

$$q_x = -K_x \frac{\partial h}{\partial x}$$

$$q_y = -K_y \frac{\partial h}{\partial y}$$

$$q_z = -K_z \frac{\partial h}{\partial z}$$

Where:

$$q = \frac{Q}{A}$$

The combination of the three individual equations is:

$$|q| = \sqrt{q_x^2 + q_y^2 + q_z^2}$$

To describe a groundwater system with every component in it. Several other parameters must be added to the governing equation. These extra parameters are the change in specific storage, the groundwater extraction, and the recharge. In a steady state model, the change in storage will be set to zero because the model is in an equilibrium.

$$S_s \frac{\partial h}{\partial t} = \frac{\partial}{\partial x} \left(K_x \frac{\partial h}{\partial x} \right) + \frac{\partial}{\partial y} \left(K_y \frac{\partial h}{\partial y} \right) + \frac{\partial}{\partial z} \left(K_z \frac{\partial h}{\partial z} \right) - Q_P + R$$

Normally it is assumed that the hydraulic conductivity in the X and Y direction are the same. In a model there is transient the storage can change. This can change because the two last parts of the equation. Pumping in the area can have different rates over the years and new wells can be established. The biggest factor to make changes in a transient model is recharge. This recharge changes over the season. But it can also change over the years due to changes in weather patterns or changes in the use of the land and changes in what crops are grown in the area. The recharge can also change due to irrigation.

Karst

Karsts are a landform that are dominated by dissolution of different carbonates. This dissolution can in mature karst landscapes have formed large caves, vertical rock features as seen in Li river, Guilin, China, and most noticeable suddenly open a large sinkhole in the ground.

Karst has for a long time only been described as these mature landscapes and large cave systems with underground rivers. But the phenomena of karst can also be described as a system that has been dissolved so that a great secondary porosity has formed in the geological unit. This dissolution of the chalk deposit will keep widening the dissolution spaces as long as the chemistry allows to.

The karst system can have different levels of matureness. This can range from small fractures that had widen due to dissolution, to the dissolution of chalk has altered the landscape as seen in Halong bay.

From a hydrogeological point of view these karst features are important to understand. Karstic flow can have a velocity as high as 5,5 km per day as found in England (MacDonald, et al., 1998). This shows that a karst system can transport possible contaminants a long way from the source very quickly.

Another important reason to understand and know if a carbonate aquifer has developed karst features is that half of the world's groundwater used for drinking water comes from aquifers

with known karst features.

Often the karst development starts at a fracture in the top of the chalk unit where acidic water enters the unit. This fracture keeps widening and can develop a network of branches. These vertical branches also increase the velocity of infiltration and becomes focused recharge areas into the chalk (Taylor & Greene, u.d.). Further on in the development of the karst these networks of branches can become so big that they collapse into themselves and become a cavity. This does not always impact the overlain geology at first. But in an event of periods of heavy rainfall the overlying deposits become saturated with water. This makes it possible for the deposits to liquify and then collapse into the cavity in the chalk. This will then form a sinkhole. If it does not form a sinkhole, it is possible that it only forms a vertical shaft. This shaft can over time form a sinkhole.

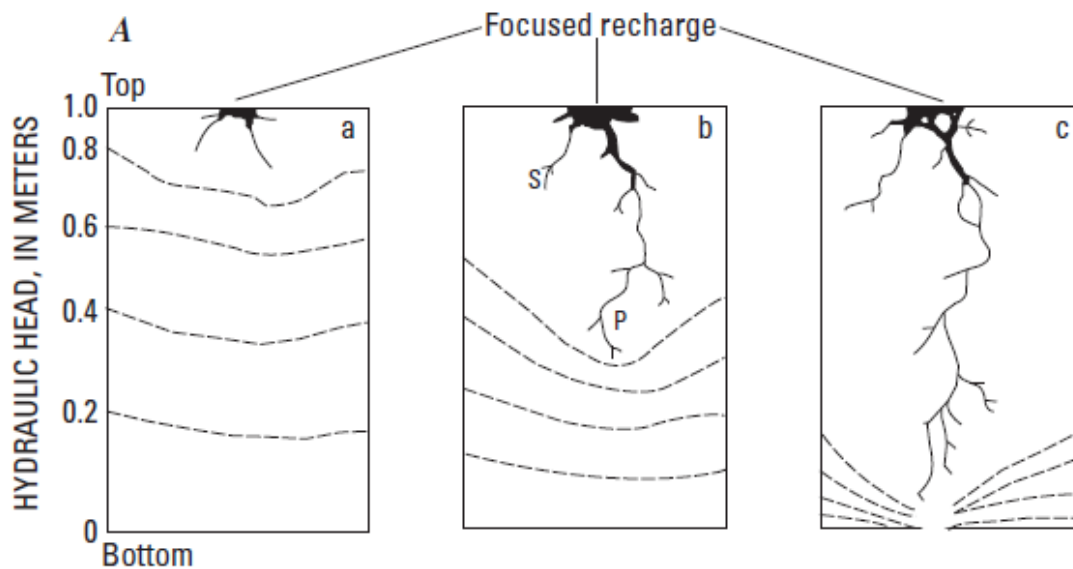


Figure 2: The figure shows the development of dissolution fractures and focused recharge. This focused recharge downwards can then lower the hydraulic head (Taylor & Greene, u.d.).

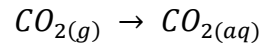
This network of dissolution branches keeps developing until it hits a planar layer or horizontal fracture that is easier to follow than keep developing a new vertical one. This horizontal branch will with time form a pipe. This pipe is called a conduit.

Sometimes a sinkhole can swallow all the overburden, so it is possible to see the carbonate unit underneath and maybe a cave. This landform is called a Karst window. This is common to find in very mature karst systems.

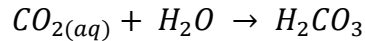
If the sinkhole is not big enough to form a karst window and there is only formed a depression at the surface. This depression will then be called a doline. This is a common landform in karst areas. Sometimes a doline is only a partly collapsed sinkhole and can later open to be a karst window (Ford & Williams, 2007).

Chemistry

The main driver for the dissolution of chalk and limestones are acidic water encountering the unit. This acidic water is mainly a product from equilibrium between CO_2 and water that creates carbonic acid. The reaction that makes the water acidic are the following:

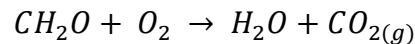


And subsequently the formation of carbonic acid:



But the amount of CO_2 available in the atmosphere is low. It is around the level of 0.003 vol%. but measurements of the amount of CO_2 in groundwater shows that it can be one or two orders of magnitude higher. The increased amount of CO_2 can be explained by root respiration and decay of organic material (Appelo & Postma, 2005)

The reaction that forms CO_2 from the organic material looks like this:



With the main sources for CO_2 established the dissolution reaction of chalk (calcium carbonate) can be described as following:



Another chemical reaction that can create even more acidity in groundwater is nitrification of ammonia. Ammonia is used as an agricultural fertilizer and can be added to fields as a chemical pure product or as manure. The nitrification reaction for ammonia is as followed:

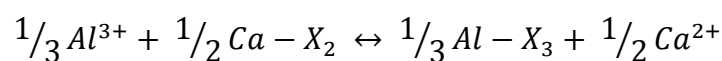


This extra acidity will end in even more dissolution of the carbonate. But many crops do not grow well in highly acidic soil. To counter this problem farmers, often add a carbonate to the soil. This then neutralize the acidity added from the nitrification of ammonia.

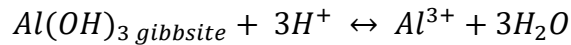
It is possible for the acidic water to be buffered and neutralize some of the acidity before it encounters and dissolve the carbonate unit. This can happen if the acidic water encounters certain minerals.

With an acid load less than 0,5 keq/ha/yr a few percent of biotite, pyroxene or hornblende is sufficient to prevent acidification (Appelo & Postma, 2005)

Field studies has also shown that different Al^{3+} containing minerals can take up the acidity. This is done by dissolution of the Al^{3+} containing mineral. This happens by the following reaction:



These minerals could be clay minerals, primary silicates, $Al(OH)_3$ or a combination of these. The buffering of the acidic groundwater is related to dissolution of Al^{3+} containing minerals. Using gibbsite as an example the buffering reactions is:



This buffering process is important in areas with thick silicate rich deposits on top of the carbonate unit. The silicate deposits could be quaternary deposits such as glacial moraines. These deposits often contain a wide range of different minerals in the different units. This could be sandy aquifers that contains different minerals like clay minerals, primary silicates or $Al(OH)_3$. In Denmark it is common to see black sand as a byproduct in gravel pits. This black sand contains large amounts biotite, pyroxene, or hornblende that can buffer the acidic groundwater.

Dissolution or corrosion of carbonates can also occur at the interface of freshwater and saltwater. This happens because of difference of concentrations in partial pressure of CO_2 between the fresh water and salt water. But these chemical processes in this mixing zone are more complicated than this. One of the elements that complicate this corrosion is redox processes that can affect the dissolved carbonate composition and change both the mixing endmember and the saturation state of the mixed waters (Appelo & Postma, 2005)

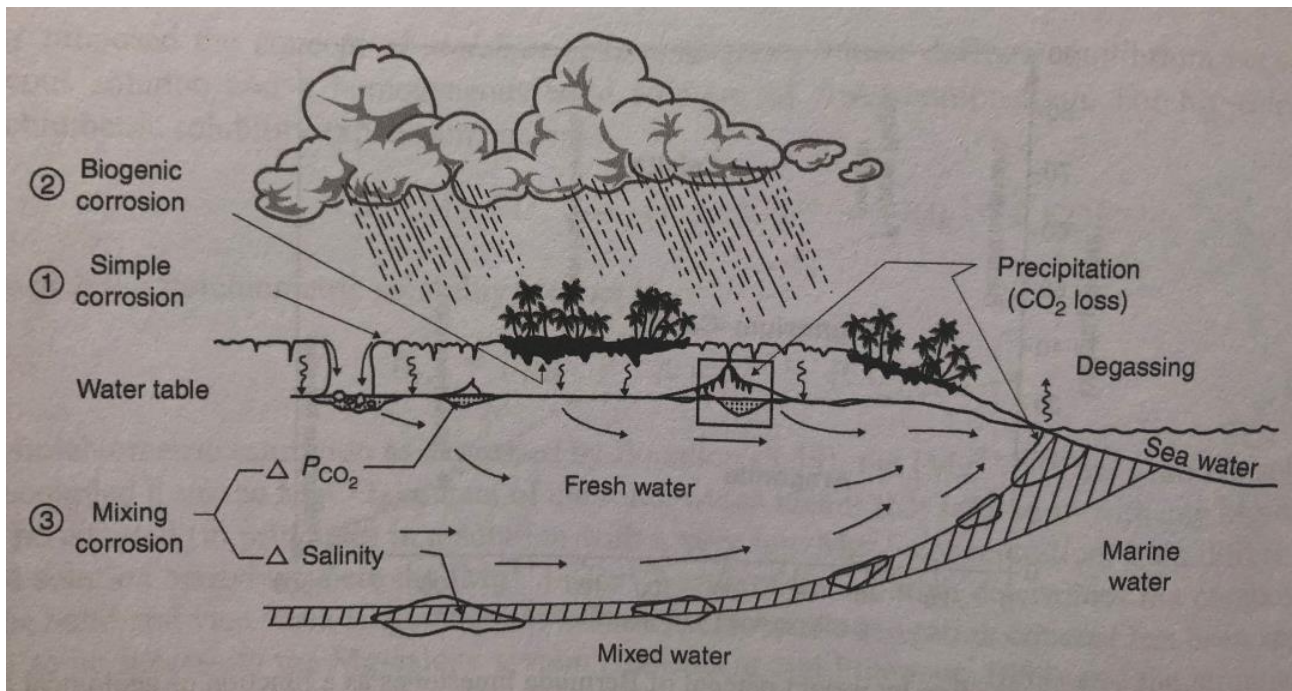


Figure 3: A conceptual model of where dissolution or corrosion of carbonates can happen. There are marked three different types of corrosion: simple corrosion, biogenic corrosion and mixing corrosion (Appelo & Postma, 2005).

Karstic flow

Due to the nature of karst, it cannot always be possible to describe or assume linear flow in the pore spaces. The dissolution channels can often be like pipes and therefore the flow can often be turbulent. But this flow changes with the amount of water that must flow through the unit (Worthington & Soley, 2017).

The Recharge to the karst system can easily spike under a heavy rainfall. And because the system can be connected directly to a

stream on the ground surface or through a sinkhole that concentrate water that otherwise would have become puddles on the surface. The Discharge the karst system must accomplish spikes very fast. This can easily increase the velocity of the groundwater in the karst. This can then push the flow from a laminar flow to a turbulent.

This turbulent flow can also happen if the karst system is penetrated by a pumping well that are screened where the conduits are located.

This turbulent flow can also transport sediments within the conduits. This can lead to further corrosion in the conduits and speed up the widening of the passages. This can also lead to wells that pump up different sediments that can lead to problems in the pipes or waterworks.

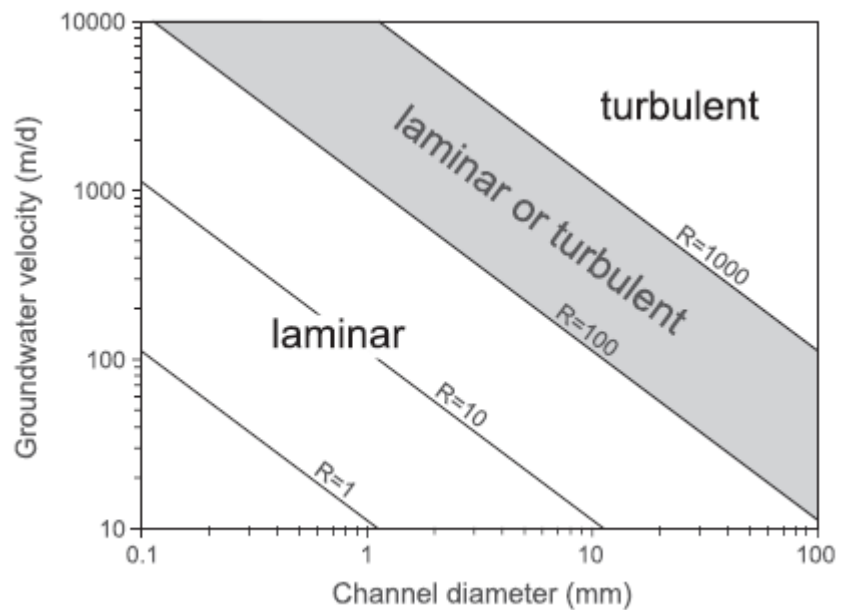


Figure 4: whether the flow is laminar or turbulent is controlled by the groundwater velocity and the diameter of the channel. conduits can have a large diameter that makes even small flows turbulent (Worthington & Soley, 2017).

TEM

Every material has a physical capability to conduct an electrical current. This can be measured using TEM (transient electromagnetic method). The method measures the resistivity (or conductivity) in a material by inducing an electrical current in it (Mussett & Khan, 2000).

For tTEM this method is set up at sleds that is towed after a vehicle. On the first sled there are a transmitter coil. On the second sled there are a receiver coil. The receiver is an induction coil. The system then transmits both a low and a high moment to collect shallow and deep data

(Auken, et al., 2018). This data is then interpreted to have a resistivity in different depths (Siemon, et al., 2009).

The Skytem system is an airborne version of the tTEM system. Skytem is often used to investigate bigger areas and deeper than tTEM. This means that Skytem often covers larger areas. But the resolution is lower compared to the one seen in tTEM (Siemon, et al., 2009)

Geological settings

Pre quaternary

The pre quaternary deposits in the area are dominated by different chalk deposits. The deepest well in the area are the Kirial well (DGU: 71.397). This is representing the pre quaternary deposits in the focus area. The oldest deposit in the area is the campanien-maastrichtien skrivekridt. Above this, there are different layers of danien chalk. The thickest deposits of these chinks are the danien bryozokalk-koralkalk, danien kalksandskalk and danien slamkalk.

The uppermost 15-25 meters are normally considered heavily fractured by the different ice advances in the area. The chalk below this fracture layer is normally considered impermeable.

Quaternary

The quaternary deposits consist of a series of quaternary sand and clay layers. The quaternary layers were deposited by a series of ice advances during the last ice age. They are deposited directly on top of the pre quaternary chalk and in some areas on top of Paleogene clay. Due to the movement of the ice the quaternary layers are in some areas heavily disturbed by ice tectonics.

Post and late glacial deposits

After the last ice age the sea broke into the low-laying areas. This then deposited different marine sediments. The largest area dominated by this is Kolindsund. These layers are dominated by marine sediments, sands and gyttja. On top of these sediments there often are lake sediments and peat.

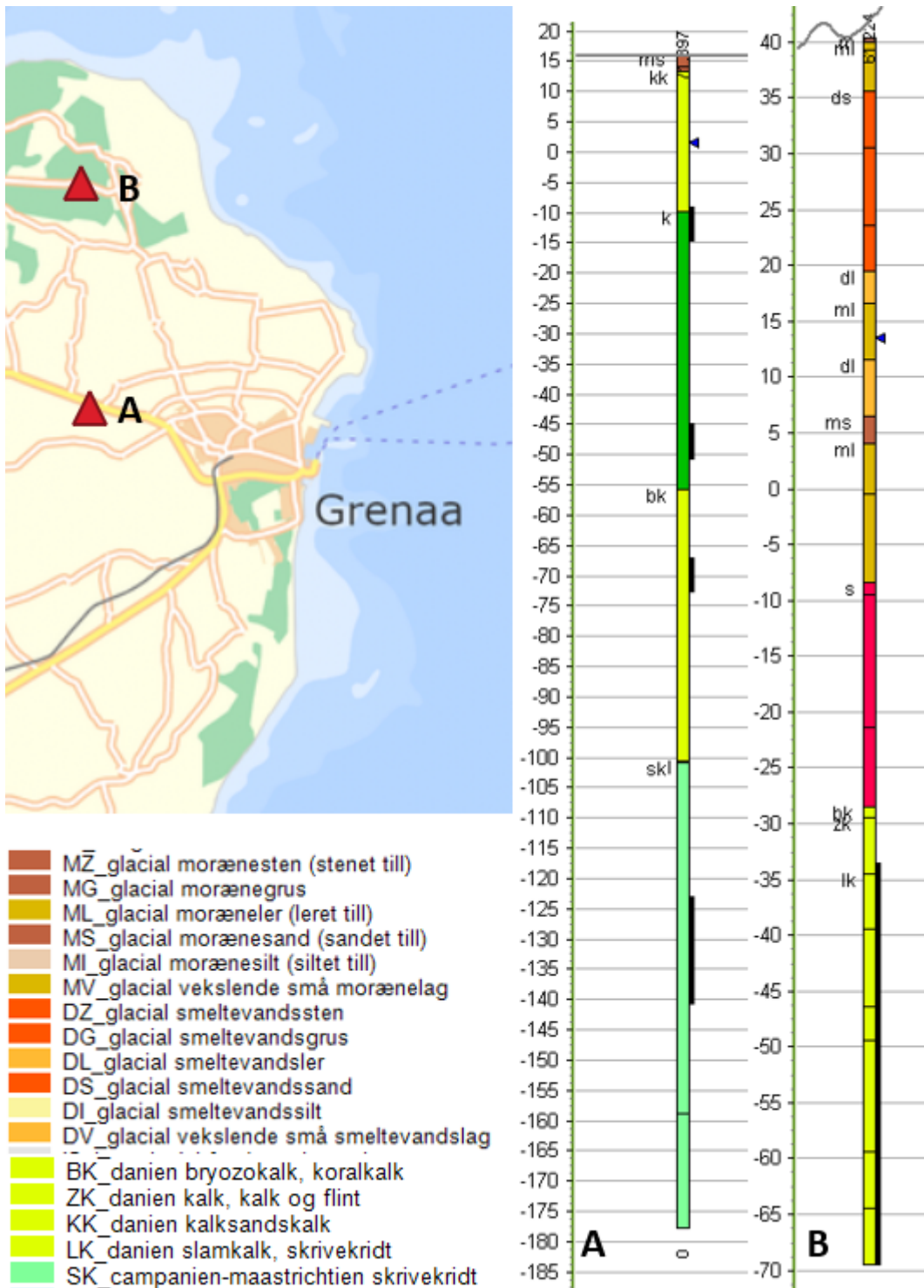


Figure 5: The geology of the area is dominated by quaternary clays and sand on top of different chalk units.

Rivers

When the work to drain Kolindsund started two channels were dug along the lake shore. This were done both on the north shore of Kolindsund and the south shore. These channels were constructed out of the material in the area and dug directly into the ground. The channels have

two purposes. The first is to drain Ryom river that has its inlet in the westernmost corner of Kolindsund. But also, to drain every smaller river that otherwise would drain into Kolindsund. Therefore, the channels were built so that every river flows into the channel directly. And then the water is let via the two channels to Grenaa river and from here to the sea.

Both to the north and to the south of Grenaa there are several smaller rivers that do not drain to Kolindsund. These smaller rivers all drain to the sea directly.

Draining

The draining of Kolindsund is done by three pumpstations. These pumpstations are situated in Alleslev, Fannerup and Enslev. The last two are the biggest ones with the biggest volume of water pumped each year. The pumps drain water directly into either Nordkanal or Sydkanal. The amount of water pumped out of Kolindsund varies with the season. In winter there is a higher volume of water drained. But also, in spring the volume of water pumped from Kolindsund is increased. This is done to fasten up the drying process of the rootzone, so the fields are ready for sowing.

To aid drain Kolindsund a series of drains were dug in former lakebed. These drains drain to several main drain channels situated in the middle of Kolindsund. These central drain channels then lead water to one of the three pumpstations.

Signs of karst in the area

Springs

In the area of Kolindsund there has been described several different springs. These springs are found through the full length of the drained area. When Kolindsund first was drained it was normal that springs would suddenly appear in the fields. This later stopped after years of active draining. But there was still area with wet fields and different springs. These springs are described very well by Korkman (Korkman, 1980).

Later in Korkman's work the origin of the water was tried to be determined. To determine this Korkman made chemical analysis and temperature analysis of each spring.

Korkman determined that the water found in several springs came partly from the channels on the outside of Kolindsund.

Large part of the channels was dug in the beach berm which is dominated by sand. The dug-up material was then used to build the dam that runs along the channels on either side of Kolindsund.

Sinkholes

Since sinkholes also are one of the most noticeable signs of karst and lidar data is freely available for all of Denmark, sinkholes were the first sign that was investigated if it is present in the focus area. This method has also been used in Thisted and Svinkløv area to identify and measure the size of possible sinkholes (Sørensen, et al., 2017). In this article there are marked several possible sinkholes in the northern part of the focus area. There has also been reported sinkholes in other parts of Jutland close to Djursland (Nilsson & Gravesen, 2018). This made it possible that these possible sinkholes were also present further south and into larger parts of the focus area.



Figure 6: Location of different sinkholes previously described.

This were also done because of the story of the drill that suddenly fell a meter and lost all the drill mud when this well as established. Unfortunately, many of the drilling logs do not have the notes from the driller anymore. In these notes there would have been a possibility for a description that could mention different problems while drilling. This could be stuff like the drill mud was lost at the top of the chalk or the drill head suddenly fell a meter.



Figure 7: Map of two wells that showed signs of karst when they were drilled.



Figure 8: shadow map showing the area around well 71.567. Note the two dolines marked with the red circle.

These possible sinkholes were noticed near to well 71.567 (see figure 8). This led to use the same shadow maps to go through rest of the focus area to see if these first two were the only one or similar possible sinkholes are present throughout.

This was done by systematical viewing the shadow map using QGIS. While viewing this shadow map each possible sinkhole were marked in the program and the named. The naming was simple numbers given in the order the possible sinkholes were discovered.

The systematic review of the area showed that these depressions were present through the whole area of the Grenaa catchment (see figure 9).

Some areas stood out with a high density of these possible sinkholes. In total three areas stood out. This was around Ålsrode, Lyngby and Voldby. The two with the highest number of possible sinkholes (see figure 9).

There were not found any possible sinkholes in the low laying areas. This could be because of the history of the area where these areas have been covered in water and is dominated by young marine sediments and different lake sediments. This sedimentation could then cover the

sinkhole if it were created before the younger sediments were deposited.
The sinkholes were often found in clusters (see figure 10 and 11).

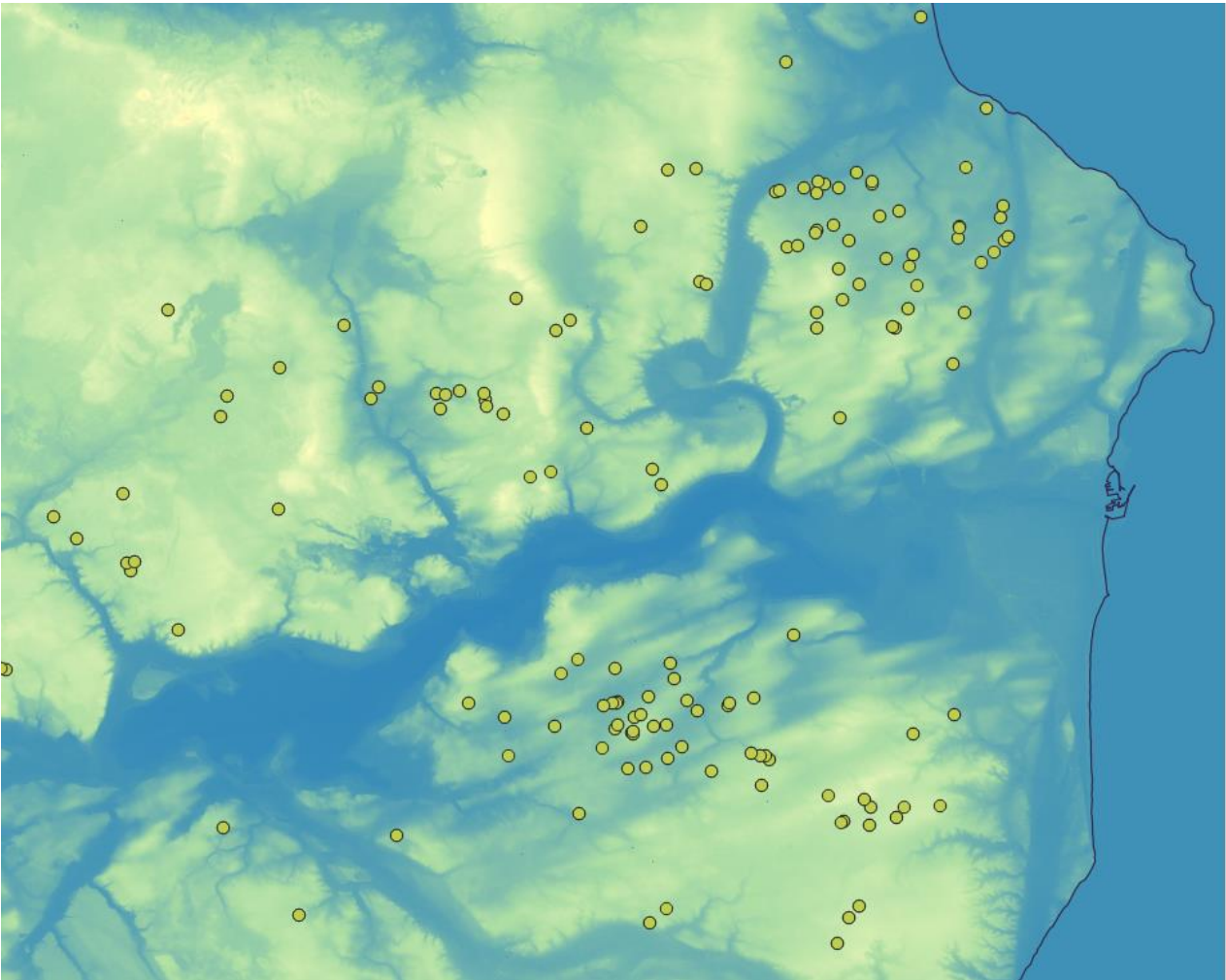


Figure 9: Map with position of the dolines observed in the area. Every dot marks a doline.

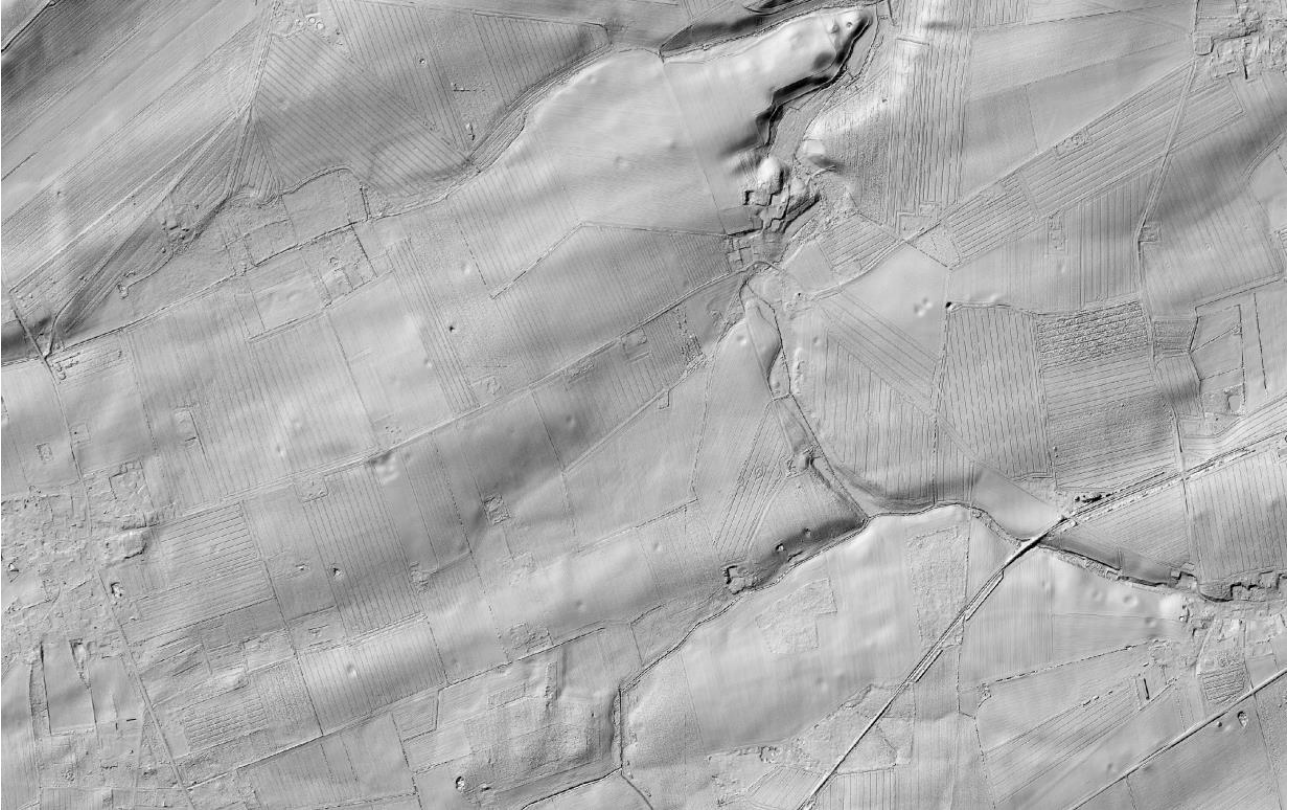


Figure 10: Shadow map of an area with a high density of dolines (see figure 11 for markings).

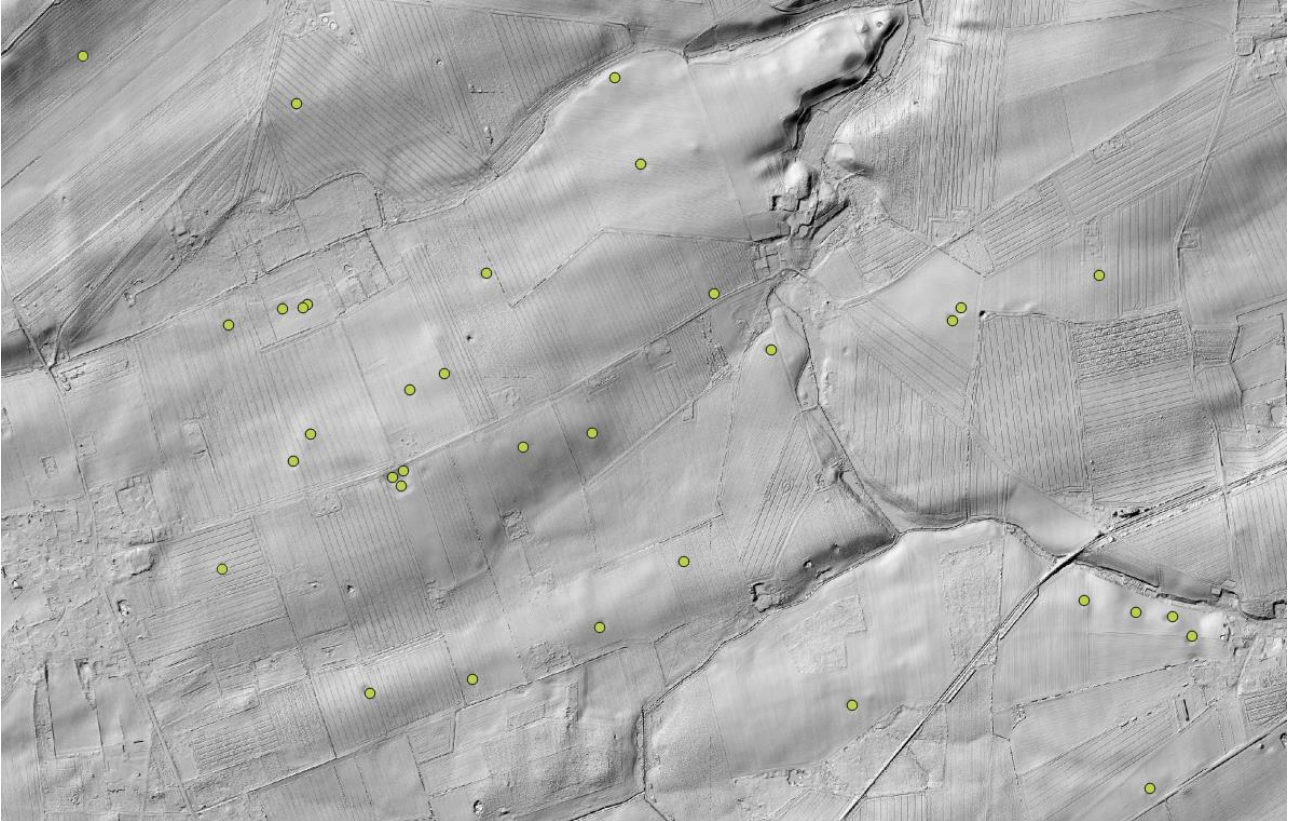


Figure 11: Shadow map of an area with a high density of dolines.

Size

To have a better understanding of the size and shape of the possible sinkholes they were all measured to be able to make statistics on them. This was done by using a GIS profile tool and a 0.4m DEM map from Kortforsyningen (it is the same data used to produce the shadow map). In this process several possible sinkholes were not measured due to their position in the landscape. This was often because of they were found on a slope, so the possible sinkhole only had one part of the depression visible. This made it impossible to define where the other side of the depression ended. If the depression were measured it would have been on a very questionable basis. Therefore, they are not part of the statistic but still marked on the map.

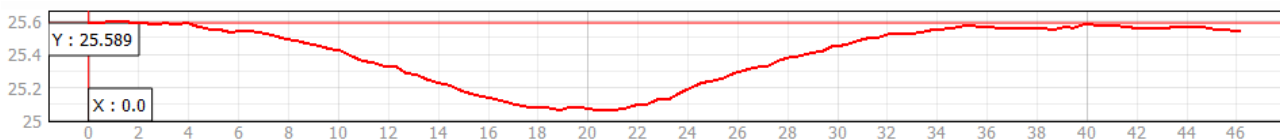


Figure 12: Cross profile of a doline. The profile is made using GIS and 0.4m DEM terrain data. The unit is meters.

The shape of the doline is similar throughout the area. It is near perfect circular depression in the landscape. There has not been found any depressions in the area that does look significant differently.

	Diameter	Depth	Ratio (Diameter/Depth)
Median	40.0	0.8	48.7
Average	42.0	0.9	57.7
MIN	22.3	0.2	17.2
MAX	91.8	3.9	166.7

Table 1: The table shows the range of sizes of the observed dolines. The unit is meters.

The diameter and depth do not vary that much. But there are some outliers in both the size of the sinkholes and the depth. But most of the sinkholes have a diameter that is around 40 meters and a depth just short of one meter.

The depth, size and ratio of the sinkholes matches what was found in Thisted and Svinkløv (Sørensen, et al., 2017). The areas in Thisted are also agricultural land and undergo the same processes of sowing and plowing. This does make the holes shallower over time.

Depth to chalk

To measure the thickness of the quaternary deposits under the possible sinkholes a map of the thickness was produced in GIS. This map was created subtracting the terrain model with the elevation of the top of the chalk in the area.

This made it possible to use the profile tool in GIS to measure the thickness. The reason to measure the thickness is that the greater the thickness of the quaternary layers are, the more they can buffer the acidic water infiltrating the area.

But also, the greater the thickness of quaternary deposits makes it more possible that the possible sinkholes are formed by dead ice and are kettles.

	Thickness of quaternary layers
Median	27.8
Average	29.5
MIN	5.9
MAX	69.1

Table 2: The table shows the range of the thickness of the quaternary layers. The unit is meters.

The thickness of the quaternary layers with a median thickness of 27.8 meters and an average thickness of 29.5 meters are high. This high thickness suggests that acidic water infiltrating the would be neutralized before reaching the carbonate layers.

Possible kettles

Due to the sediments deposited on top of the chalk there is a possibility for that the possible sinkholes could be formed by blocks of ice left in the moraine and slowly melted and then formed these depressions in the landscape. To understand if these possible sinkholes are made from dissolution of chalk or by ice left in the moraine further work must be carried out. This could include GPR, geo-electrical survey core drilling and exposing the geological layers by excavation.

If it is a kettle hole the sedimentary layers are only disturbed in the quaternary layers. And there is a possibility that the kettles contain peat and gyttja. This often form in kettle holes because they become lakes after the ice block has melted.

The high average thickness of the quaternary layers suggests that the possibility for the holes being a remanent of dead ice is strong.

Systematic walkthrough for specific yield and drawdown

To better understand the areas capacity for yielding water the wells in the area were analyzed. This were done using alle the available data for the wells. The data were collected from the Jupiter database. A map of specific yield was then created using GIS and a contour tool.

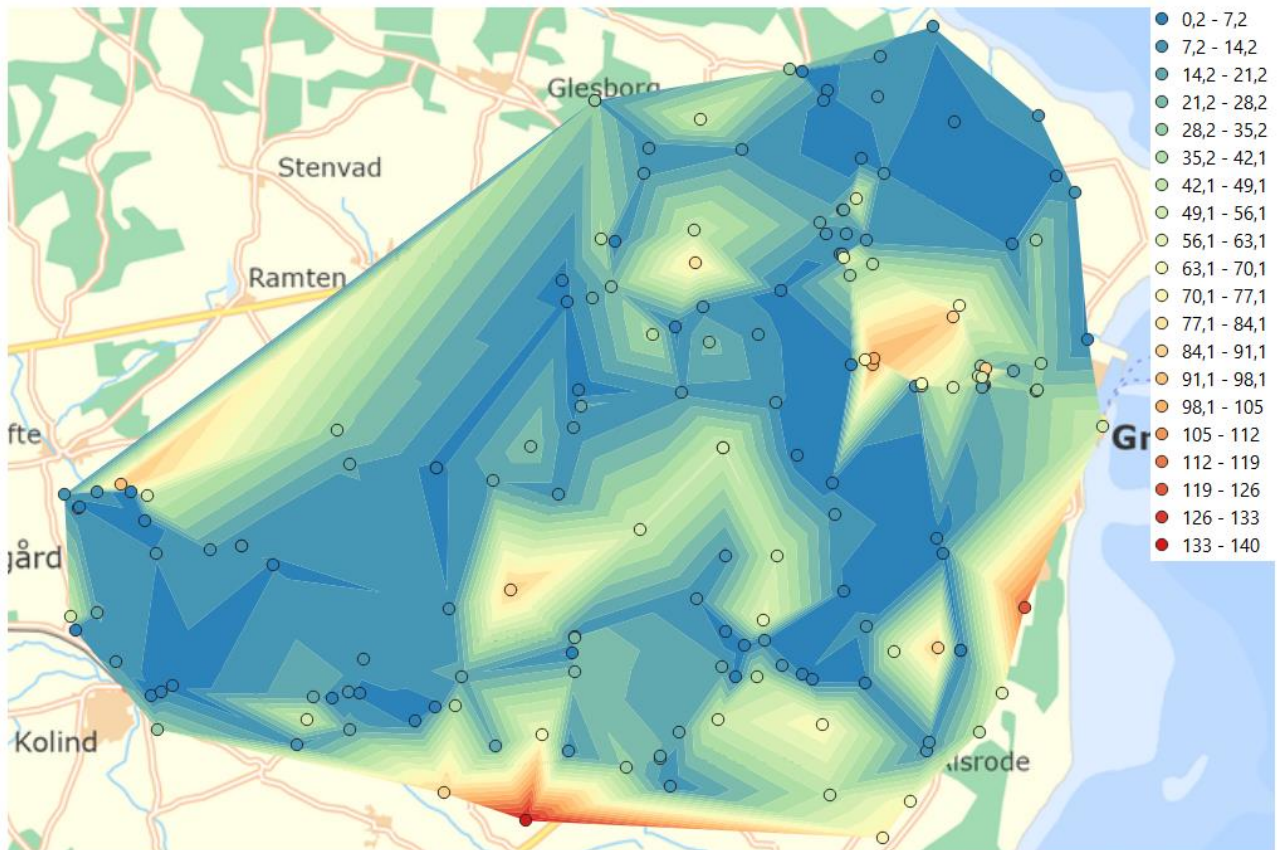


Figure 13: The figure shows the specific yield of the wells in the area.

The map shows that the wells situated north of Grenaa has a high specific yield. There are also some bands of wells that has a high specific yield. But there is no larger area or direct system between areas and the specific yield. Also, that a well with a high specific yield can be located next to a well that has a low specific yield.

To see if these wells with a high specific yield, could be a clue of karstification. The drawdown of each well was mapped. If the wells with a high specific yield also has a low draw down. It could be a sign of karstification.

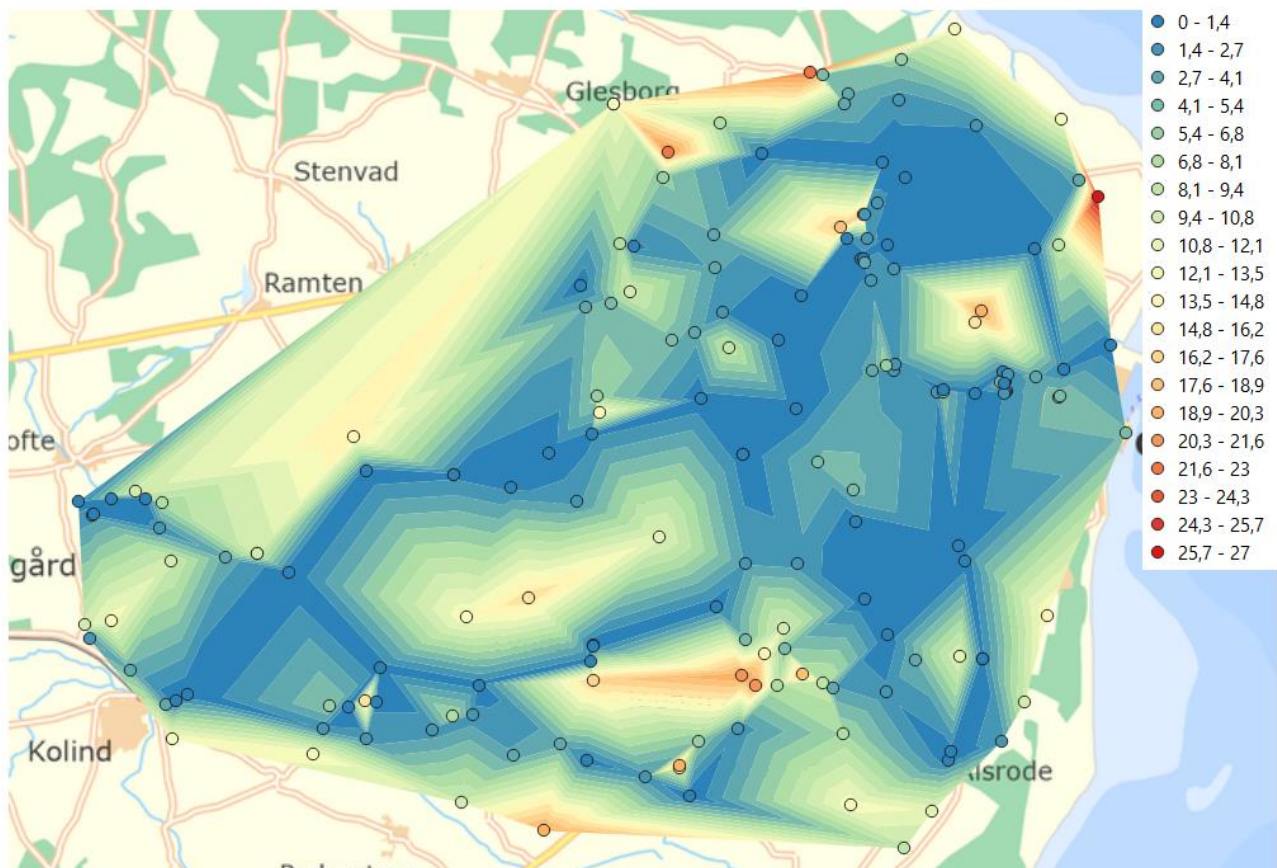


Figure 14: The maps shows the drawdown of the wells in the area.

The map shows that there is no clear system in which wells that has a low draw down. Only a couple of wells north of Grenaa has a low drawdown and a high specific yield. This map does not consider which type of geology the well is situated in. But it does show that there is no system between specific yield and drawdown.

Enslev pumpstation spring

At the Enslev pumpstation there are located the biggest known spring in the area. It is in the drain channel that leads drain water from Kolindsund to the pumpstation. The spring were already known when the new Enslev pumpstation were build. At this time, it was necessary to pump away large amount of water to sufficient lower the groundwater in the area. The groundwater lowering was so big that it interfered with the pumping of groundwater for drinking in the nearby town of Enslev. It was also reported the drinking water quality was lowered at the Enslev school (Korkman, 1980).

The position of the spring is interesting because it is in a drain channel. This position and the amount of water that discharge from the spring reverses the low in the drain quickly after the

pumps stop. The average backflow from the spring is $0,4 \frac{m^3}{s}$. This flow changes over the course of the year. This is due to the changes in the hydraulic gradient in the area (Korkman, 1980).

The position of the spring can be seen on figure 15. Where the figure says rist (metal grid) and beton (concrete) is where the dam holding out 'Nordkanal is starting. The rest of the building and pumpstation is placed as part of the dam. This puts the spring right op next to the dam and Nordkanal.

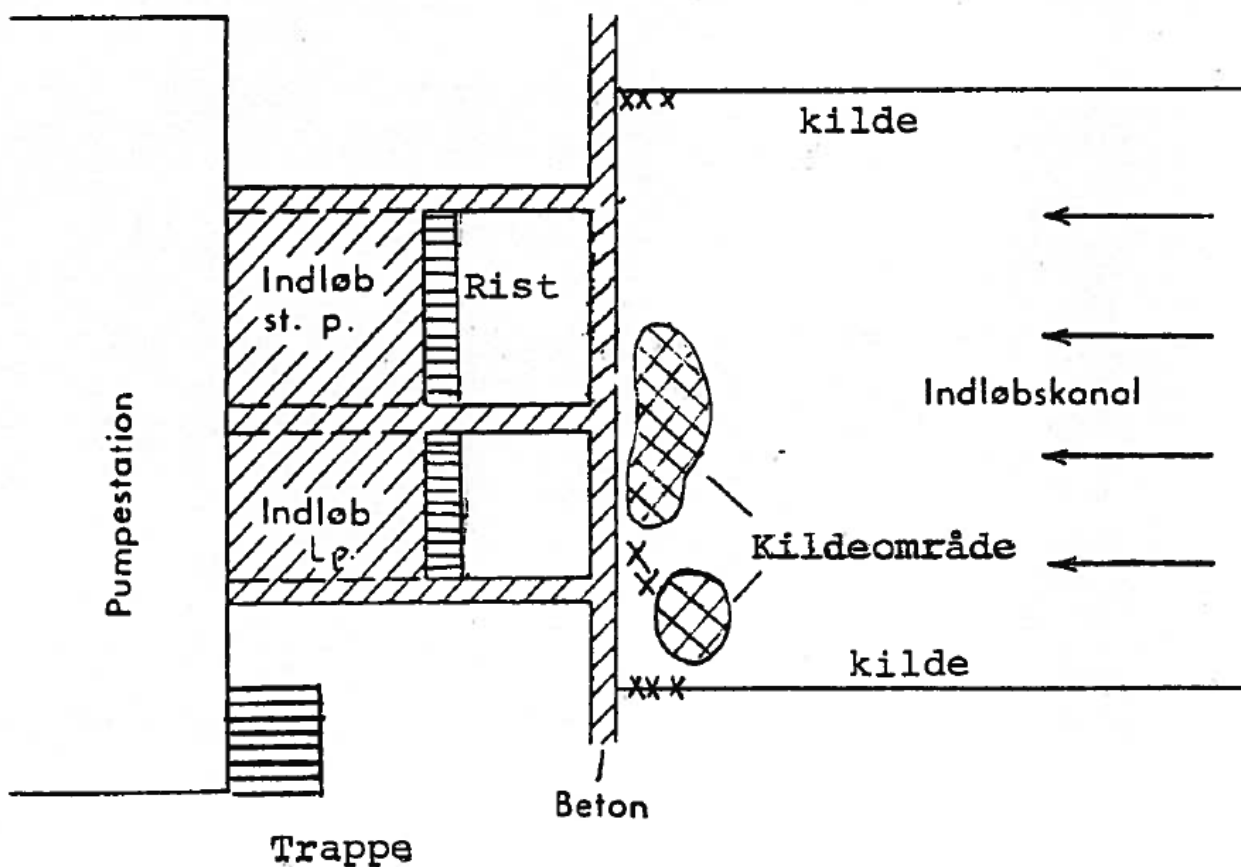


Figure 15: The figure shows the position of the spring at Enslev pumpstation. The x's marks smaller springs. The small springs in the channel sides are not active all year around (Korkman, 1980).

Korkman (1980) has also found that there is a correlation between the backflow in the drain and the water level in the outer channel. This is of course also part of the hydraulic gradient. And furthermore, Korkman reports that the outer channel in the Enslev area most certain are built directly on top of the chalk (Korkman, 1980). And considered that this chalk is fractured by ice tectonics the hydraulic conductivity can be high.

Looking at the topsoil map produced by GEUS. The area at the pumpstation is dominated by saltwater gravel. This again can have a high hydraulic conductivity that can feed the spring or

aided the loss of channel water to the drained Kolindsund (see figure 16).

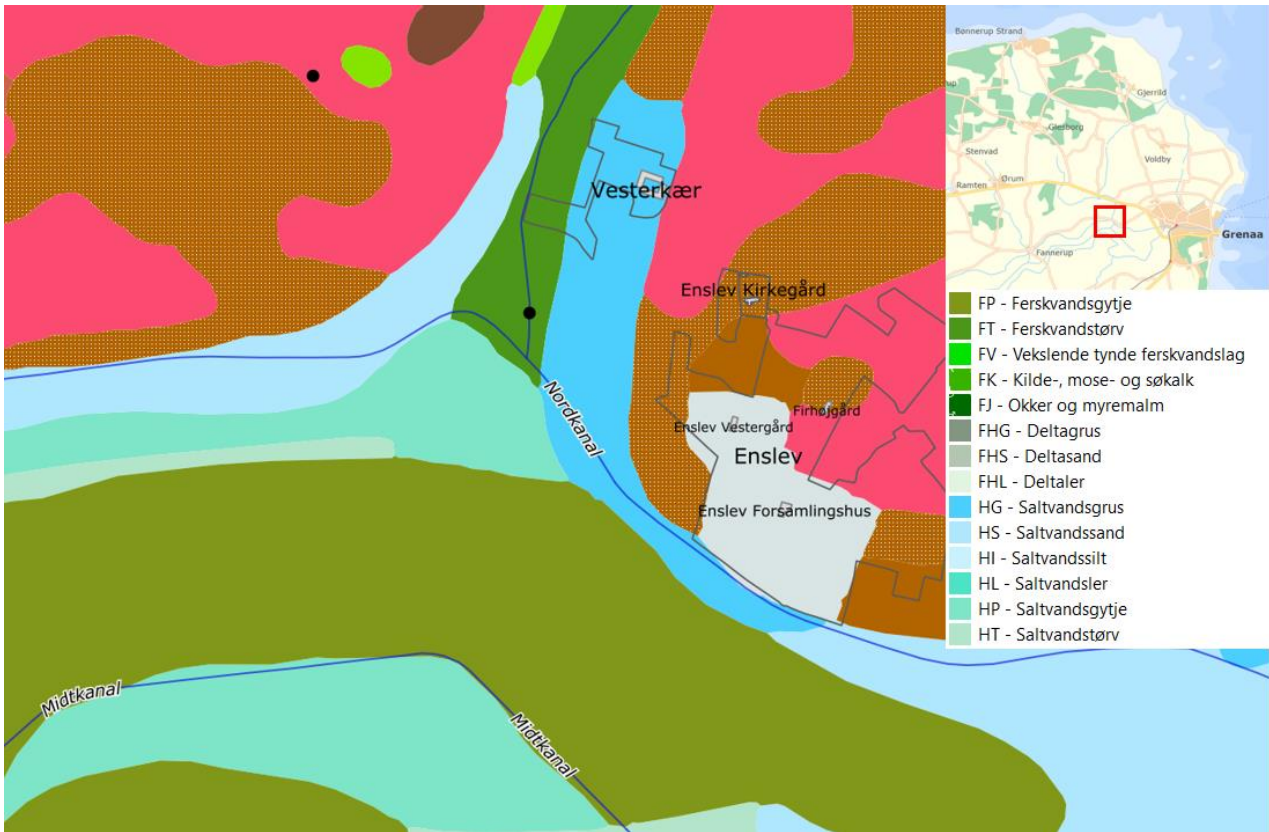


Figure 16: Map of the soil type at one meter below terrain. The map is produced by GEUS and shows the area around Enslev.

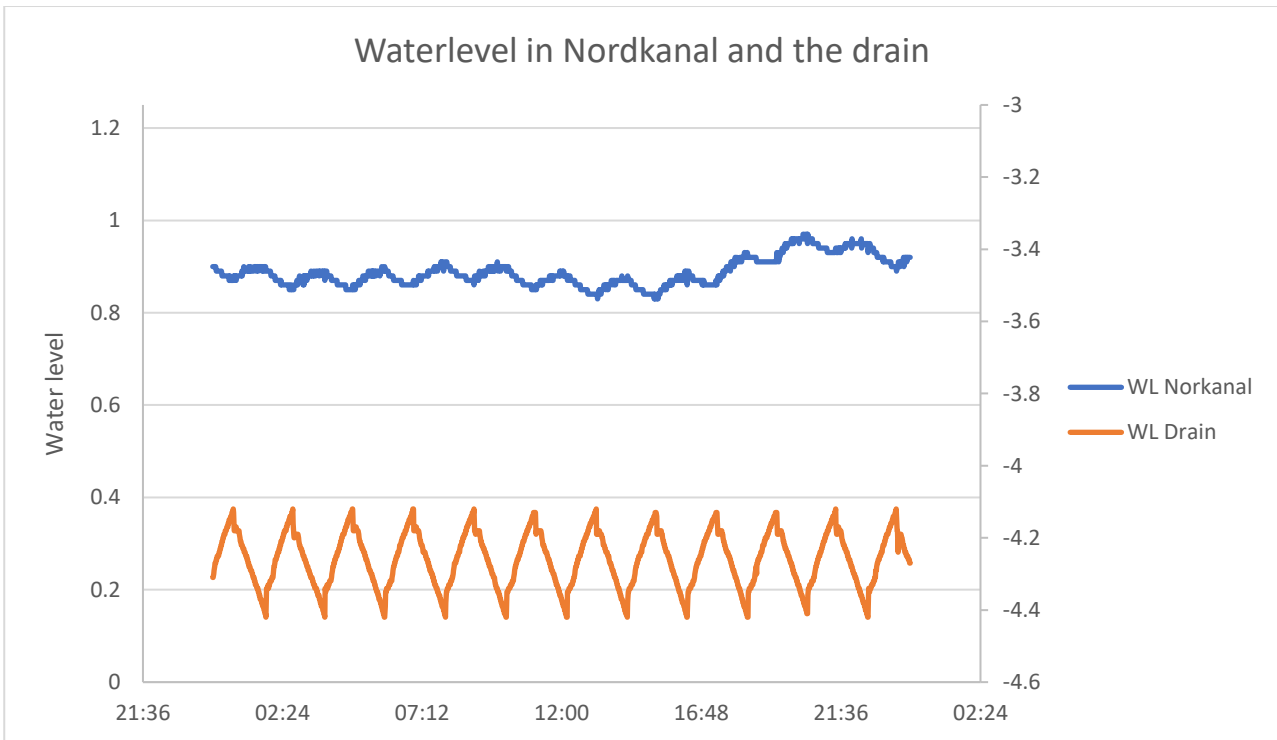


Figure 17: The figure shows the water level on the outside of the pumpstation in Nordkanal, and in the drain on the inside of the pumpstation. The day showed is 19-02-2020. The unit is meters above sea level.

Looking at the water level in the two channels on either side of the pumpstation it shows that the fluctuations in water levels are somewhat correlated. The water level in the drain channel has a regular fluctuation. This is due to the pump is controlled by the water level and is turned on when it gets too high and again turned off when the water level hits a certain level. This fluctuation in the drain channel has a cycle that is a little over two hours long.

The water level in Nordkanal has a fluctuation that is also due to the contributing rivers in the area that Nordkanal drains. On an hourly scale the water level rises slightly when the pump tourn on and then again falls slightly when the pump is turned off.

Positions of measurements

Several different measuring points have been installed around the pumping station to increase the knowledge of the area. In this analysis three different measuring points are used. The three points consist of two points situated directly in the channels. One in the drain channel and one in the outer channel 'Nordkanal'. The last point is a well situated west of the pumpstation. measuring point 24.26 consist of a doppler radar, a water level diver and a temperature measuring device. This makes it possible for this measuring point to give information about temperature, flow, and water level. It is situated as close as possible to the pumpstation as possible without measuring interference from turbulent flow caused by the pump and the spring.

The outside measuring point called 24.25 is situated in the channel called 'Nordkanal'. It measures temperature and water level.

The last measuring point is the well B25 adjacent to the pumpstation on the Kolindsund side of

'Nordkanal'. It measures hydraulic head of the groundwater and its temperature.



Figure 18: The map shows the position of measurement points around the Enslev pumpstation.

Flow

When the pump is turned off measuring point 24.26 measures negative flow. That means that water is running from the pumpstation and into the rest of Kolindsund. This backflow continues until the pump once again starts. In this period the water level in the drain channel rises. While the pump is turned off the temperature in the drain channel rises. Right after the pump is turned on the temperature falls rapidly. On the outside of the pump station in the 'Nordkanal' the temperature is still falling while the pump is turned on. But midway through the pumping the temperature starts increasing towards the temperature in the drain channel.

This difference in reaction can be explained by the position of 24.25 so it does not measure the pump water directly and therefore is influenced by the flow in 'Nordkanal'. But also, by the distance from the pumpstation to 24.26. This causes a delay in the water to react to the starting of the pump. And therefore, it will still flow backwards for a little while after the pump is turned on. And the same happens when the pump is turned off. Here the water in the drain channel will flow towards the pump for a little while due to the difference in water level.

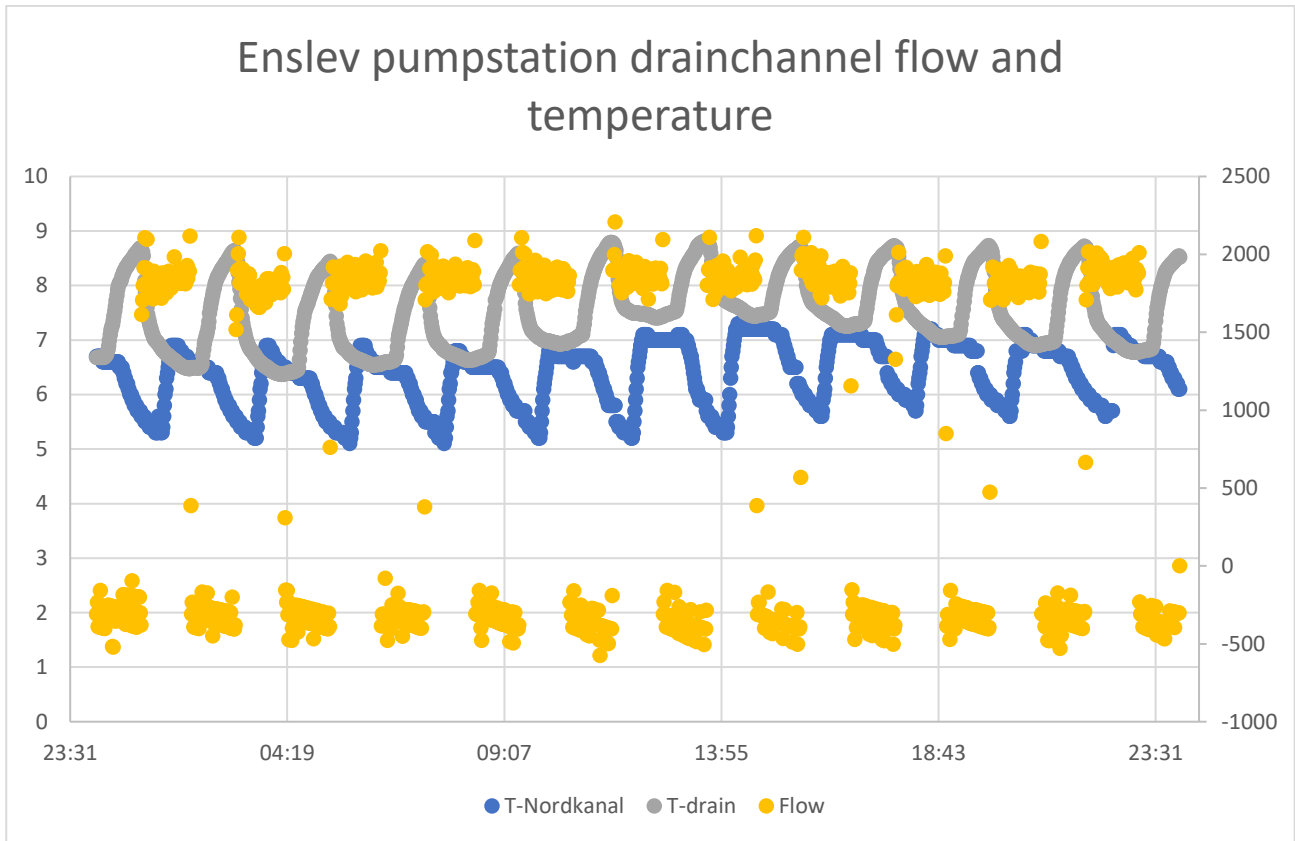


Figure 19: The graph show the temperature on the outside of the pumpstation and the inside (primary axis (degrees Celsius)) and the flow in the drain channel (secondary axis (litres per second)).

To investigate the possible fluxes into the drain channel and data available a simple conceptual model was drawn up. It shows that there are two possible fluxes into the drain channel. One flux is the groundwater and the other is the return water from the outer channel 'Nordkanal'.

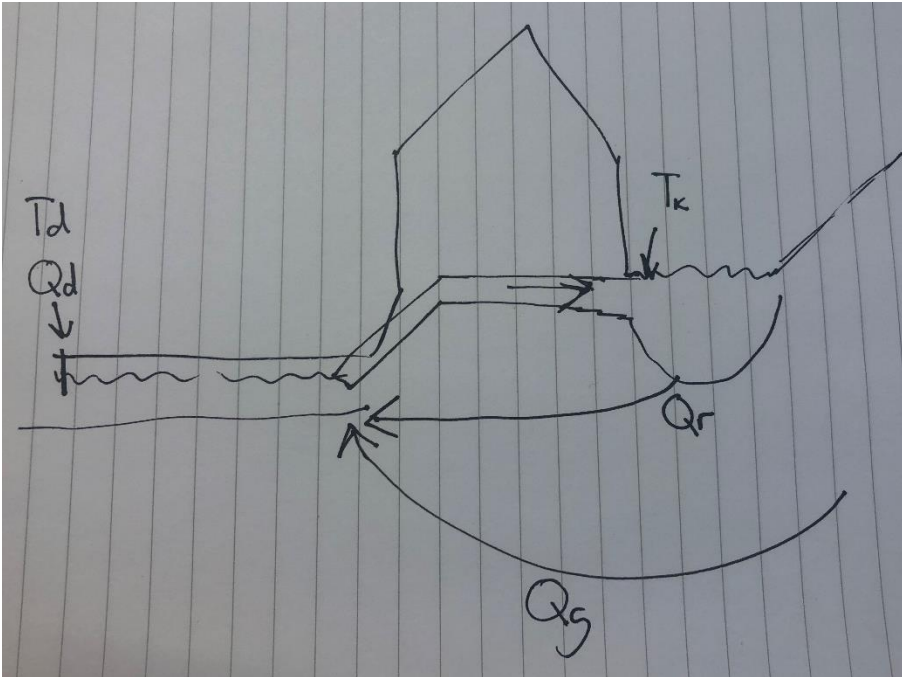


Figure 20: The figure shows a conceptual model of the waterflow feeding the spring and what is measured where.

To calculate how much of the water that comes from the spring is coming from the outer channel 'Nordkanal'. A mass and energy balance equation were used.

$$Q_{groundwater} * T_{groundwater} + Q_{channelwater} * T_{channelwater} = Q_{drainwater} * T_{drainwater}$$

This made it possible to make an equation that is equal zero and then solve the equation for the two unknown parameters $Q_{groundwater}$ and $Q_{channelwater}$. The equation was:

$$Q_{groundwater} * T_{groundwater} + Q_{channelwater} * T_{channelwater} - Q_{drainwater} * T_{drainwater} = 0$$

It was noticed that the backflow in the drain channel change a lot from minute to minute. And sometimes the flow stops for a minute and the next minute has a much higher flow. Based on this it was decided that the calculation of the different flow components on an average of the last 30 minutes of the backward flow.

To make this equation work with the data available, it was assumed that the groundwater reaching the spring has the same temperature as the well B25. It was also assumed that the return water from the channel has the same temperature as the water measured on the outside of the pumpstation at measuring point 24.25.

The day analyzed was 19-02-2020 and every backflow over the course of the day had the different flow contributors calculated.

Q Groundwater	Q channel retur	Q total	Q Drain 30min average	δdrain
175.8	150.5	326.3	331.6	-5.3
183.1	156.9	340.0	350.3	-10.3
191.4	164.1	355.5	359.4	-3.8
181.5	153.9	335.5	331.5	3.9
186.0	157.4	343.5	338.4	5.0
214.4	176.3	390.7	379.8	11.0
213.3	179.8	393.0	374.2	18.8
204.2	180.7	384.9	374.1	10.8
154.6	135.8	290.4	285.9	4.5
155.1	135.0	290.1	288.9	1.2
170.7	147.1	317.7	317.9	-0.2
185.8	160.0	345.7	345.4	0.4

Table 3: Shows the calculated flow contributors. It is divided into return water from the channel, groundwater, and the total calculated volume. It also shows the 30-minute average observed flow and the differences between the flows. The unit is litres per second.

It shows that the flow with these two water fluxes could be calculated precise. The difference between the calculated and the observed flow are at the most 18,8 liters per second too high and at its lowest it is 10,3 liter per second too low.

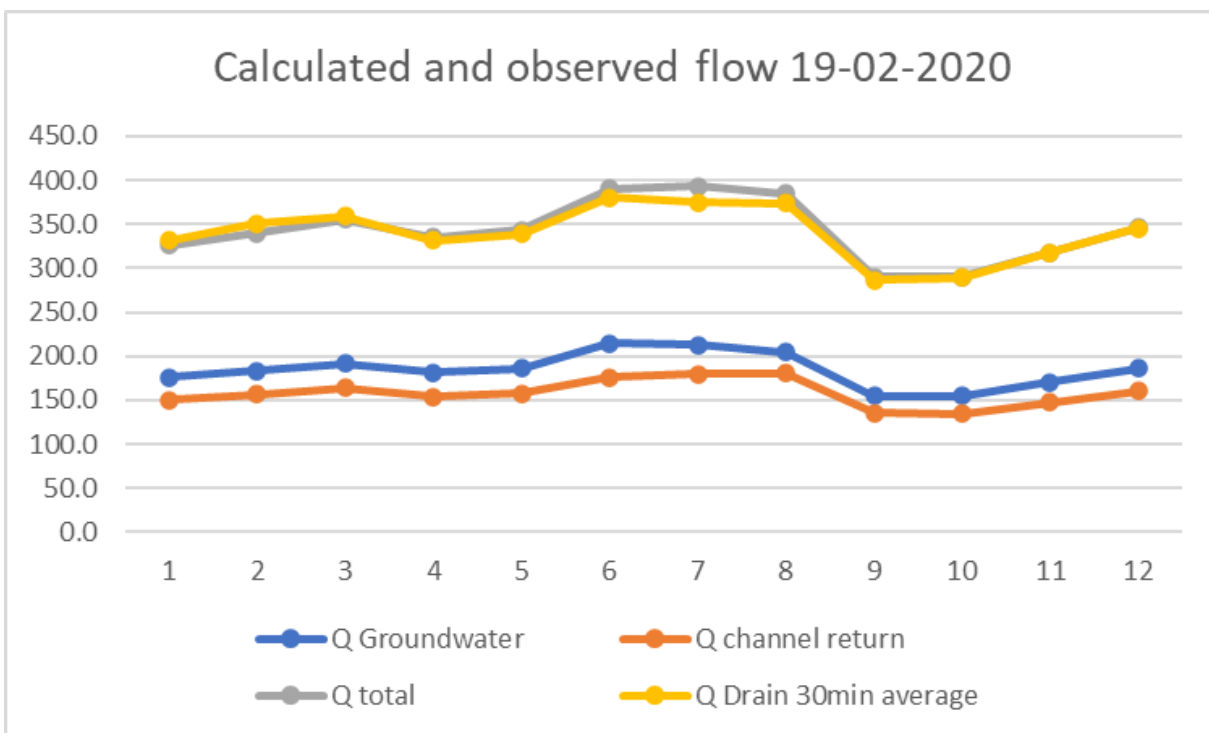


Figure 21: Shows the calculated flow contributors. It is divided into return water from the channel, groundwater, and the total calculated volume. It also shows the 30-minute average observed flow and the differences between the flows. The unit is litres per second.

The calculation of flow shows that the water flux that returns from the outer channel 'Nordkanal' contributes a little under half of the total water in the drain channel when it has a flow away from the pumpstation.

Looking at the flow in the drain channel (figure 22) and the water level in Nordkanal there is no hourly correlation.

But there has been found a correlation between the flow in the drain channel and the water levels in the 'Nordkanal'.

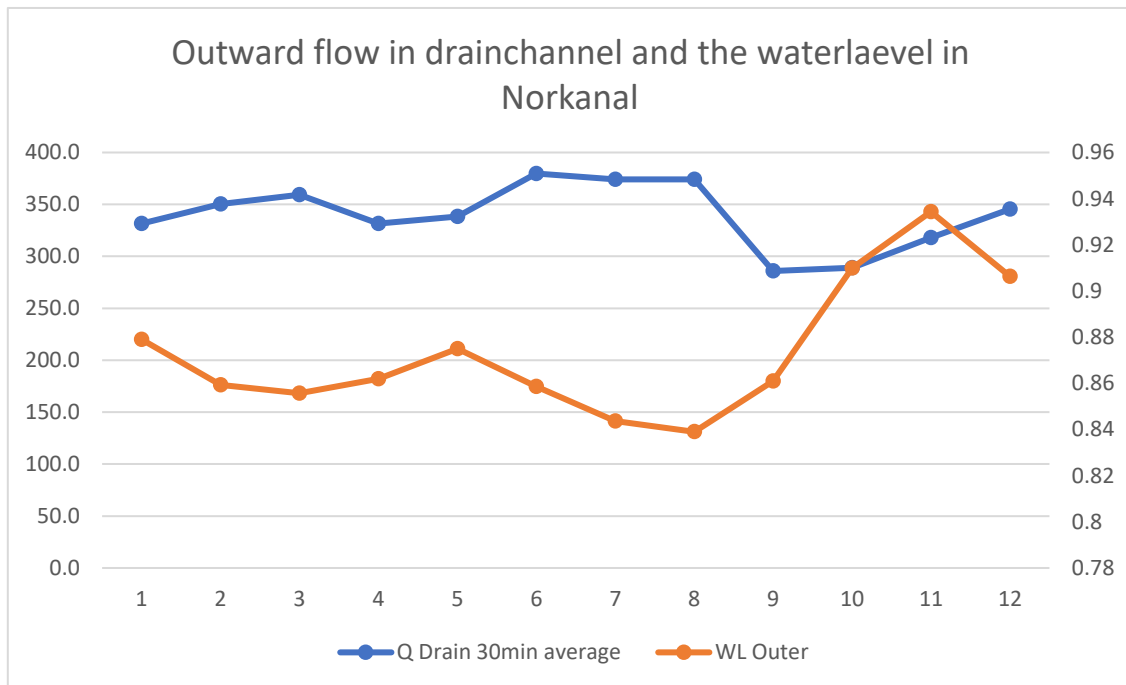


Figure 22: Shows the flow in the drain channel away from the pumpstation and the water level in the outside channel. The unit is litres per second and meters above sea level.

New geological model

To investigate a possible better way to model groundwater flow in the chalk aquifers. A new geological model was suggested. This suggestion was made by the company WSP Denmark. They were working with a farmer north of Grenaa to establish a high yielding pumping well to be used for irrigation. This work was done with an investigation of the subsurface using TTEM together with capacity test on newly dilled wells.

Looking at the newly made TTEM lines there were found a remarkable difference in the resistivity of the calk in the area. The top 10 meters of the chalk have a relative low resistivity compared to the chalk below. This shift in relative resistivity is sharp and present throughout the area where the TTEM were made north of Grenaa. A new well and a capacity test then showed that the well could produce a satisfying amount of water for irrigation. This then led to investigate that if this pattern of resistivity of the chalk were present throughout the focus area. On the background of this pattern of resitivity and the high yield well it where assumed that this high resitivity layer where a layer that where either fractured in a way that it could

support a high flow. Or that the high resistivity chalk represented areas where flow were mainly in conduits.

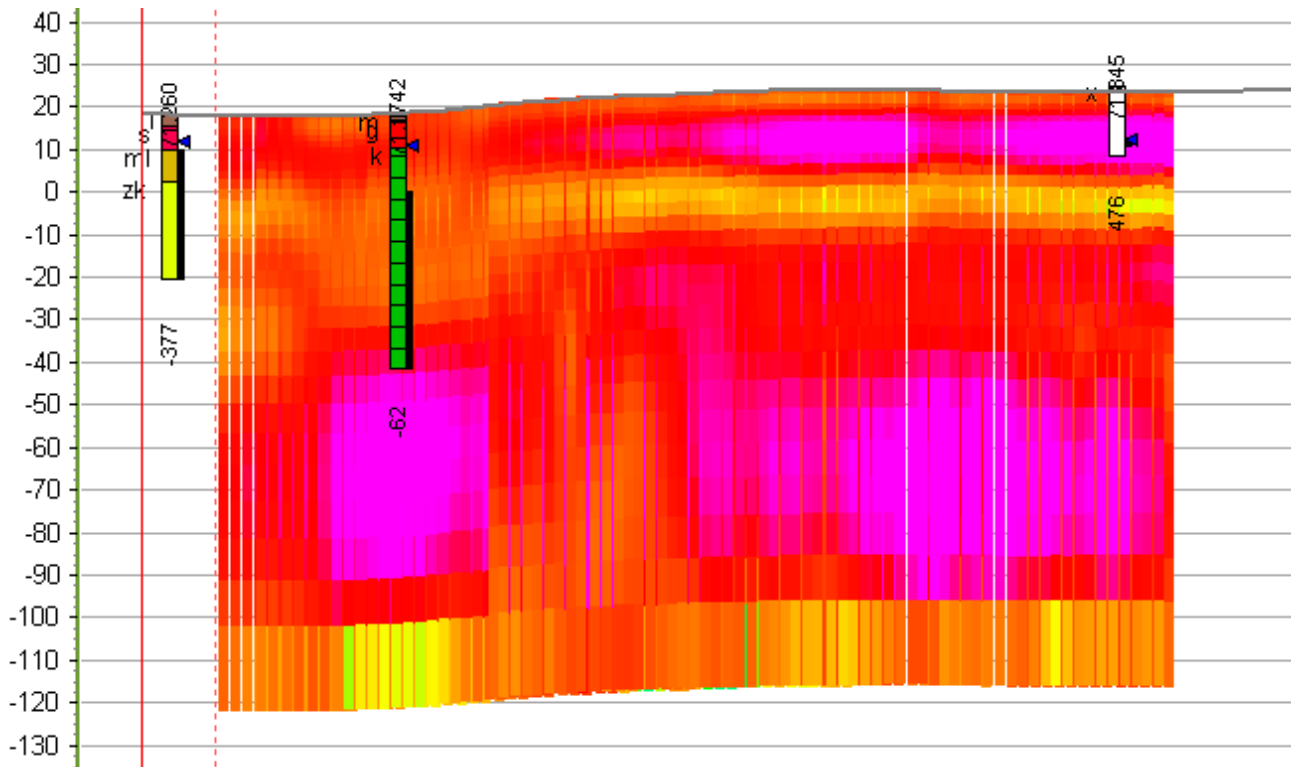


Figure 23: tTem profile from north of Grenaa

SKYTEM investigation

To investigate this SKYTEM data covering the area north of Kolindsund was collected from the GERDA database. This data covers most of the area around Kolindsund and all the way to the

coast to the north. It also covers parts of the area south of Kolindsund (Rambøll, 2014).

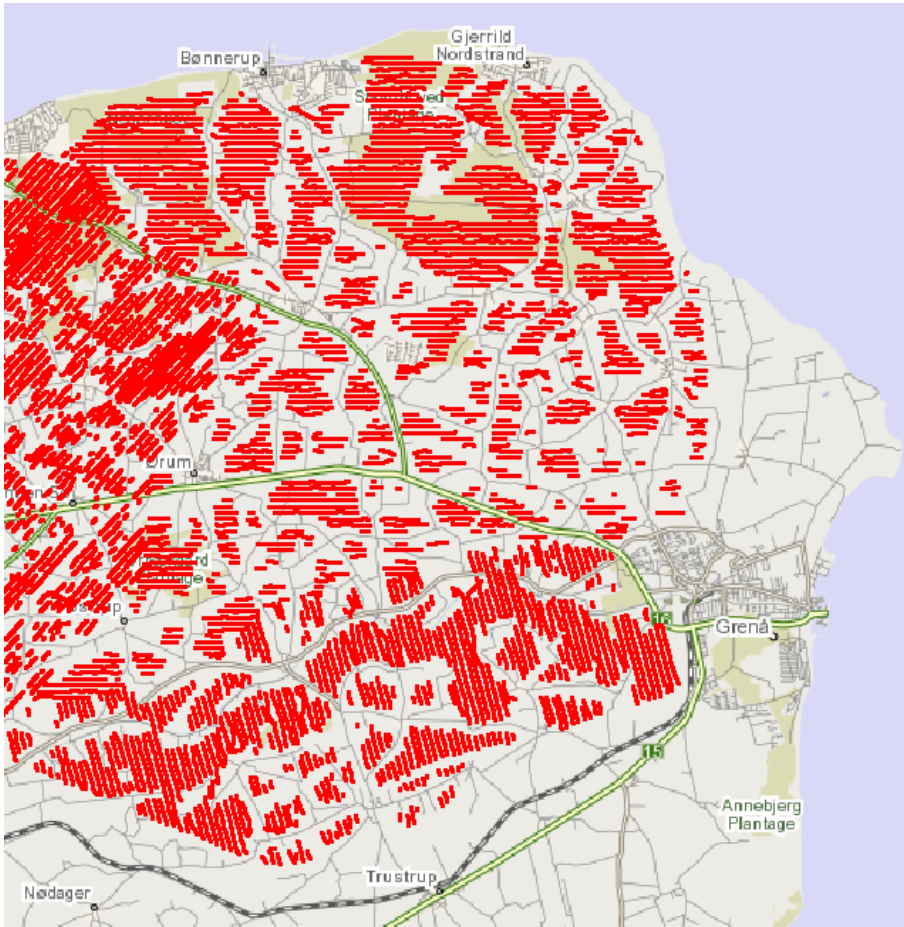


Figure 24: The maps show the locations where there is SKYTEM data available.

The program used to interpret was Geoscene3D. Using Geoscene a 3d interpretation was made. This was done by interpolating the SKYTEM data into 5-meter-thick slices. To cover a larger area each datapoint were set to cover 50 meters in radius. this made the data cover more of the areas that was not measured. This makes it possible to make a preliminary investigation of the resistivity in the chalk layer by layer.

First the TTEM profiles were used to find an interval in relative resistivity and if there were a certain interval that could be of interest. This was done by comparing the TTEM and the SKYTEM data in the small areas where both were present. This also showed that there is a significant difference in detail and the measured resistivity. TTEM has a higher vertical resolution than SKYTEM. This makes TTEM better to identifying relative sharp interfaces between geological layers compared to SKYTEM. But the depth of penetration of the TTEM is shallower than the one seen on SKYTEM. The SKYTEM data has a lack of detail but this makes It possible to have a deeper penetration. This deep penetration makes it useful to identifying the saltwater-groundwater interface below the focus area.

This quick analysis showed that there is a different in resistivity for the interval 40 meters below sea level to 80 meters below sea level throughout the area

This correspond to the same interval that was identified with the TTEM north of Grenaa. In some areas hare this interval thicker. The analysis also shows that there are several areas situated in low laying valleys that shows a low resistivity. This is most likely due to either fossil seawater or seawater that has been drawn up due to drainage in the area.

at 40 meters below sea level Kolindsund is the most prominent area with this presumed saltwater. But in the low laying area that runs from Enslev to the north towards the sea are there also at 40 meters below sea level a lower resistivity that gets lower the closer it comes to the sea see figure 25 and 26.

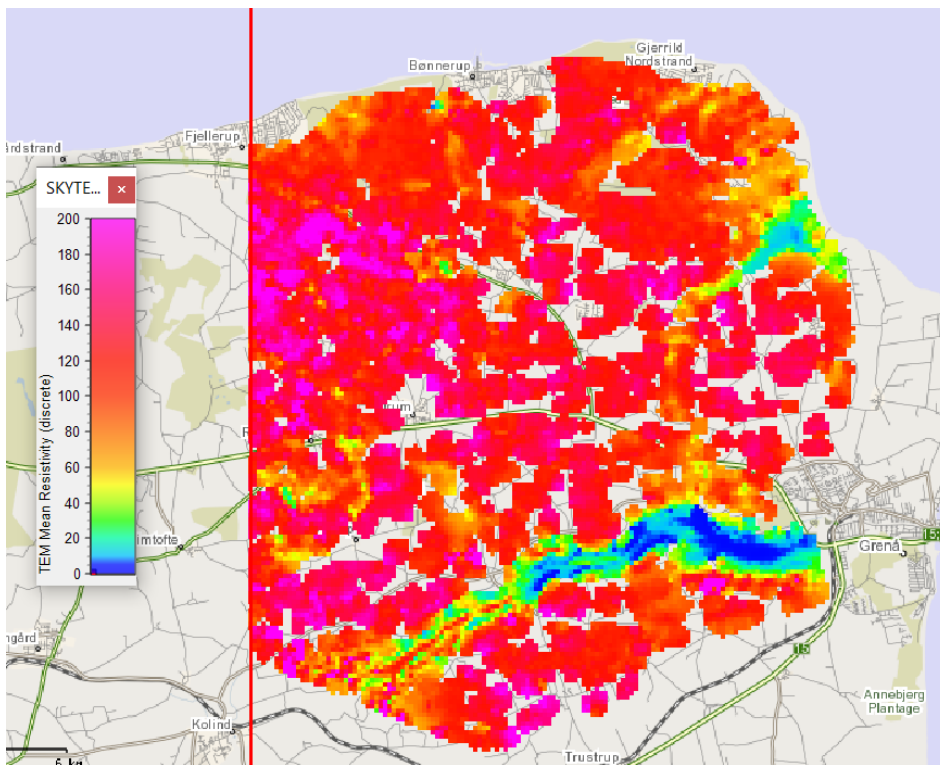


Figure 25: the map shows the mean resistivity for 40 meters below sea level.

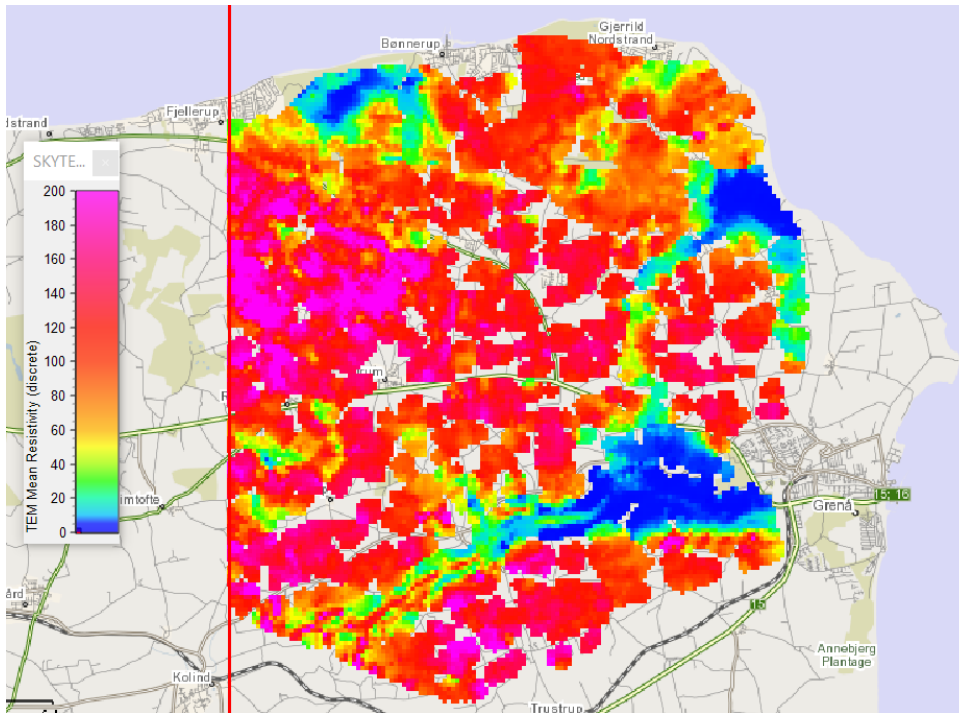


Figure 26: the map shows the mean resistivity for 80 meters below sea level.

Data

To make a new geological model the data available were considered. The data for the area were collected from the Jupiter and GERDA databases directly to the modelling program Geoscene3D. The types of data available in the Jupiter database were wells drilled throughout the area. From the GERDA database two different types of data were available. The first was SKYTEM. This data covers the northern part of the focus area and all the area adjacent to Kolindsund (see figure 24). The other main part of geophysical data retrieved from GERDA was TTEM. This is a more local land borne investigation than the SKYTEM. The TTEM was available for two areas. One area situated north of Grenaa and one south-west of Grenaa at the wellfield area of Homå (see figure 27).

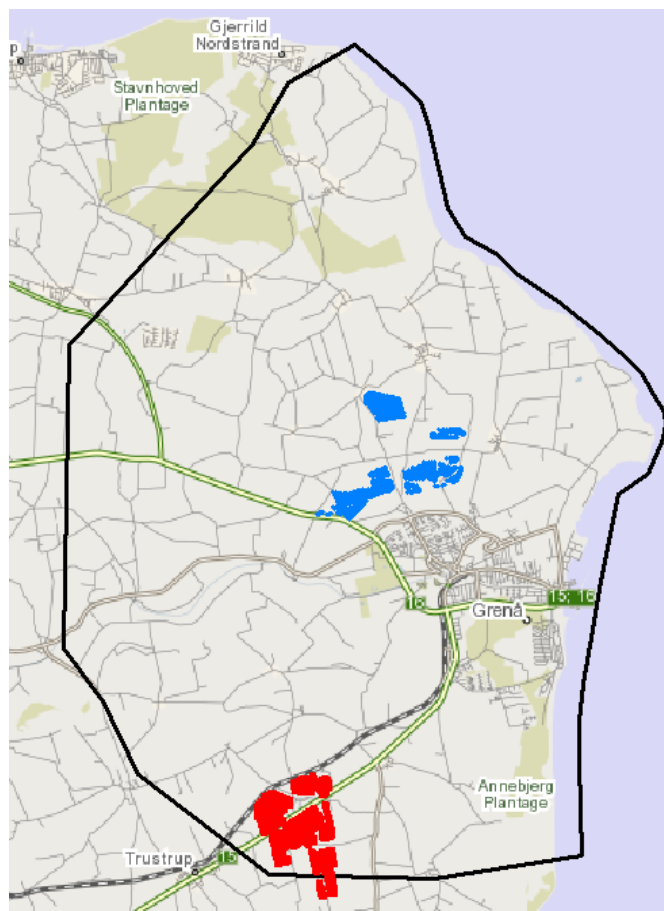


Figure 27: The maps show the areas with available tTem data.

Interpretation

To interpolate the different data in the area a grid of profiles was laid out throughout the area (see figure 282). It was made sure that the grid and the work area covered the whole area and as much TEM data around the area. There were made 10 north-south going profile lines and 13 east-west going profile lines. In the area where TTEM was available several extra short profiles lines were made. This was done to make a higher precision of the geological model in areas where TTEM provided high detail data.

These profile lines were set to import adjacent wells to the profile line at a distance of 50 meters for the initial interpretation. Later in the interpretation work the distance to adjacent wells were increased to 200 meters and then to 500 meters.

The layers were interpreted as series of support dots. These the program Geoscene3D can then use these dots to make an interpretation of a surface throughout the area. These dots were then used to make a temporary surface. This surface was used to adjust the interpolation up and down if necessary, before the final interpolation. Sometimes the layer interpolation was far off when it came to the quaternary layers. This meant it were necessary to place support

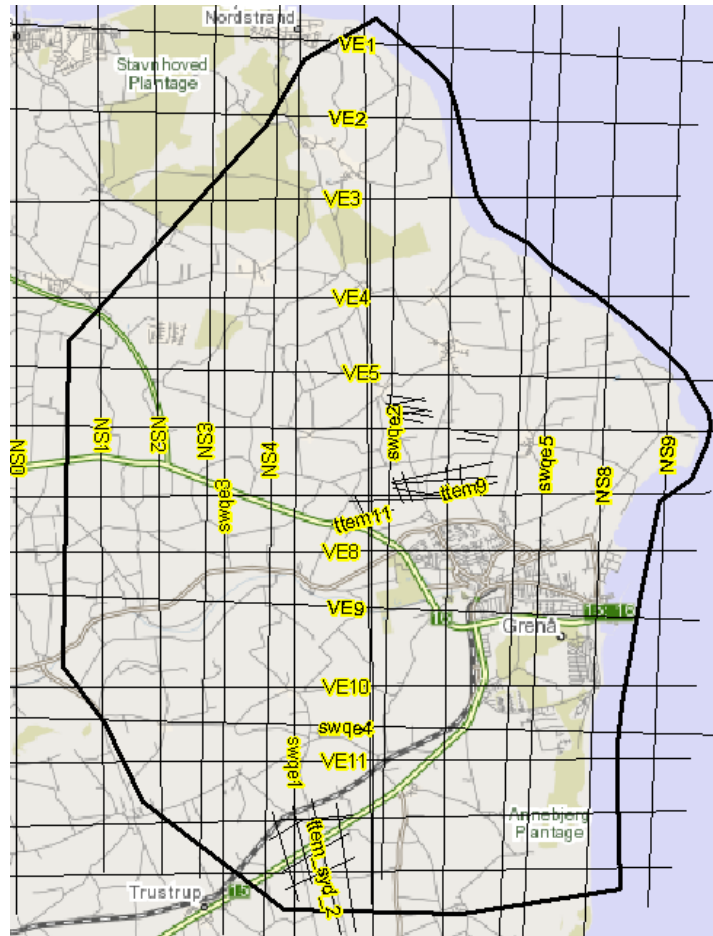


Figure 28: The map shows the profile line created to help interpret the geology. Note the extra short profiles at the area with tTEM.

points. These support points do not represent the real geology. But it does weight an area higher in the interpolation such this area's unit's surface is either pulled up or down so it can match the data.

For the final interpolation Kriging were used. This made the interpolation smoother so that "shark teeth" was removed.

The next tool used to finalize the model were adjusting the layers in relation to each other. This made sure that the surface of the interpreted unit could not cross over each other.

The first layers that were interpreted were the chalk layers. The layers were defined by the relative resistivity. The top layer is a low resistivity layer. The top of the chalk was mainly defined by lithology listed on the wells. Every time a well had some sort of chalk the top of this were marked. The middle chalk layer was dined with high resistivity. And the bottom was defined with a lower resistivity at around 20 to 0 ohm. This bottom represents the freshwater saltwater interface. These three layers were interpreted as four surfaces defined by the top of the three layers and the bottom of the model. This bottom surface was defined by the low resistivity that comes from the deep saltwater below the area.

The next step for interpretation were the quaternary sediments. These were interpreted as two different sandy units and two different clay units. The layering was as followed from the bottom. A clay layer, a sandy layer, a clay layer and at the top a sandy layer. Layers that are less than 5 meters thick were collapsed and set as one of the four layers.

Due to the sedimentation history of the area, there are many small thin layers that cannot be traced from well to well. These thin layers that also could be lenses of different sediments were ignored and the prevailing unit were interpreted as one single unit. One thing that also could interfere with the different layers encountered in the wells is ice tectonics. This can make fault lines in the sediments and make them overlap each other. See figure 29 to 31 to see the process.

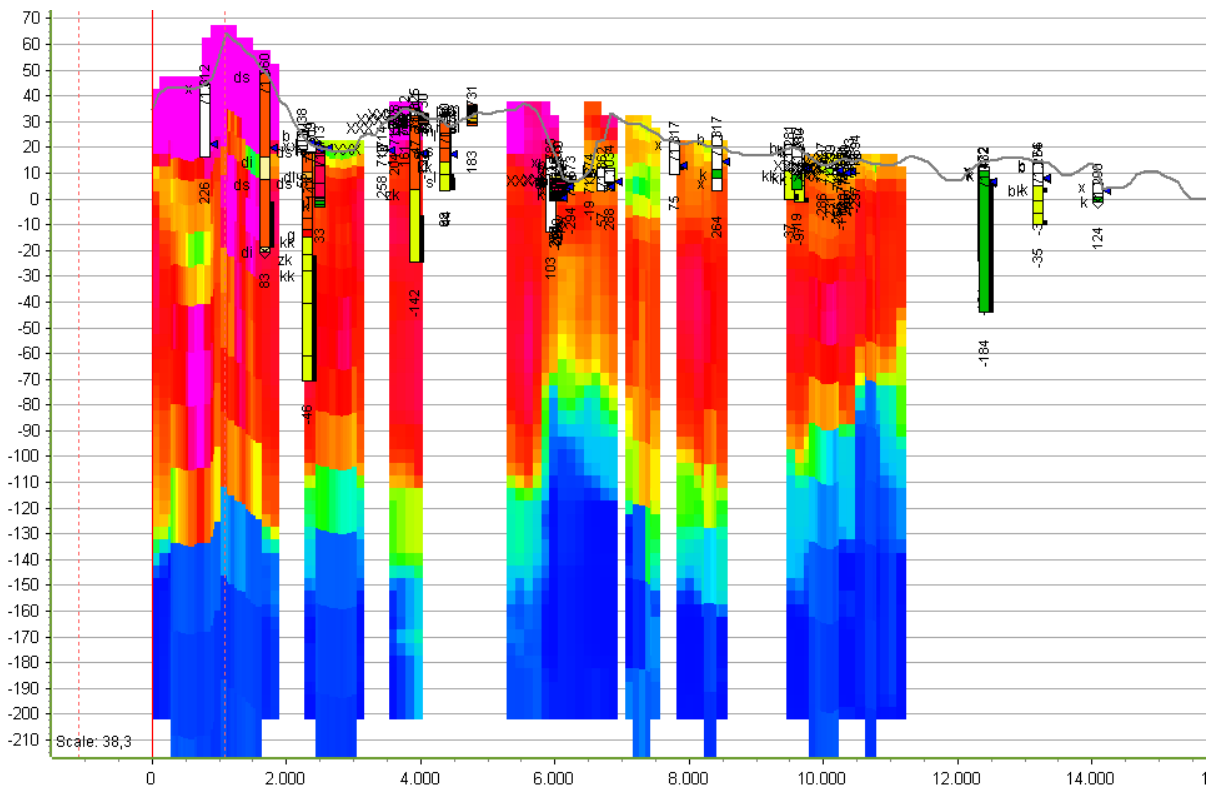


Figure 29: a west-east profile line along ve5 profile line. It shows wells and SKYTEM for the area.

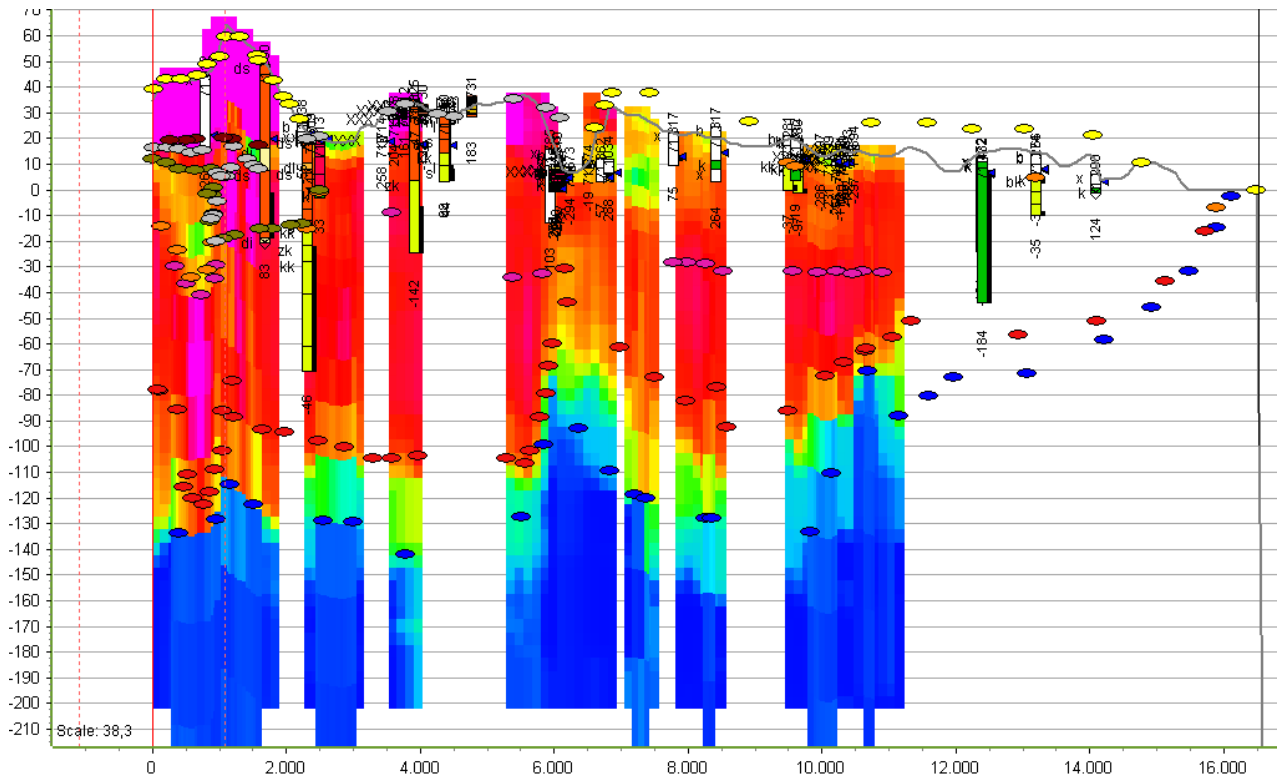


Figure 30: a west-east profile line along ve5 profile line. It shows wells and SKYTEM for the area. The profile line also shows interpolation dots.

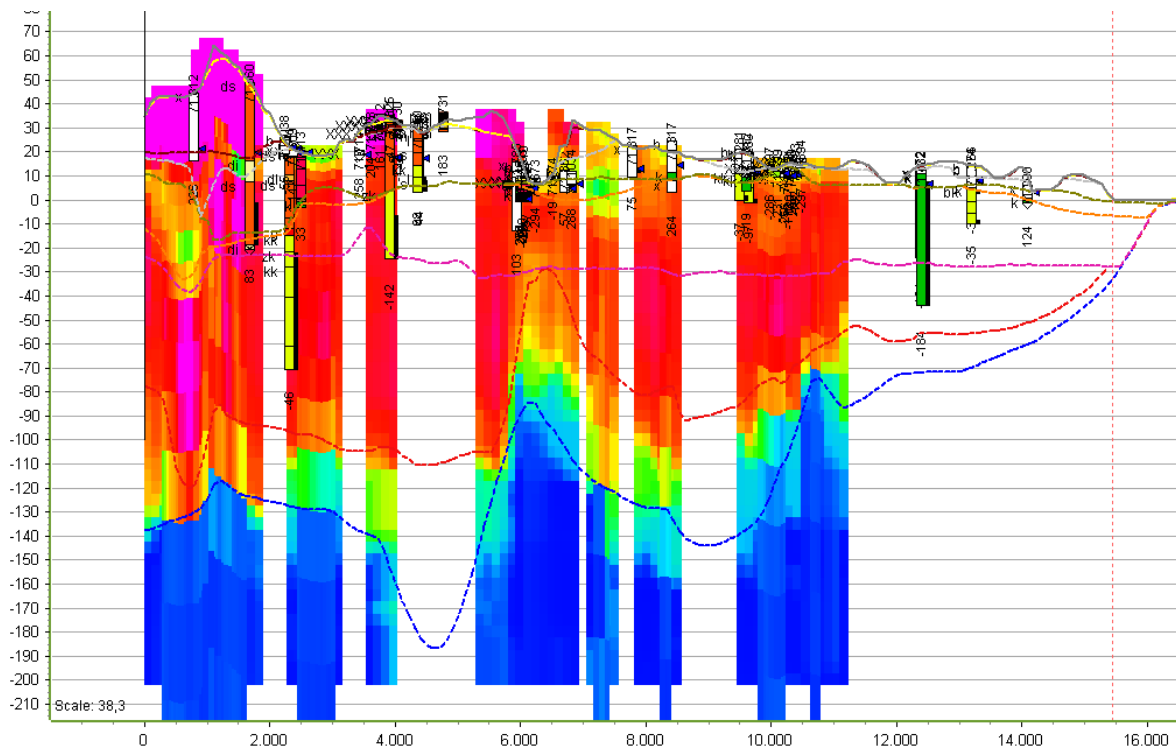


Figure 31: a west-east profile line along ve5 profile line. It shows wells and SKYTEM for the area. it also shows the interpolated surfaces after Kriging and adjusting.

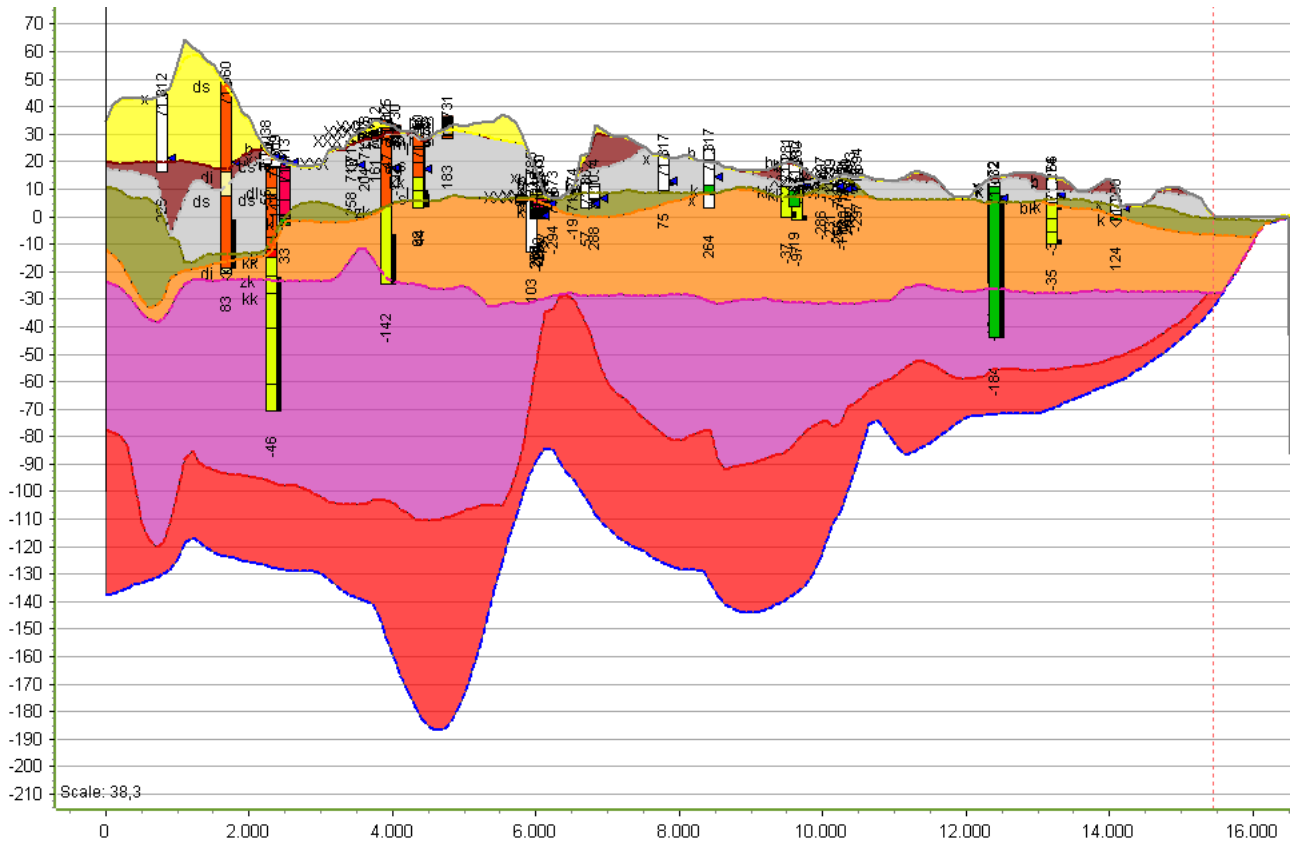


Figure 32: a west-east profile line along ve5 profile line. It shows wells and the final layers.

The final geological model

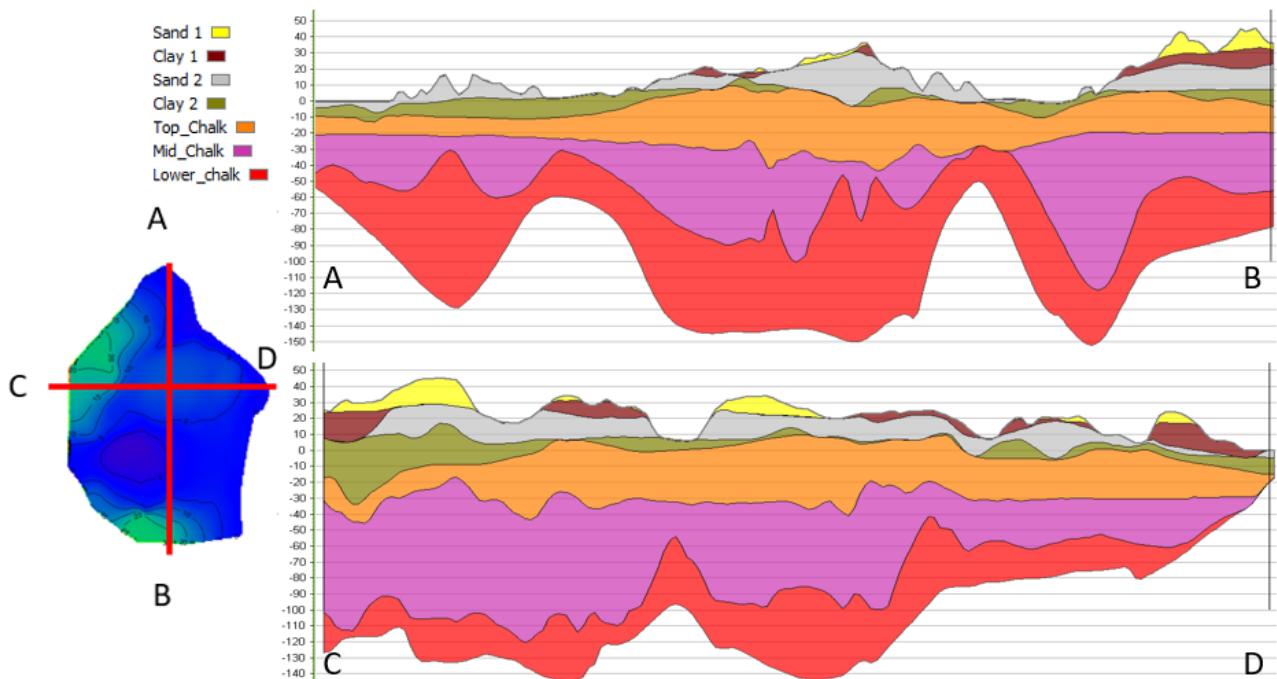


Figure 33: The final geological model.

The final geological model consists of three chalk layers and four quaternary layers. The chalk layers were defined by using SKYTEM that measured the relative resistivity.

The four quaternary layers consist of two clay layers and two sandy layers. These layers are defined by the wells. Skytem and TTEM were used to interpret between the wells. There is large areas in the new model where SKYTEM or tTem were not available and here is the chalk layers just an interpolation from the areas where the data was available.

Flow logs

Within the focus area there are several wells that have undergone geophysical investigation and most interesting there has been made a flow log in these wells. They are mostly located in the southern part of the focus area around the Homå well field and Vejlbj well field. There are also some located in this area, but they are outside the focus area and therefore there is no model or skytem to compare them to.

In the northern part of the area there are three wells that have a flow log.

Flowlogs to tem

Within the area there are three wells that has undergone a well log and have SKYTEM data in the vicinity. These wells are located in the northern part of the area near Gjerrild.



Figure 34 Shows the position of the three northern wells that have undergone flow logging.

61.219

The well is situated in Albæk plantage. It is the deepest of the three wells reaching a depth of 100 meters below sea level. It is screened in most of the chalk and only cased in the top and an open well for the rest of the well. See the full log in appendix B.

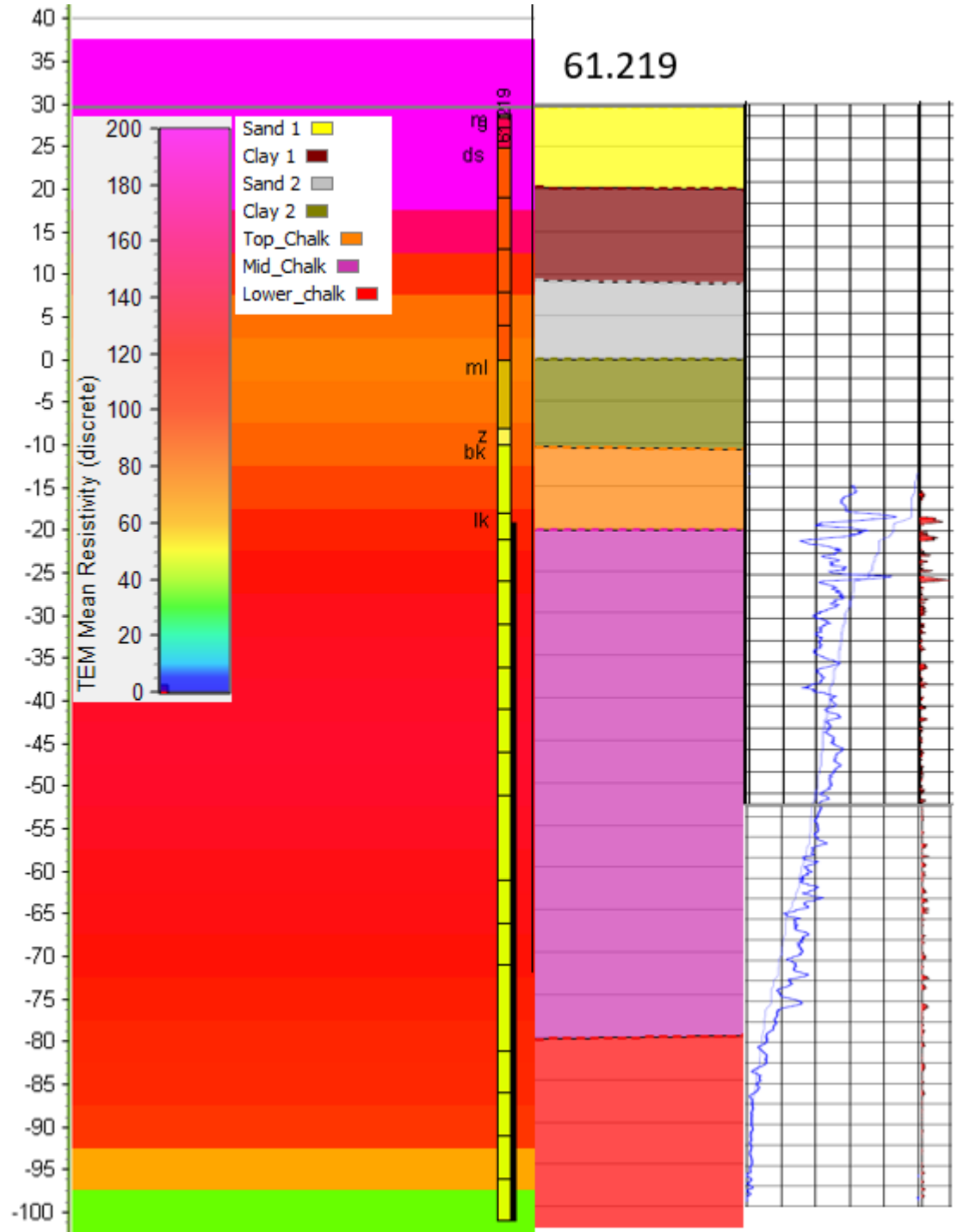


Figure 35: shows the interpolated SKYTEM, final geological model and the flow log.

When the area was interpreted it was done along the profile lines and therefore there are not interpreted geology using this well. This is clear in the geological model on figure 35. In the top

part of the well there are interpreted a layer of clay that does not exist in the well.

The highest resistivity in the well is around 120 - 140 ohms. This is lower than what is found in other areas.

The low resistivity in the top layer of the chalk is not visible. This could be due to the clay layer on top that has a low resistivity. This mask the differences in the chalk if it is there.

The flow log shows that the water flow ins at small step through most of the well. The biggest in flow are found in the to 10 meters of the well. This matches the traditional theory of fractured chalk in Denmark. This says that the top 10 to 20 meters are fractured due to ice tectonics.

61.221

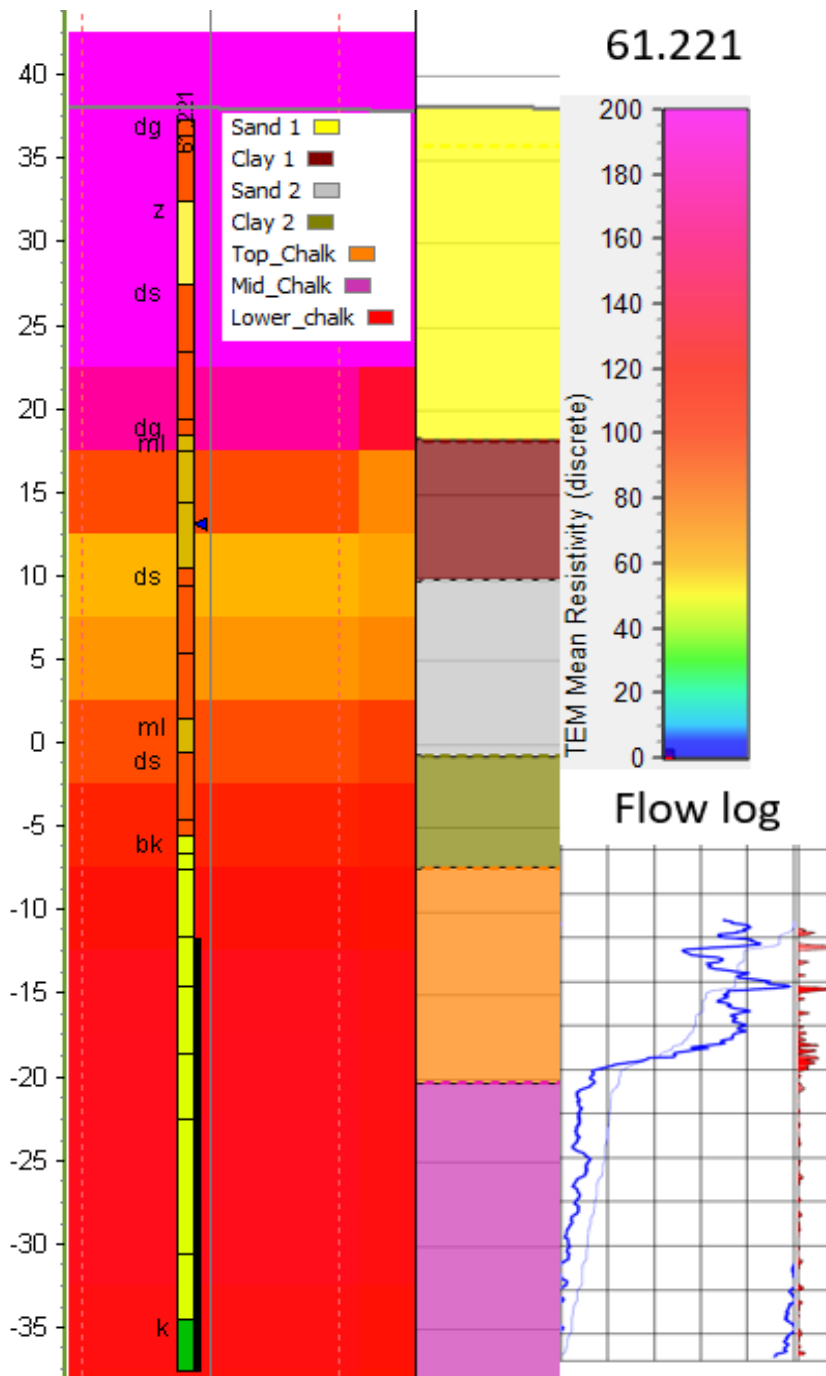


Figure 36: shows the interpolated SKYTEM, final geological model and the flow log.

The well is situated in Albæk plantage. The well reaches a depth of 35 meters below sea level. It is cased in the top part of the well through the quaternary layers and into the top of the chalk. Here the well becomes an op well. This well is quite close to 61.219 so the same irregularities with the geological interpretation is found at this well. The resistivity is around 110 ohms. The low resistivity chalk cannot be found

at this well. It could again be averaged out in the top where the clay is.

The flow log shows that 80% of the water flows into the well in the first 10 meters below the casing and then for here on down the water only trickles into the well

This again matches the traditional theory of fractured chalk in Denmark. This says that the top 10 to 20 meters are fractured due to ice tectonics. See the full log in appendix C.

61.149

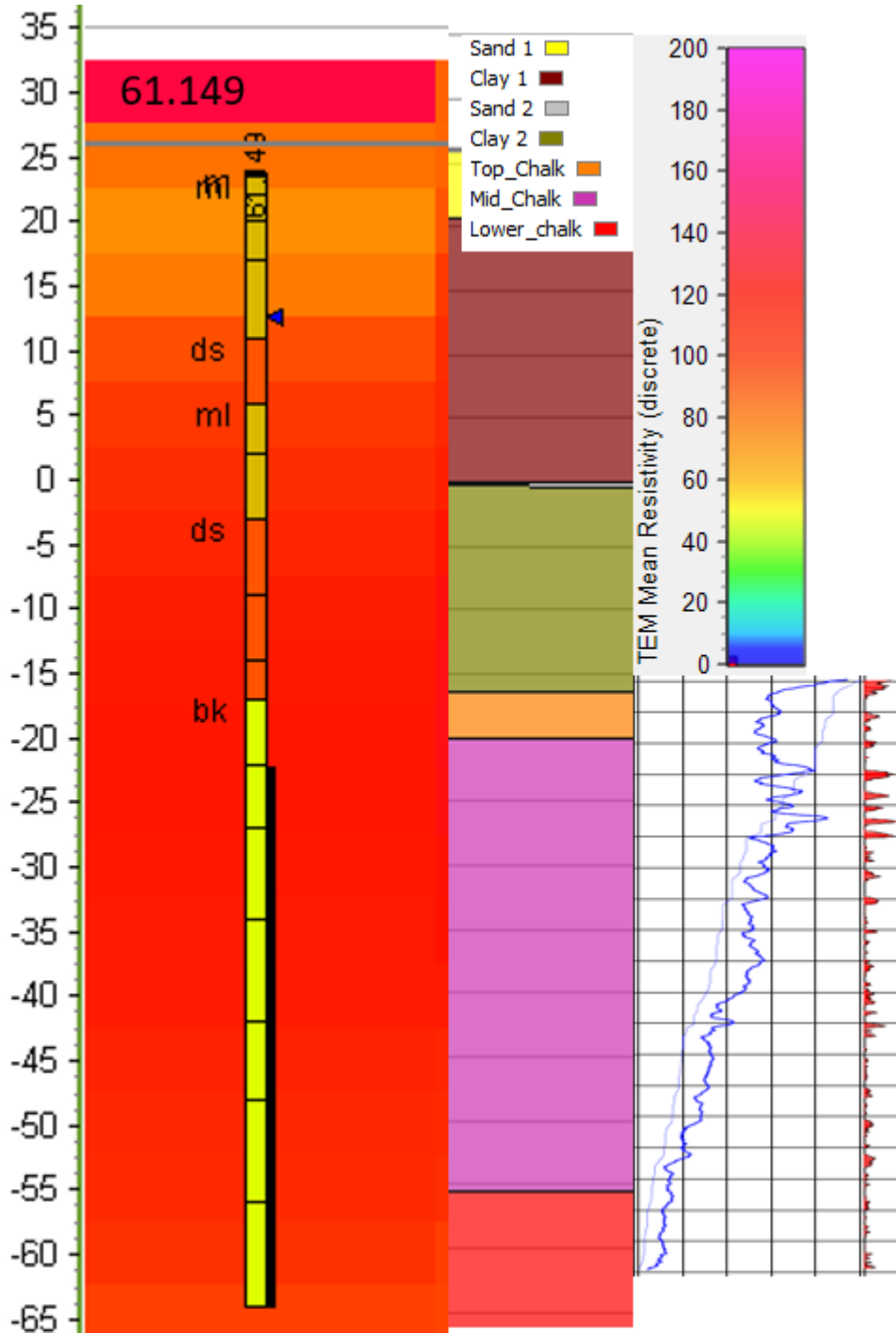


Figure 37: shows the interpolated SKYTEM, final geological model and the flow log.

The well is situated in Hemmed plantage. It reaches a depth of 65 meters below sea level. It is cased in the top part of the well through the quaternary layers and into the top of the chalk. Here the well becomes an op well for the rest of its depth. This well is close to 61.219 and 61.221 so the same irregularities with the geological interpretation is found at this well.

The resistivity is around 110 ohms. The low resistivity in the top layer of the chalk is not visible. Looking at the resistivity the chalk seems to be uniform.

The flow log shows that the water flow in through most of the well. The biggest in flow are found in the to 15 meters of the well. Here 60% of the water flows into the well. This matches the traditional theory of fractured chalk in Denmark. This says that the top 10 to 20 meters are fractured due to ice tectonics.

Compared to 61.219 and 61.221 the flow into this well is much more even through the well. See the full log in appendix A.

Flow logs to model

In the southern part of the focus area there are four wells that are situated within the geological model.

Most of the wells in this area have been used to interpret the geology. But the geological model does not fit the geology found in the wells perfectly. This can be due to restrictions in the interpolation algorithm used. other wells in the area can be fitted quit well and others are only close to a good fit.

The nearest TEM used to interpret the chalk is situated 2 km to the south west.

71.394 and 71.443

The geology for the two wells fit well but common to them both the geology is pulled down, so the quaternary layers lay too deep as well as the chalk is a little too deep.



Figure 38: Shows the position of the four southern wells that have undergone flow logging.

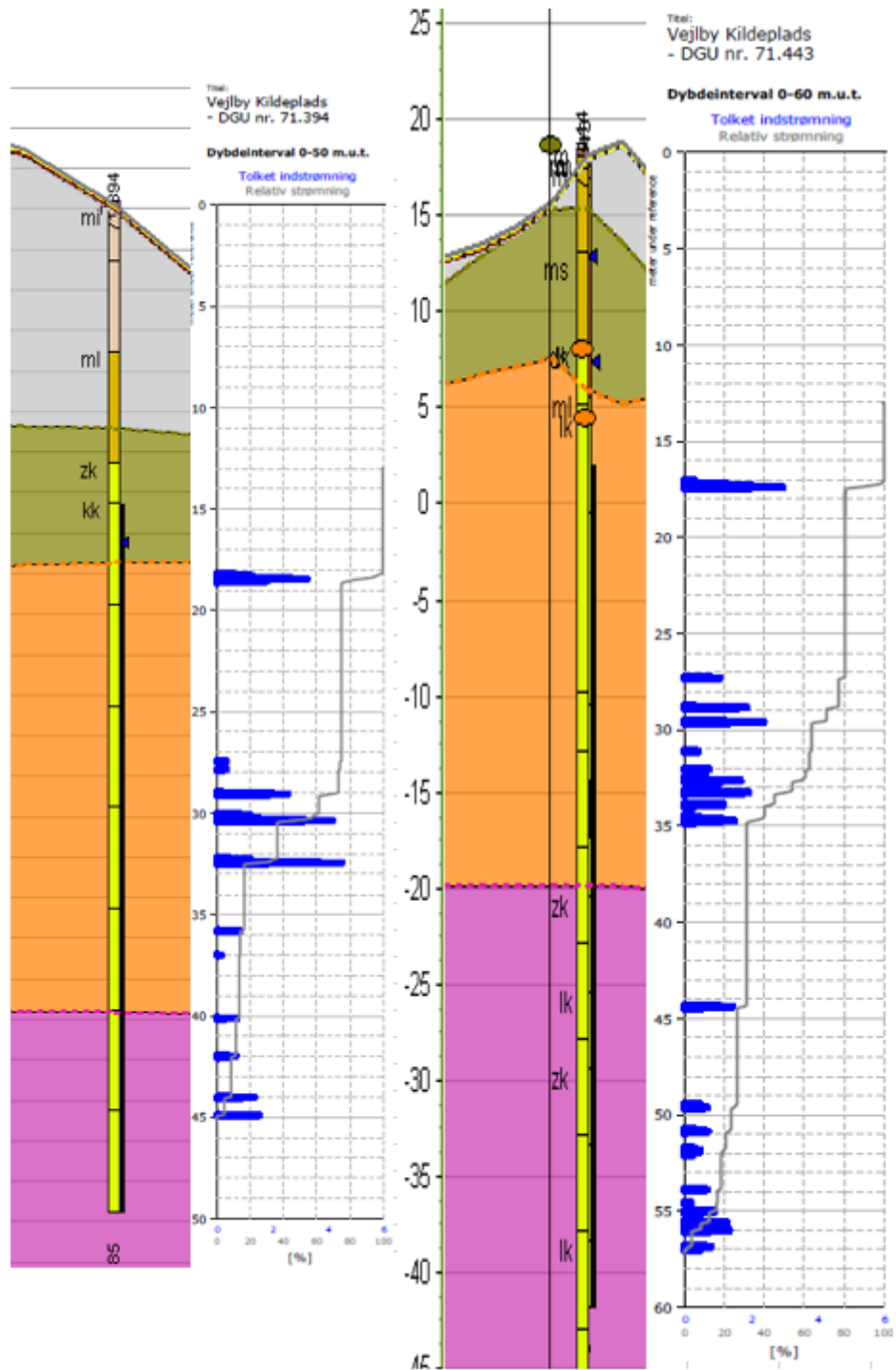


Figure 39: shows the final geological model and the flow log.

71.394 is cased the top part of the well through the quaternary layers and into the top of the chalk. Here the well becomes an open well for the rest of its depth. The well is 50 meters deep and reaches 32 meters below sea level. See the full log in appendix E.

71.443 is cased the top part of the well through the quaternary layers and into the top of the chalk. Here the well becomes an open well for the rest of its depth. The well is 60 meters deep

and reaches 43 meters below sea level. See the full log in appendix F. The flow log for both wells shows that large parts of the flow into the wells comes from very narrow parts of the well. These narrow parts could be large fractures or conduits. These patterns are seen in the whole length of both wells. It is a pattern that is seen in both the top layer of the chalk but also in the middle chalk unit.

81.310 and 71.393

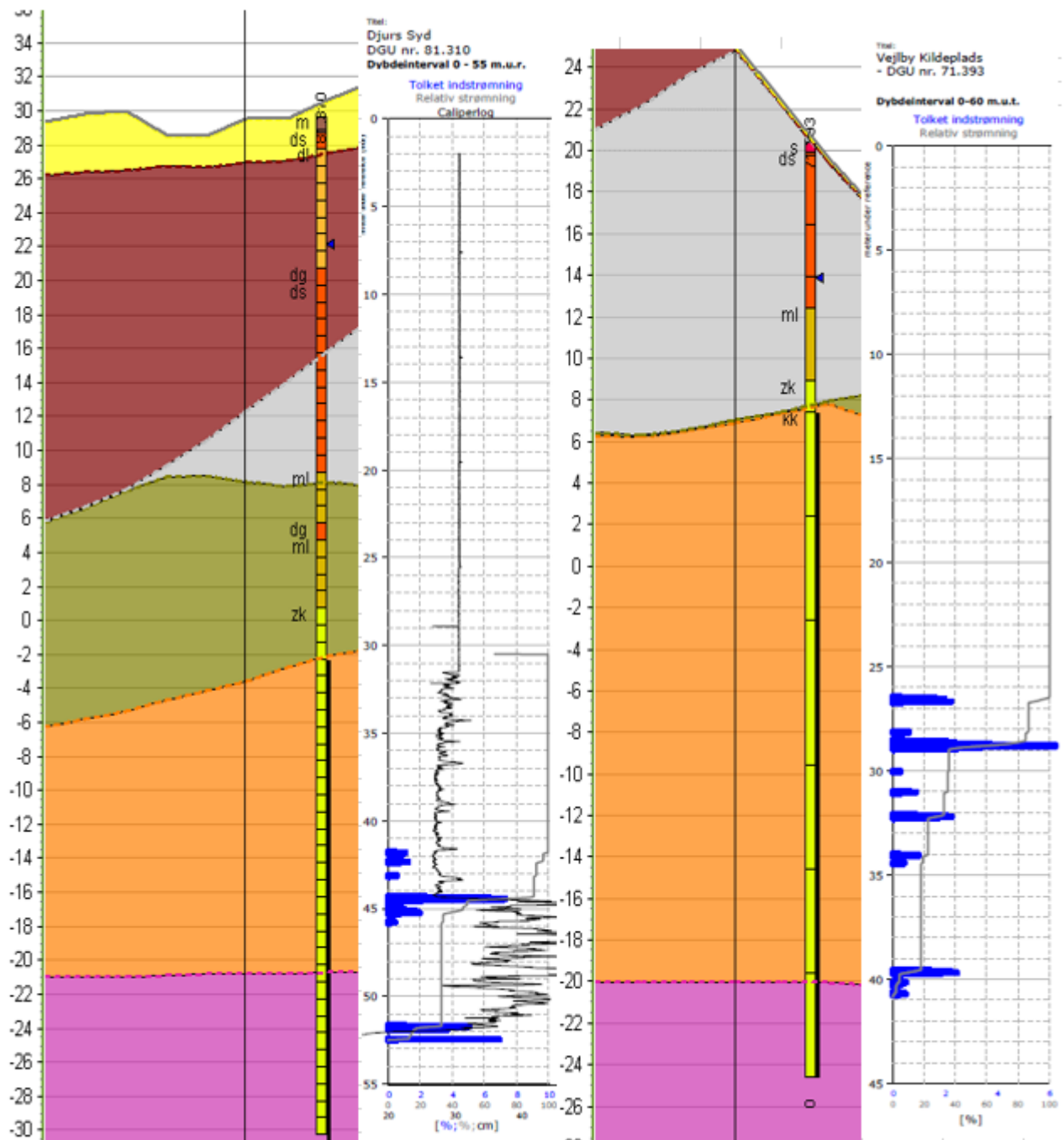


Figure 40: shows the final geological model and the flow log.

71.393 is cased the top part of the well through the quaternary layers and into the top of the chalk. Here the well becomes an open well for the rest of its depth. The well is 45 meters deep and reaches 25 meters below sea level. See the full log in appendix D.

81.310 is cased the top part of the well through the quaternary layers and into the top of the chalk. Here the well becomes an open well for the rest of its depth. The well is 60 meters deep and reaches 30 meters below sea level. See the full log in appendix G.

The flow log for both wells shows that large parts of the flow into the wells comes from very narrow parts of the well. These narrow parts could be large fractures or conduits. These patterns are seen in the whole length of both wells except for the top of the two wells. The first ten meters appears to produce no water.

Flow logs areas

These flow logs shows that there is a difference where the flow into the wells is located. South of Kolindsund there are a flow pattern that is in the full length of the well. North of Kolindsund it is different here most of the flow happens in the top of the well and then recede towards the bottom of the well.

These differences in well flow patterns suggest that there is a difference in the hydrogeology of the chalk in the north part of the area compared to the south part of the area.

Model cutout

To try to make different models to investigate how to model this area in a better way. It was decided to make a finer discretization to make the model more precise. This led to make the model smaller and only represent part of the catchment. This was done to lower computing time of the model when simulated in MIKE SHE.

To find the new area the original regional model using a grid size of 200 meters were used. The model cutout was decided on where it was possible to make a no flow boundary.

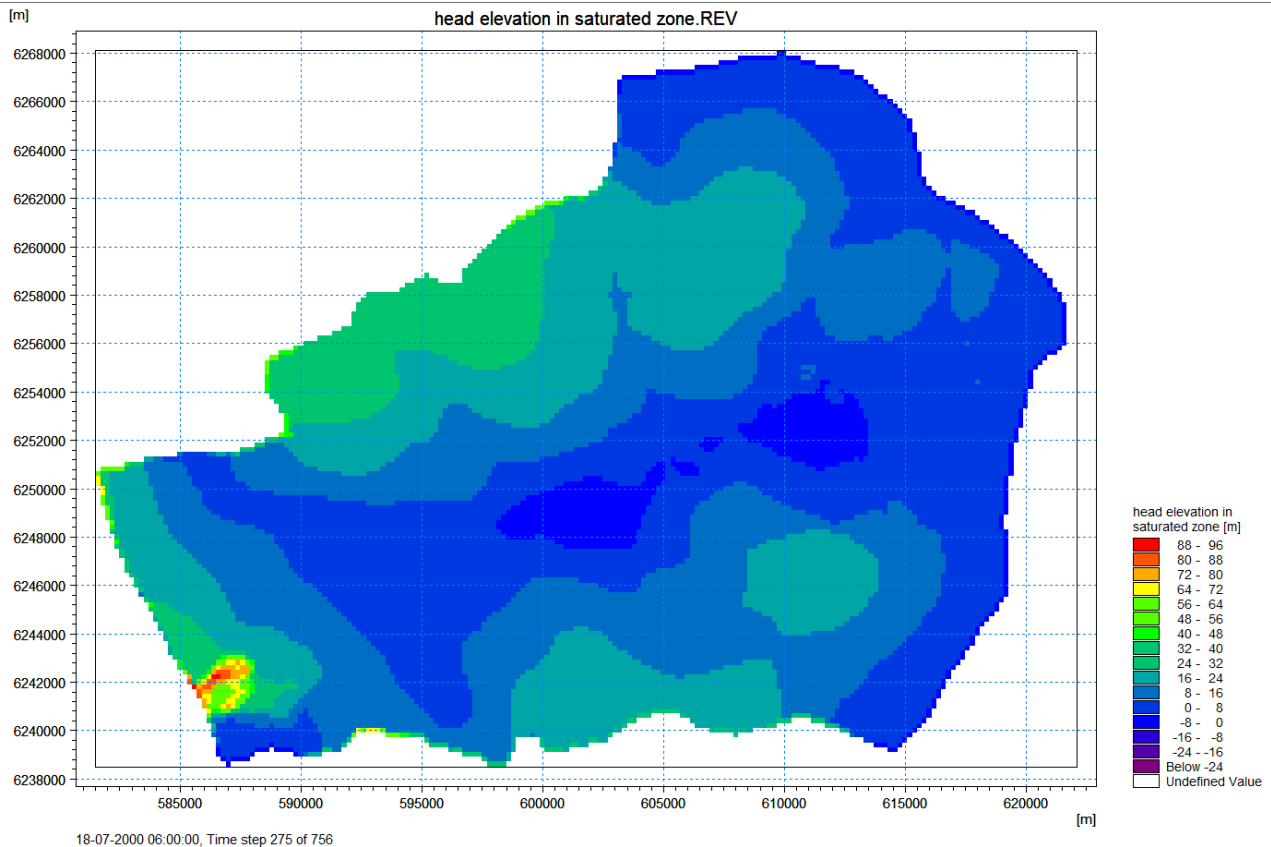


Figure 41: The hydraulic head in the upper most chalk layer for the original model for the catchment. It is made with a grid size of 200 meters.

Boundary conditions

To make this smaller focus area a new smaller model was staked out. To do this new boundary conditions were found for an area that also contained a large amount of the possible sinkholes. The sea was chosen to be one boundary. On the background of the old model of the Grenaa river catchment simulated head a new model was outlined with no-flow boundaries inland. The river model where not cut due to problems encountered with this in the MIKE river module. The no-flow boundary where set to be from the sea to the Homå high head, from here it crosses Kolindsund to Fannerup. From Fannerup it traces perpendicular to the isopotential lines to the Glesborg high head. From here it traces perpendicular to the isopotential lines to the sea at Gjerrild.

The no-flow boundary is set under the assumption that the groundwater under natural conditions will flow perpendicular to the isopotential lines. This means that the water should not cross the boundary.

At the bottom of the model there is also made a no-flow boundary. This no-flow boundary is where the freshwater meets the saltwater underneath the area. Due to difference in density of the two solutions a no-flow can be assumed.

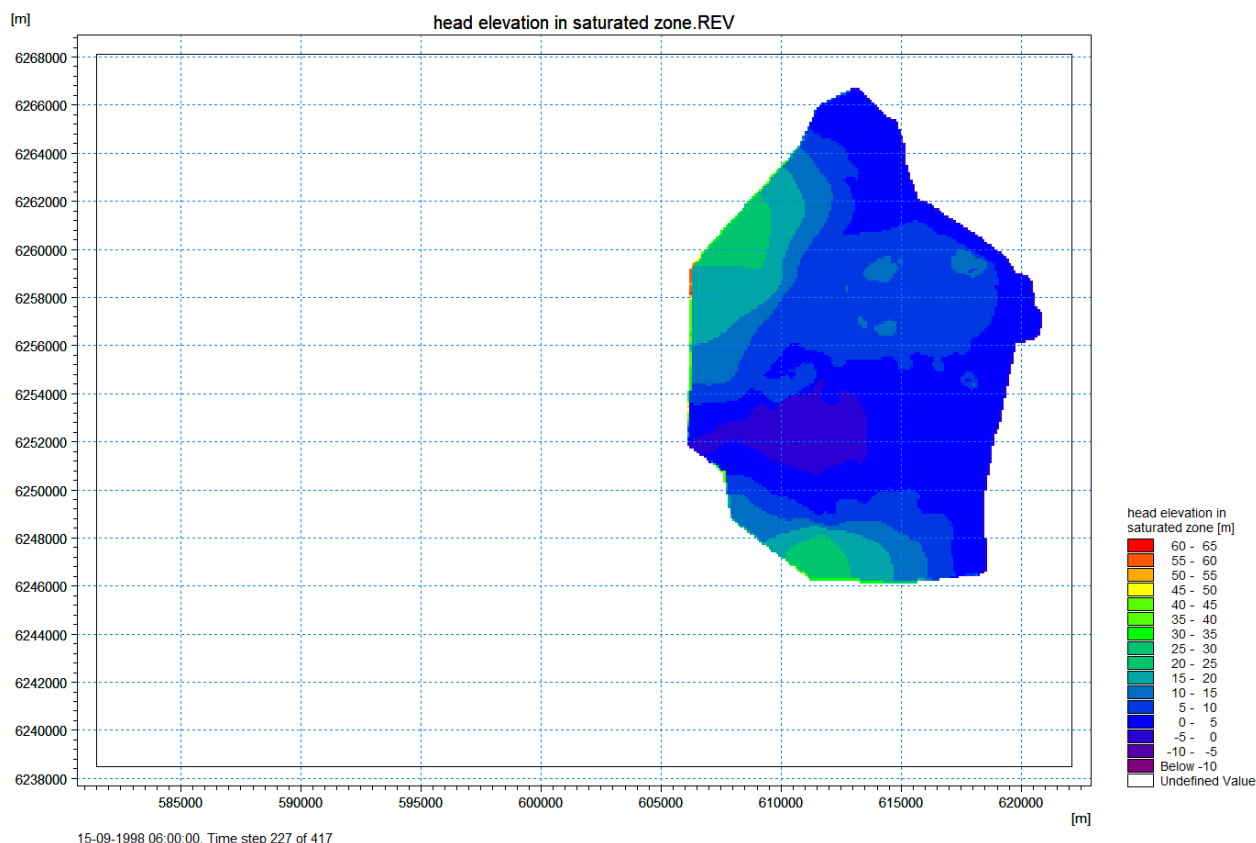


Figure 42: The area of the new flow model. The large white area is not cut due to the river model.

Model setup

The three different models were set up with many parts being the same. The only difference between them were made in the geology. Every model was made to have a grid size of 100 meters. The simulations start at 1st of January 2005 and end at 31st of December 2018.

Land use

The data for land use in the area are data that are public available for Denmark. The data contain information of which crop is used on the different areas. It also contains information of forest composition and developed areas.

The information is the used together with data about crop development and leaf area index for the different plants and crops.

Climate

The climate data are public available in Denmark. The data is collected by DMI and can be collected. The climate data used in the models are temperature, precipitation, and reference evapotranspiration.

Temperature

The temperature is based on station measurements the stations are placed throughout Denmark. These stations take the measurements at a height of two meters above terrain.

Precipitation

The precipitation is based on station measurements. These rain gauges are placed throughout Denmark. The data collected by the rain gauges is then interpolated to cover all of Denmark.

Reference evapotranspiration

The reference evapotranspiration is calculated by DMI and public available. The evapotranspiration is calculated using Penmann's equation with data also collected by DMI and then interpolated to cover Denmark.

Unsaturated zone

To calculate the flow in the unsaturated zone a two-layer approach were used. This were chosen to minimize the computing time of each model. The data needed is the soil composition and the ET surface depth.

The soil data are available to the public in Denmark. The data consist of which soil is in the area. Each soil type has its own properties. These properties are then put into MIKE SHE to calculate the unsaturated flow.

River

To simulate the rivers draining the area a MIKE River model were used. This model is the same as in the regional model for the area. The only thing that was changed were the connections between the rivers to fit the new discretization of 100 meters. Note that Nordkanal, Sydkanal and part if midterkanal is cut so that it does not simulate a correct discharge based on the new models.

Pumps

The pumping in the area is done using the pumps in Allelev, Fannerup and Enslev. All three pumps fere set to have a fixed rate of pumping. Allelev has $0,6 \frac{m^3}{s}$, Fannerup has $1,5 \frac{m^3}{s}$ and Enslev has $2 \frac{m^3}{s}$. The pumping was set to have a start and stop based on the water level in the drain channel. These water level intervals are: For Allelev, start at -4.8 meter and stop at -5.1 meters. For Fannerup, start at -4.6 meters and stop at -4.95 meters. For Enslev, start at -4.15 meters and stop at -4.45 meters.

Geological model

The geological model comes from the Dk model. It is built of thirteen different layers. Two of these layers are chalk units, one is Pleistocene clay, and the rest are quaternary layers of alternating sand and clay.

The two chalk units are constructed with a fixed thickness. The bottom of the model is defined as a no-flow boundary. Within the valley that contains Kolindsund there are three units constructed as lenses in MIKE SHE. These three units are sand, clay and peat.

Many of the layers are barely present in the new model. This is the Pleistocene clay and several

of the quaternary sands and clays. This can be seen in the cross sections of figure 43 as bands of layers close together. These bands are there because the model operates with a minimum thickness of each layer as a minimum of 0,5 meters.

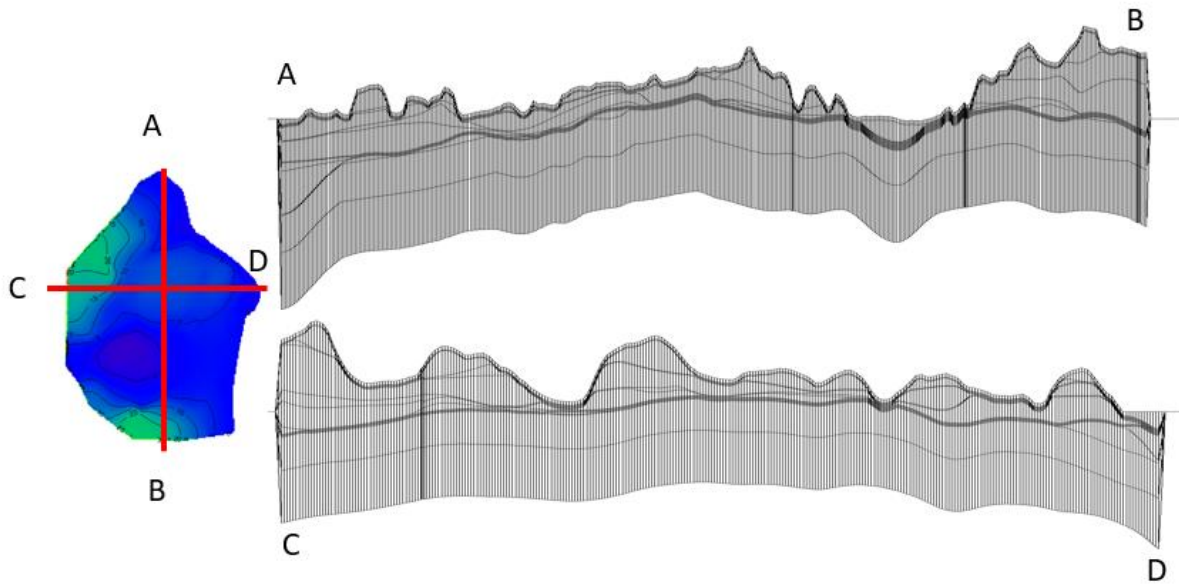


Figure 43: The geological model that is used for the two models based on the DK model.

Sensitivity analysis

To decide which parameters should be optimized a sensitivity analysis were made. This analysis was made as a central analysis with a perturbation fraction of 0.2. The evolution period was 1st of January 2010 to 31st of December 2018.

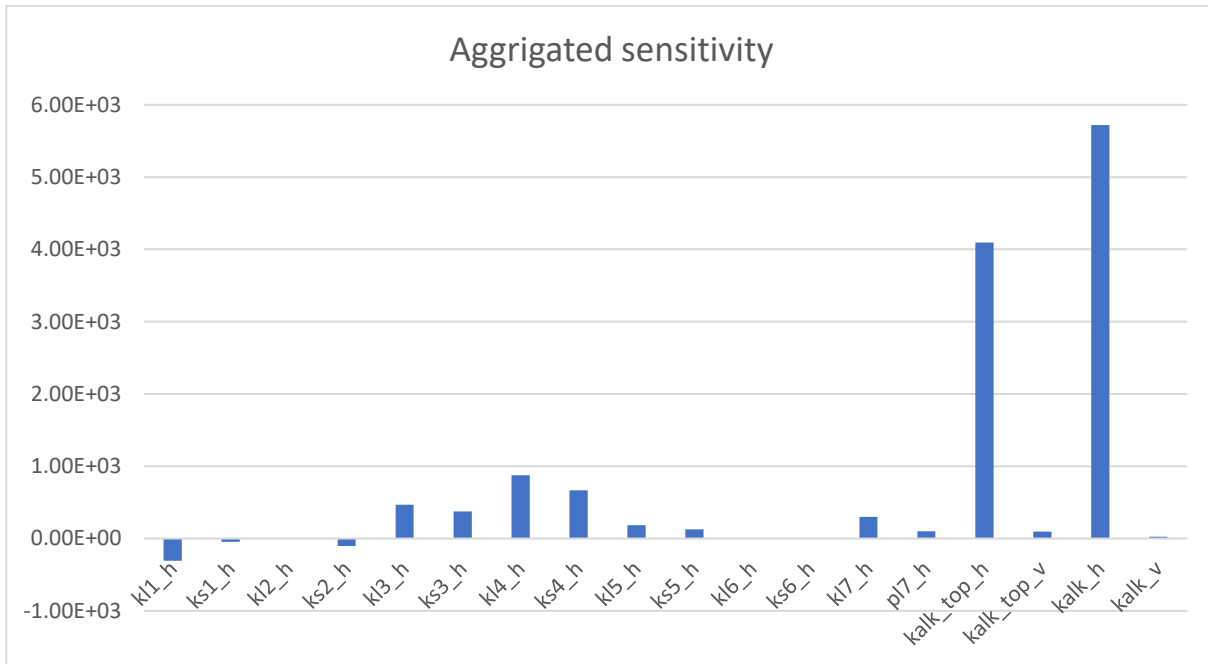


Figure 44: The sensitivity analysis for the model cut out based on the regional model.

The sensitivity analysis shows that the most sensitive parameters are the horizontal conductivity of the two chalk units. Of the quaternary layers the most sensitive parameters are the horizontal conductivity of KS3, KL3, KS4 and KL4 which are two clay units and two sandy units. The anisotropy factors are set to be 0.1 for all four units.

Covariance matrix

The covariance matrix shows if any of the parameters analyzed in the sensitivity analysis are correlated. This were calculated by the MIKE Autocal tool. To get the covariance matrix to be calculated there was removed three layers from the analysis that is not present in the area. The layers were KL2, KL6 and KS6

	kl1_h	ks1_h	ks2_h	kl3_h	ks3_h	kl4_h	ks4_h	kl5_h	ks5_h	kl7_h	pl7_h	kalk_top_h	kalk_top_v	kalk_h	kalk_v
kl1_h	1.00E+00	-4.15E-02	-1.68E-02	-1.39E-02	-3.37E-02	1.57E-02	-1.68E-02	-6.39E-02	9.43E-03	7.91E-03	-5.78E-02	-7.84E-02	5.53E-03	8.33E-02	-6.65E-02
ks1_h	-4.15E-02	1.00E+00	-4.56E-02	7.23E-03	5.77E-02	-3.33E-02	2.68E-03	-3.78E-01	-3.38E-03	-1.34E-01	-2.68E-01	-1.24E-01	-1.26E-02	1.35E-01	-1.36E-01
ks2_h	-1.68E-02	-4.56E-02	1.00E+00	2.40E-01	-4.57E-02	8.71E-02	-2.62E-02	-4.08E-02	-1.86E-02	-1.65E-01	-1.82E-01	1.81E-02	4.51E-02	-2.46E-02	-4.72E-02
kl3_h	-1.39E-02	7.23E-03	2.40E-01	1.00E+00	-4.14E-02	1.00E+00	-4.16E-01	-5.52E-01	-2.40E-02	3.32E-01	4.32E-02	-6.51E-02	1.83E-03	-7.08E-02	-1.68E-02
ks3_h	-3.37E-02	5.77E-02	-4.57E-02	-4.14E-02	1.00E+00	-4.16E-01	-5.52E-01	-2.40E-02	3.32E-01	4.32E-02	-6.51E-02	1.83E-03	-7.08E-02	-1.68E-02	-9.68E-03
kl4_h	1.57E-02	-3.33E-02	8.71E-02	-9.50E-03	-4.16E-01	1.00E+00	-5.96E-02	-5.75E-02	8.13E-02	-5.25E-02	1.89E-02	-3.55E-02	-1.21E-02	5.79E-03	4.60E-02
ks4_h	-1.68E-02	2.68E-03	-2.62E-02	1.31E-02	-5.52E-01	-5.96E-02	1.00E+00	7.76E-02	-7.39E-01	5.08E-02	1.03E-02	4.86E-02	-1.94E-02	-5.32E-02	1.87E-02
kl5_h	-6.39E-02	-3.78E-01	-4.08E-02	-7.84E-03	-2.40E-02	-5.75E-02	7.76E-02	1.00E+00	-1.36E-02	-2.51E-01	-6.50E-02	2.48E-02	-1.51E-01	-2.70E-02	-5.20E-02
ks5_h	9.43E-03	-3.38E-03	-1.86E-02	-2.55E-02	3.32E-01	8.13E-02	-7.39E-01	-1.36E-02	1.00E+00	-1.65E-02	4.25E-02	-1.18E-01	-1.13E-01	1.19E-01	-4.67E-02
kl7_h	7.91E-03	-1.34E-01	-1.65E-01	-6.40E-02	4.32E-02	-5.25E-02	5.08E-02	-2.51E-01	-1.65E-02	1.00E+00	-8.35E-02	8.72E-02	-1.80E-01	-9.03E-02	-2.48E-01
pl7_h	-5.78E-02	-2.68E-01	-1.82E-01	-8.99E-02	-6.51E-02	1.89E-02	1.03E-02	-6.50E-02	4.25E-02	-8.35E-02	1.00E+00	-6.64E-02	-3.79E-02	6.83E-02	-1.02E-01
kalk_top_h	-7.84E-02	-1.24E-01	1.81E-02	-1.32E-02	1.83E-03	-3.55E-02	4.86E-02	2.48E-02	-1.18E-01	8.72E-02	-6.64E-02	1.00E+00	-5.88E-03	-9.96E-01	-4.50E-03
kalk_top_v	5.53E-03	-1.26E-02	4.51E-02	1.67E-02	-7.08E-02	-1.21E-02	-1.94E-02	-1.51E-01	-1.13E-01	-1.80E-01	-3.79E-02	-5.88E-03	1.00E+00	-6.04E-03	-2.94E-01
kalk_h	8.33E-02	1.35E-01	-2.46E-02	2.19E-02	-1.68E-02	5.79E-03	-5.32E-02	-2.70E-02	1.19E-01	-9.03E-02	6.83E-02	-9.96E-01	-6.04E-03	1.00E+00	1.91E-02
kalk_v	-6.65E-02	-1.36E-01	-4.72E-02	-1.56E-02	-9.68E-03	4.60E-02	1.87E-02	-5.20E-02	-4.67E-02	-2.48E-01	-1.02E-01	-4.50E-03	-2.94E-01	1.91E-02	1.00E+00

Figure 45: Covariance matrix for the new cut out model based on the regional model.

The covariance matrix shows that no parameters are correlated. If the parameters were correlated the value calculated would be very close to one.

Distributed hydraulic conductivity for the chalk layers model.

In the DK model the chalk layers are modeled with a hydraulic conductivity that are heterogenic. This heterogeneity is interpolated from data that is collected during different pump tests to create a map with differentiated hydraulic conductivity.

The two maps are as followed:

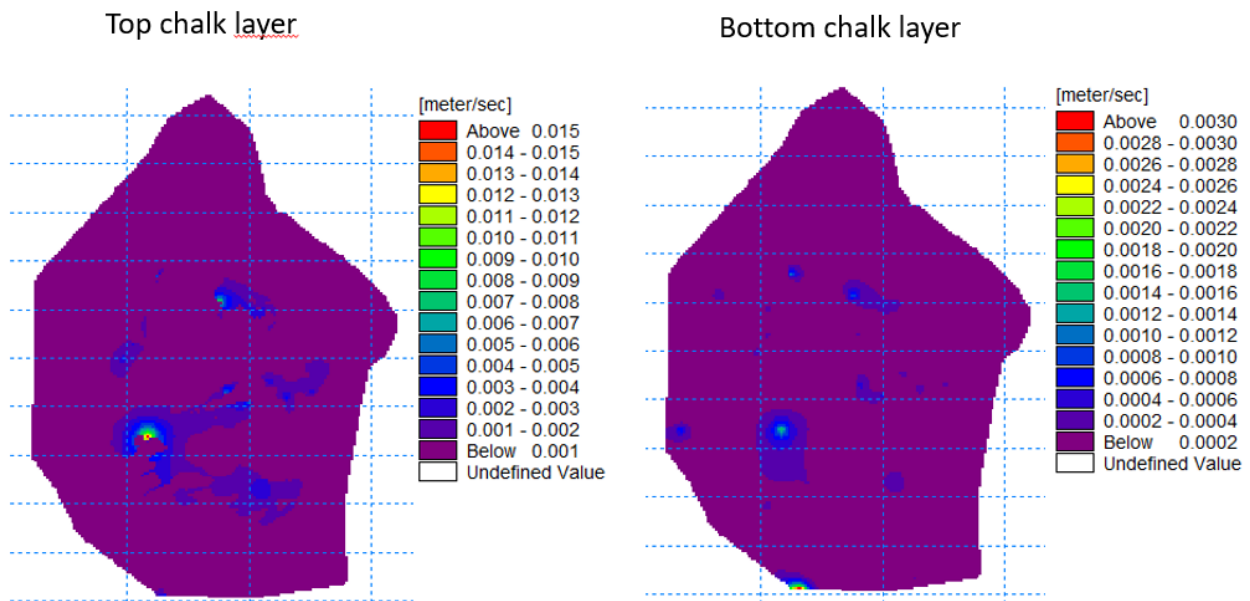


Figure 46: The distributed hydraulic conductivity for the two chalk layers.

For this model there are not changed anything in the geology from the original regional model. The only thing that is changed is the hydraulic conductivities in four quaternary layers. Which layers to change was made based on a sensitivity analysis made on the model. The most sensitive layers were then calibrated using MIKE Autocal were KL3, KS3, KL4 and KS4. The layers are two quaternary clay layers and two quaternary sand layers.

Mike Autocal used 450 runs distributed over nine loops.

Distributed hydraulic conductivity for the chalk layers model results.

The results of the auto calculation were found and is showed below together with the other hydraulic conductivities. The optimized parameters are shown in green. For KS4, KL3 and KL4 the vertical hydraulic conductivity was optimized, and KS was optimized at the horizontal

hydraulic conductivity. The anisotropy factor between the horizontal and vertical hydraulic conductivity were set to be 0.1.

	KL1	KS1	KL2	KS2	KL3	KS3	KL4	KS4	KL5	KS5	KL6	KS6	KL7	PL7	Kalk Top	Kalk
Horizontal K	6.10E-07	1.86E-05	6.10E-09	3.73E-05	1.26E-05	2.98E-05	5.56E-07	2.15E-04	2.80E-06	9.61E-05	1.52E-07	9.61E-05	1.52E-07	3.01E-07	x	x
Vertical K	6.10E-09	1.86E-06	6.10E-10	3.73E-06	1.26E-06	2.98E-06	5.56E-08	2.15E-05	2.80E-07	9.61E-06	1.52E-08	9.61E-06	1.52E-08	3.01E-08	x	x

Table 4: The table shows the hydraulic conductivities for the model. The green values are the optimized values obtained in the auto calculation. The unit is meters per second.

Comparing the calibrated parameters to table values gives: KL3 is optimized to be within table values for silty sand. KS3 is within table values silty sand and clean sand. KL4 is within the table values for glacial till. KS4 is within table values for clean sand. All table values are from “Groundwater science” (Fitts, 2013).

Before calculating the statistics for the model and collecting the results the model was runed one more time using the new optimized parameters and with a new hot start file. The hot start file used is the one from the final run of the parameter optimization. The date used for the hot start is 31st of December 2018.

Mean head.

To see how the model is on an average basis, the mean head where calculated. The mean head for the uppermost chalk layer is displayed in figure 47. This layer where chosen because the top of the chalk is nearly the same across the model except in Kolindsund.

The model has three hydraulic head mounts. These hydraulic head mounts follow the topography of the area. Kolindsund can be seen with the lowest hydraulic head in the area. Here the head is below the sea level.

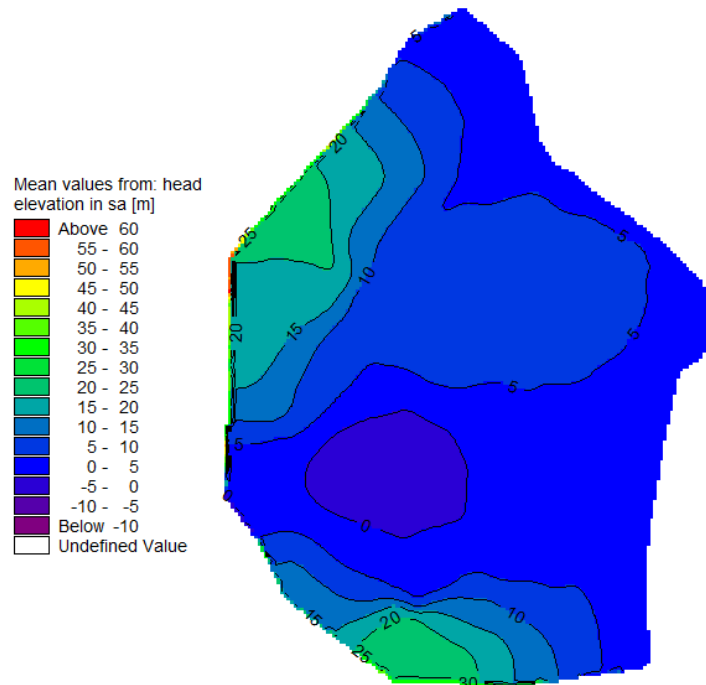


Figure 47: Shows the mean head for 2005 to 2018.

Well timelines

The fluctuation in hydraulic head is easier to view as a timeline.

Four different wells have been selected to show the different functions through the years. These wells are 71.483, 71.522, 71.757 and 71.770.



Figure 48: The maps show the position of the four wells that are chosen to show timelines for the hydraulic head.

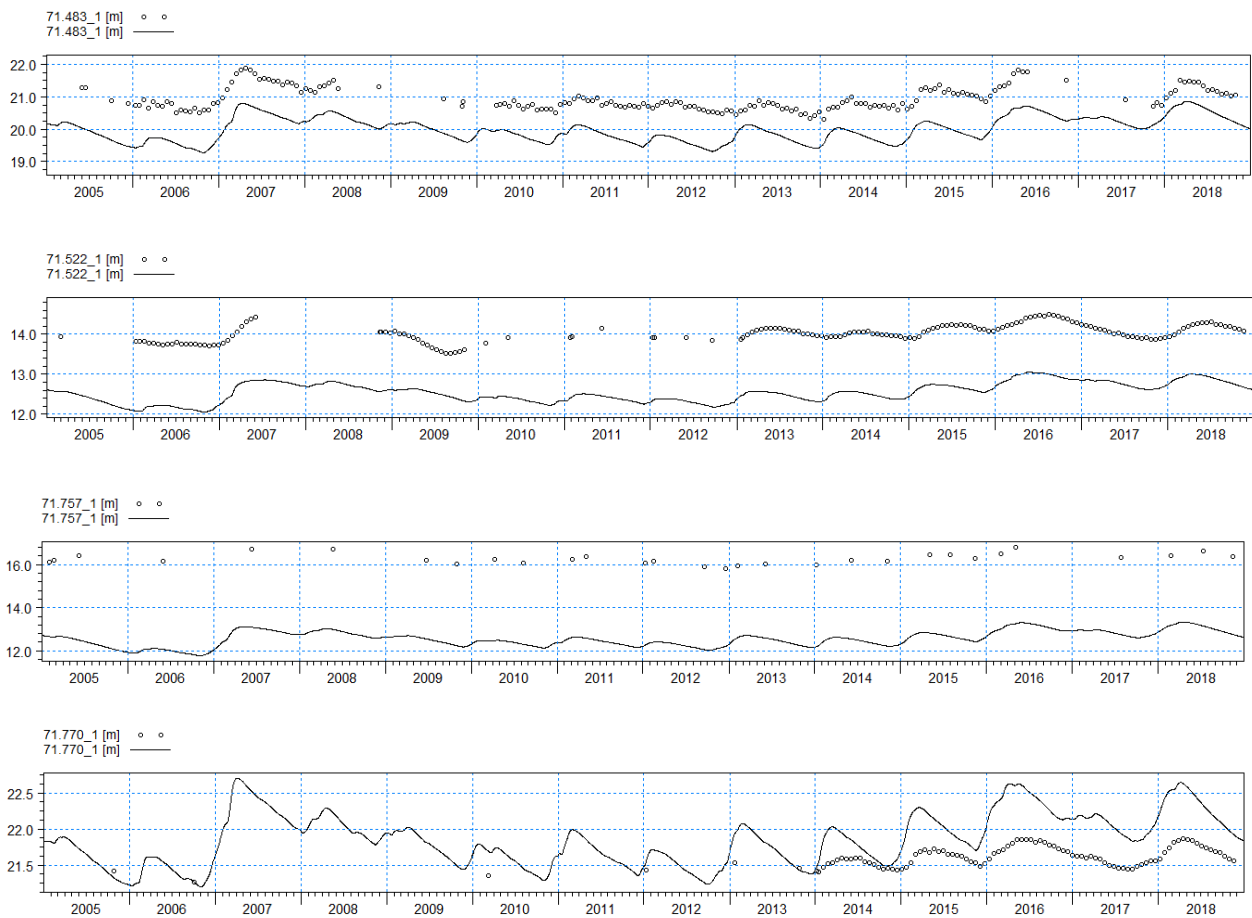


Figure 49: The four timelines show the hydraulic head in each well. The black line is the simulated head, and the dots are the observed hydraulic head.

71.483, 71.522 and 71.757 shows that the model simulates a lower head than what is observed over the years. The model does simulate the yearly fluctuations that are observed in the wells. Well 71.770 is simulated with a higher hydraulic head than what is observed. The model highest hydraulic head is simulated spikier than what is observed.

Enslev pumpstation

From the analysis of the spring at Enslev pumpstation it is known that the pump turns on at around a two-hour interval. In the summer there is a little more time between the pumping.

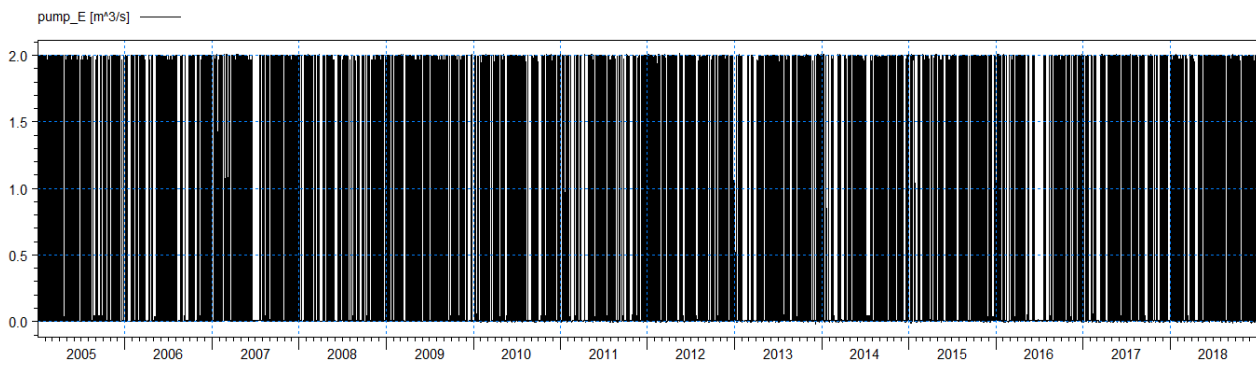


Figure 50: the volume of pumped water per second at Enslev pumpstation for the period 2005 to 2018.

Looking at the timeline it can be seen that the pumps at Enslev Pumpstation is at work for a large part of the simulated time. But there are times where the pumps do not pump for long periods of time.

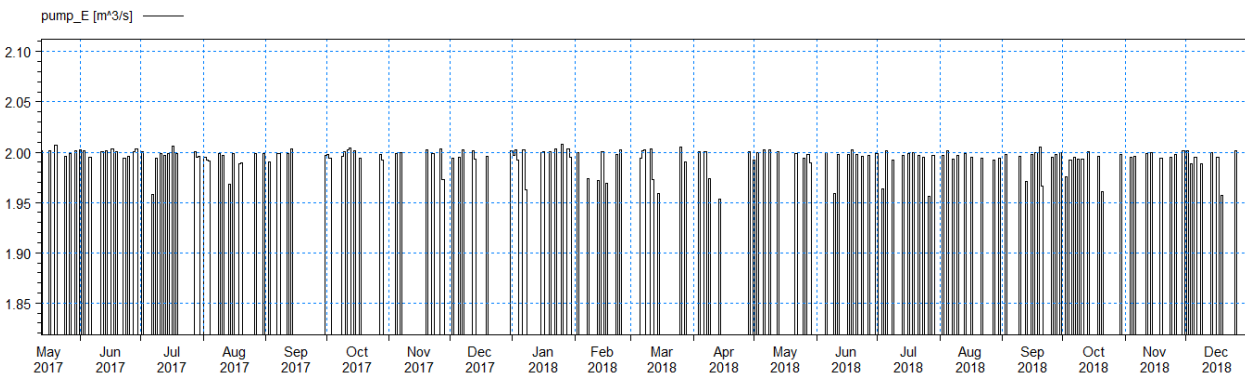


Figure 51: the volume of pumped water per second at Enslev pumpstation for the period May 2017 to December 2018.

Zooming in at the timeline to a monthly basis, it can be seen that the pump is at work for most of the time through the simulated period. But there are periods up to three weeks where the pump is not turned on. These shutoffs range from days to around three weeks.

Skærvad stream

The only stream in the area that is not cut in any point by the new boundaries are Skærvad stream. This stream is situated north of Kolindsund and connects to Nordkanal at Enslev.

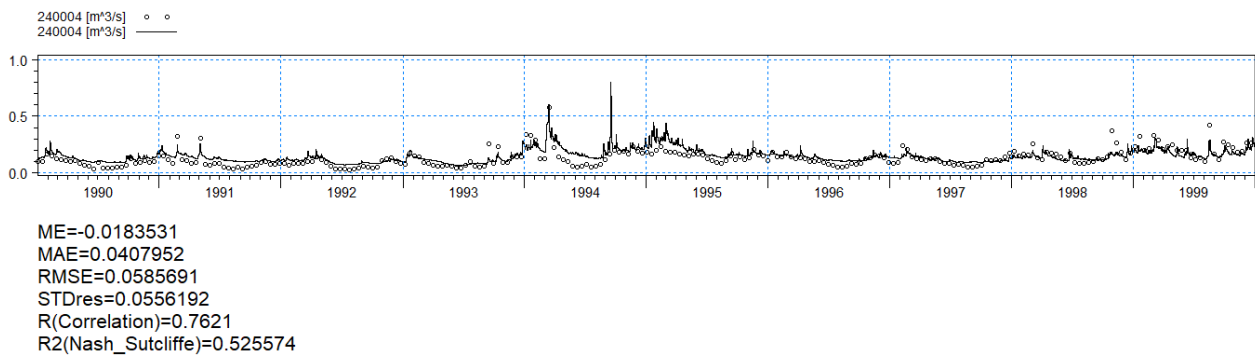


Figure 52: The discharge for Skærvad stream and the calculated statistics.

The plot of the discharge shows that the model is capable at simulating the discharge precisely. The model simulates a little too much discharge. But most of the time the model is nearly on point.

Mapped mean error.

To better view where the model has the biggest deviations three maps were produced using the mean error for the different observation wells. The error is calculated using $E = Obs - Sim$ and then calculating the mean of all these errors. This means if the model simulates too much water the mean error is negative. If the model simulates too little water the mean error is positive.

The Three different maps consist of a map that shows every mean error, one with the mean error for quaternary units and one map showing the mean error for the chalk units.

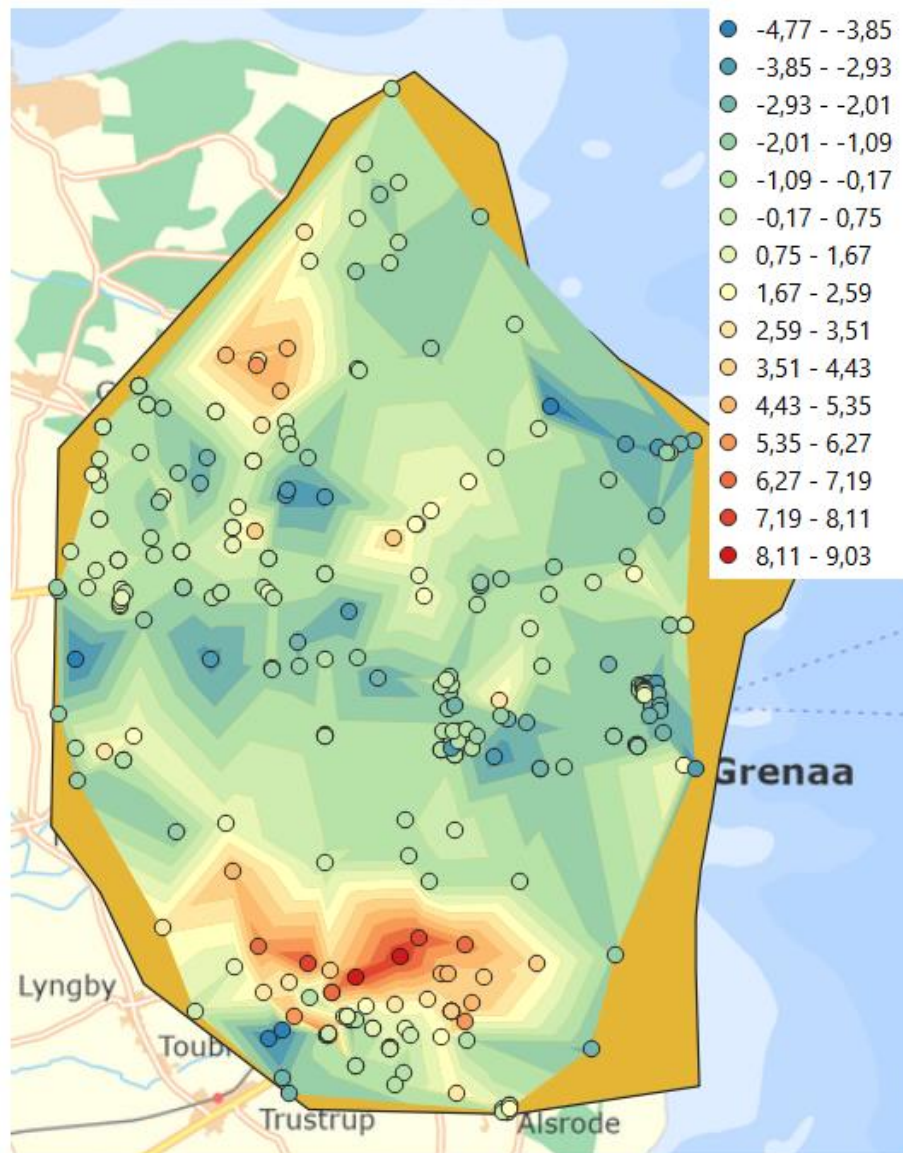


Figure 53: Map of the mean error for each well in the area. The map is for all the wells.

The map show that the model has problems with simulating the hydraulic head in the southern half of the model. Here there is a large area there has a lack of water. In the middle and eastern part of the model, the model generally simulates too much water. In the north western part of the model the model simulates too little water also. The differences between wells in the same areas are high. This can be due to complex geology that the model does not consider.

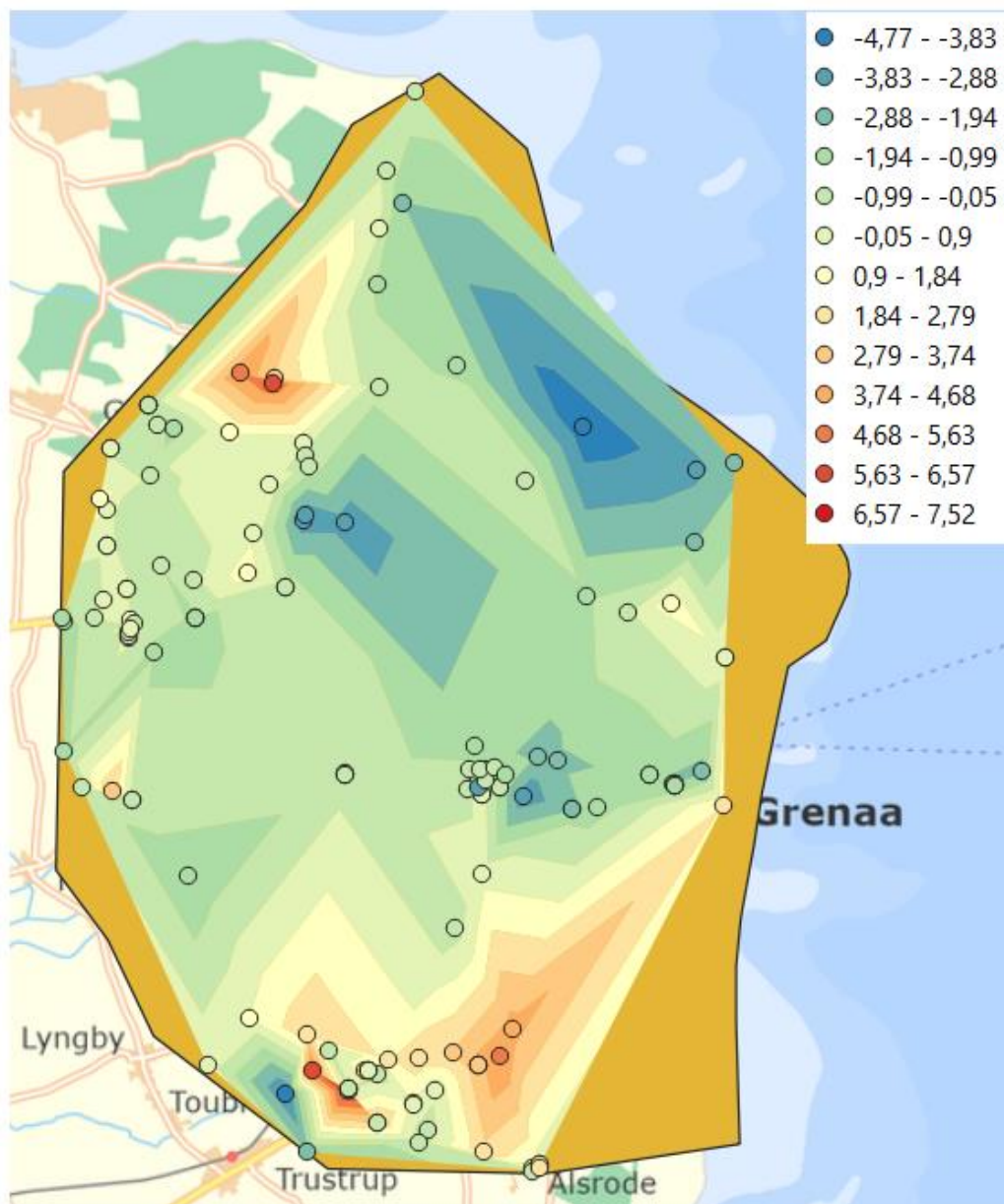


Figure 54: Map of the mean error for each well in the area. The map is for the wells screened in the quaternary layers.

For the quaternary layers, the model mean error also shows large differences. The southern part of the model simulates too little water. This is the same in the north western part of the model. Overall is the model quite capable to simulate the hydraulic head in most of the quaternary units. But these layers are thin in most of the area. The areas to the south and north west also contains thick quaternary layers. These areas also contains many small lenses and local existing layers that can create perched aquifers.

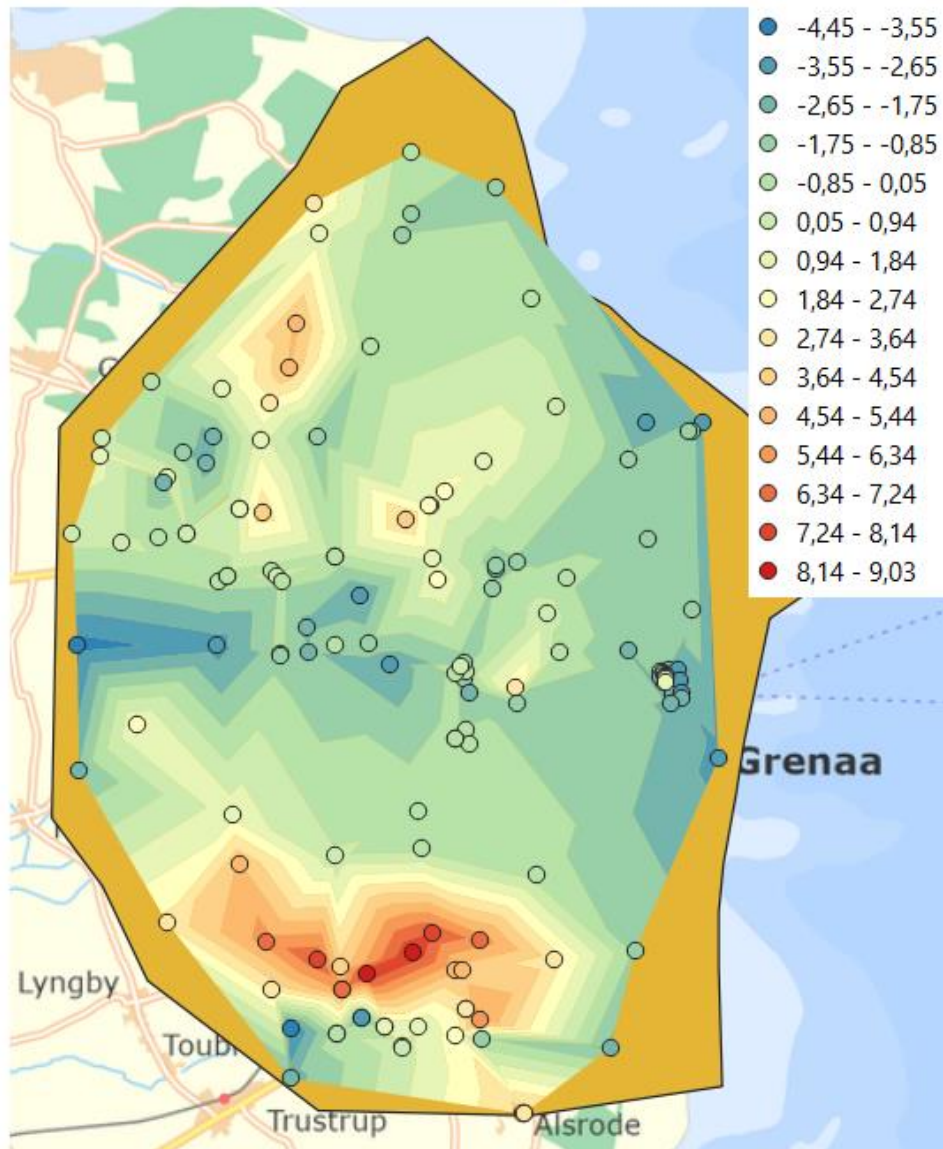


Figure 55: Map of the mean error for each well in the area. The map is for the wells screened in the chalk layers.

For the Chalk layers the mean error calculated for each well shows great differences throughout the area. The southern part of the model simulates too little water. This is the same in the north western part of the model. The middle and north western part of the model generally simulates too much water. Locally there are great differences in the mean error.

Statistic

To better understand the overall fit of the model the root mean square errors were collected. The method to show the RMSE values are box and whisker plot.

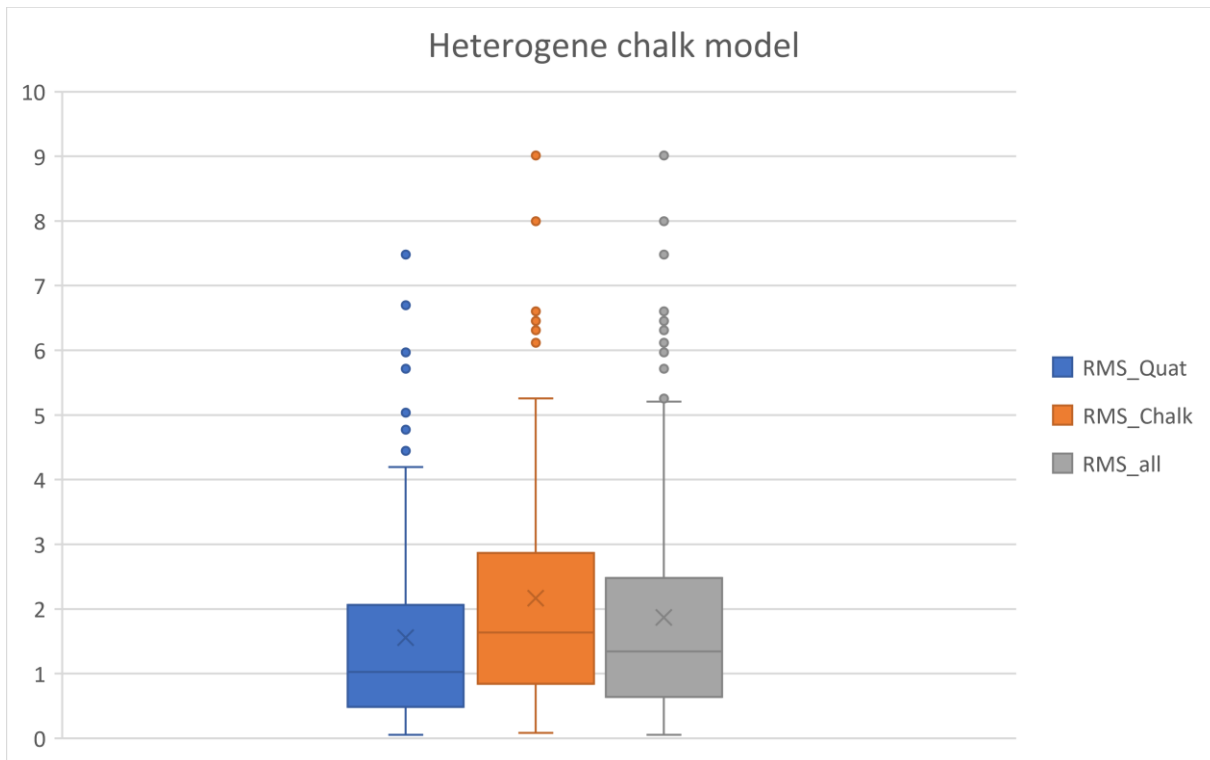


Figure 56: Box and whisker plot with the RMSE values for the model. The values are split into quaternary layers, chalk layers and all the layers.

The box and whisker plot shows the first quantile (line with a bar end), second quantile (lowest part of the box), the median (the line in the box), the average (the x), the third quantile (the upper part of the box), the fourth quantile (line with a bar end) and the outliers defined by the third quantile + 1.5 * the inter quantile range.

This shows that the model is best at simulating the hydraulic head in the quaternary layers. The quaternary layers have a wide range of outliers.

The RMSE for the chalk layers are higher in every quantile compared to the quaternary layers.

The outliers of the chalk layers are also higher than what is simulated for the quaternary layers.

Uniform dk model

To better compare the new geological model the model with heterogeneity chalk were made homogenic in every layer. This were also done to see if the heterogeneity model were better performing than a homogenic model.

The change to the model is the hydraulic conductivities in four quaternary layers and the two chalk layers. Which of the quaternary layers that were chosen to change was made based on a sensitivity analysis made on the model. The most sensitive layers were then calibrated using

MIKE Autocal were KL3, KS3, KL4 and KS4. The layers are two quaternary clay layers and two quaternary sand layers.

Uniform dk model results

The results of the auto calculation were found and is showed below together with the other hydraulic conductivities. The optimized parameters are shown in green. For KS4, KL3 and KL4 the vertical hydraulic conductivity was optimized, and KS was optimized at the horizontal hydraulic conductivity. The anisotropy factor between the horizontal and vertical hydraulic conductivity were set to be 0.1. the parameter optimization was set to optimize both the horizontal and vertical conductivity of the two chalk layers.

	KL1	KS1	KL2	KS2	KL3	KS3	KL4	KS4	KL5	KS5	KL6	KS6	KL7	PL7	Kalk Top	Kalk
Horizontal K	6.10E-07	1.86E-05	6.10E-09	3.73E-05	9.08E-07	1.52E-05	3.32E-06	1.15E-04	2.80E-06	9.61E-05	1.52E-07	9.61E-05	1.52E-07	3.01E-07	3.63E-05	4.32E-05
Vertical K	6.10E-09	1.86E-06	6.10E-10	3.73E-06	9.08E-08	1.52E-06	3.32E-07	1.15E-05	2.80E-07	9.61E-06	1.52E-08	9.61E-06	1.52E-08	3.01E-08	1.88E-03	1.26E-03

Table 5 The table shows the hydraulic conductivities for the model. The green values are the optimized values obtained in the auto calculation. The unit is meters per second.

Comparing the calibrated parameters to table values gives: KL3 is optimized to be within table values for silt and glacial till. KS3 is within table values silty sand. KL4 is within the table values for silty sand and silt. KS4 is within table values for clean sand. Chalk top (kalk top) is within the table values for limestone and fractured basalt. Note that the hydraulic conductivity for the vertical is Much higher than the horizontal. It is within the range for gravel. Chalk (kalk) is within the table values for limestone, fractured basalt, and glacial till. Note that the hydraulic conductivity for the vertical is Much higher than the horizontal. It is within the range for gravel. All table values are from “Groundwater science (Fitts, 2013).

Mean head.

To see how the model is on an average basis, the mean head where calculated. The mean head for the uppermost chalk layer is displayed in figure 57. This layer where chosen because the top of the chalk is nearly the same across the model except in Kolindsund.

The model has three hydraulic head mounts. These hydraulic head mounts follow the topography of the area. Kolindsund can be seen with the lowest hydraulic head in the area. Here the head is below the sea level.

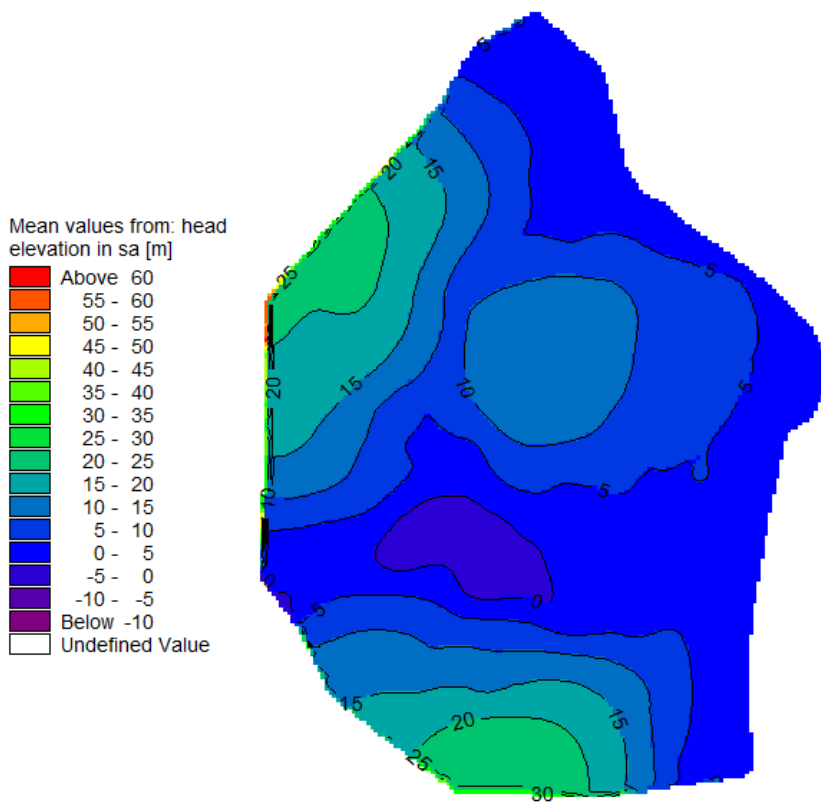


Figure 57 Shows the mean head for 2005 to 2018.

Well timelines

The fluctuation in hydraulic head is easier to view as a timeline.

Four different wells have been selected to show the different functions through the years. These wells are 71.483, 71.522, 71.757 and 71.770.



Figure 58 The maps show the position of the four wells that are chosen to show timelines for the hydraulic head.

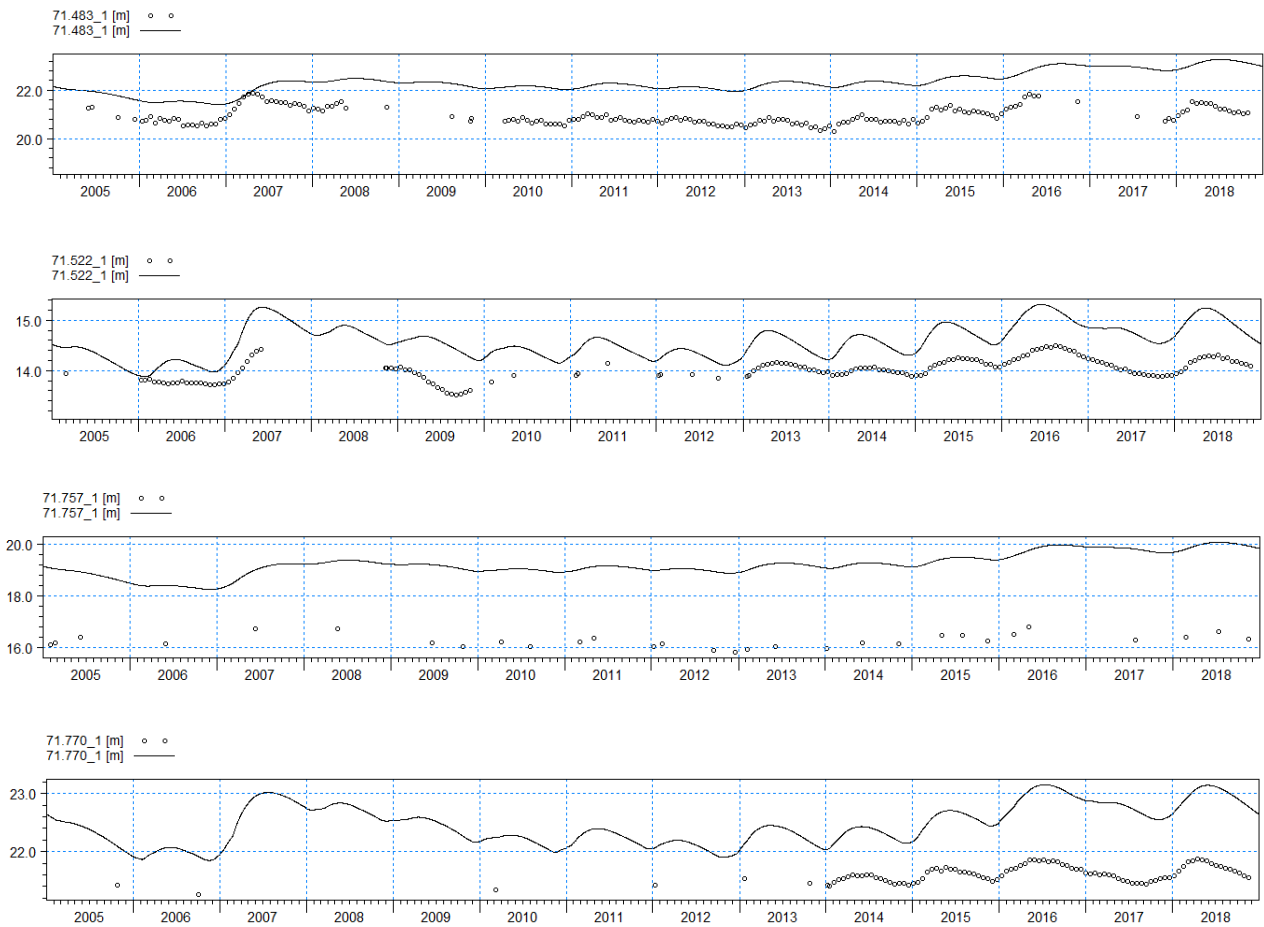


Figure 59 The four timelines show the hydraulic head in each well. The black line is the simulated head, and the dots are the observed hydraulic head.

For all four wells the model simulates a higher hydraulic head than the one that was observed. The model does simulate the yearly fluctuations that are observed in the wells.

Enslev pumpstation

From the analysis of the spring at Enslev pumpstation it is known that the pump turns on at around a two-hour interval. In the summer there is a little more time between the pumping.

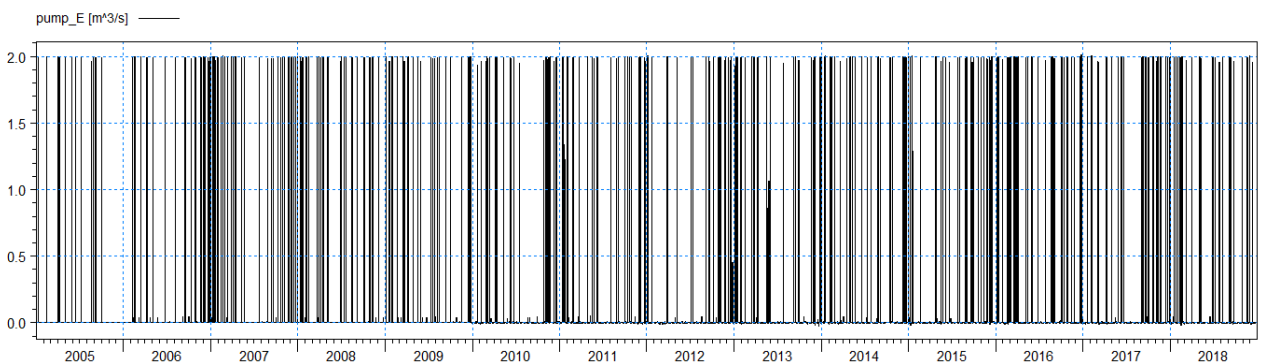


Figure 60 the volume of pumped water per second at Enslev pumpstation for the period may 2017 to December 2018.

Looking at the chart it can be seen that there is large gaps in the timeline where the pump doesn't pump any water. And also, that there are long time between the pumping each month.

Skærvad stream

The only stream in the area that is not cut in any point by the new boundaries are Skærvad stream. This stream is situated north of Kolindsund and connects to Nordkanal at Enslev.

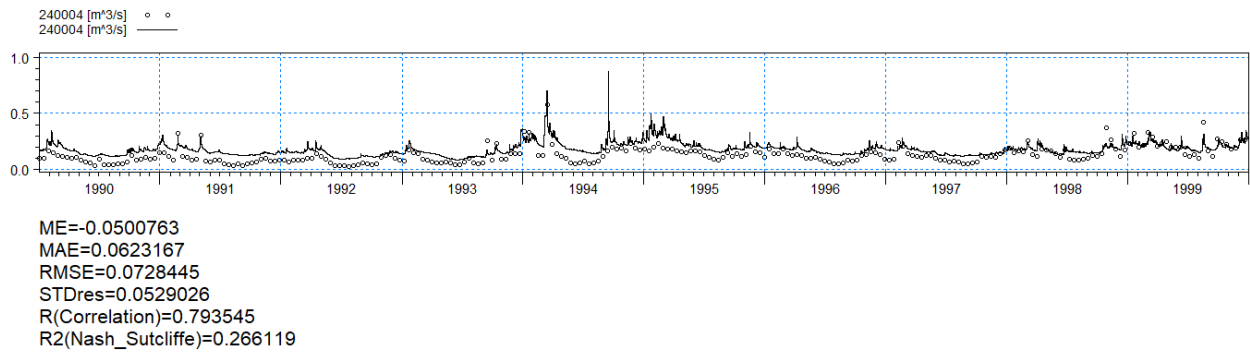


Figure 61 The discharge for Skærvad stream and the calculated statistics.

The plot of the discharge shows that the model is capable at simulating the discharge precisely. The model simulates a little too much discharge.

Map statistic

To better view where the model has the biggest deviations three maps were produced using the mean error for the different observation wells. The error is calculated using $E = Obs - Sim$. This means if the model simulates too much water the mean error is negative. If the model simulates too little water the mean error is positive.

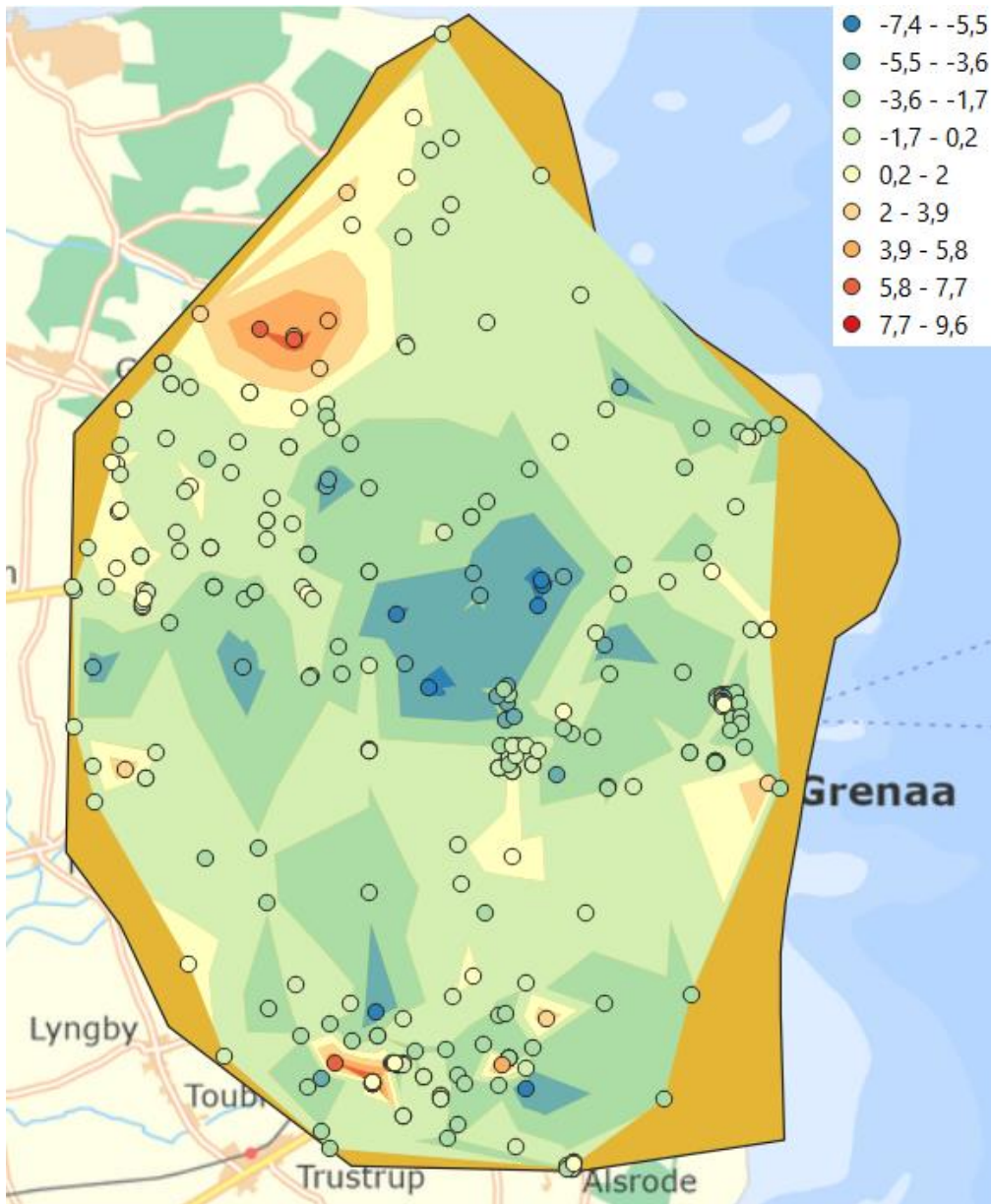


Figure 62 Map of the mean error for each well in the area. The map is for all the wells.

The map shows that the model simulates too high of a hydraulic head in most of the area for all the different layers. In the north western part of the model is there an area that the model simulates a head lower than the one that was observed.

The differences between wells in the same areas are high. This can be due to complex geology that the model does not consider. The differences between wells near each other can also be because of bad measurements or heterogeneity geology.

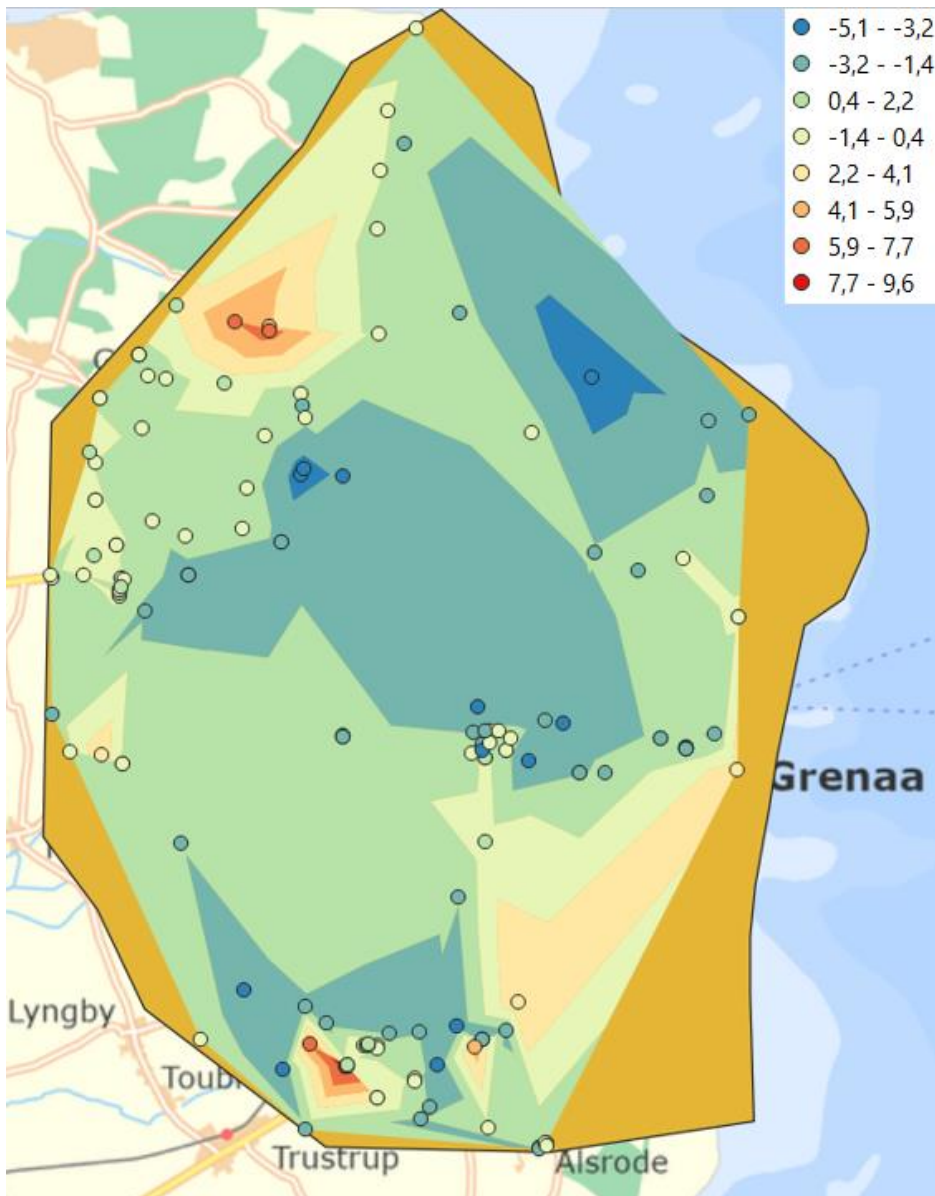


Figure 63 Map of the mean error for each well in the area. The map is for the wells screened in the quaternary layers.

For the quaternary layers, the model does also large differences in the mean error. The model does simulate too low hydraulic head overall. But there are smaller area and wells that simulates too high of a hydraulic head. Within a small area there are large differences in the hydraulic head. This can be due to complex geology that the model does not consider that there is a perched aquifer in the real world. The differences between wells near each other can also be because of bad measurements or heterogenic geology.

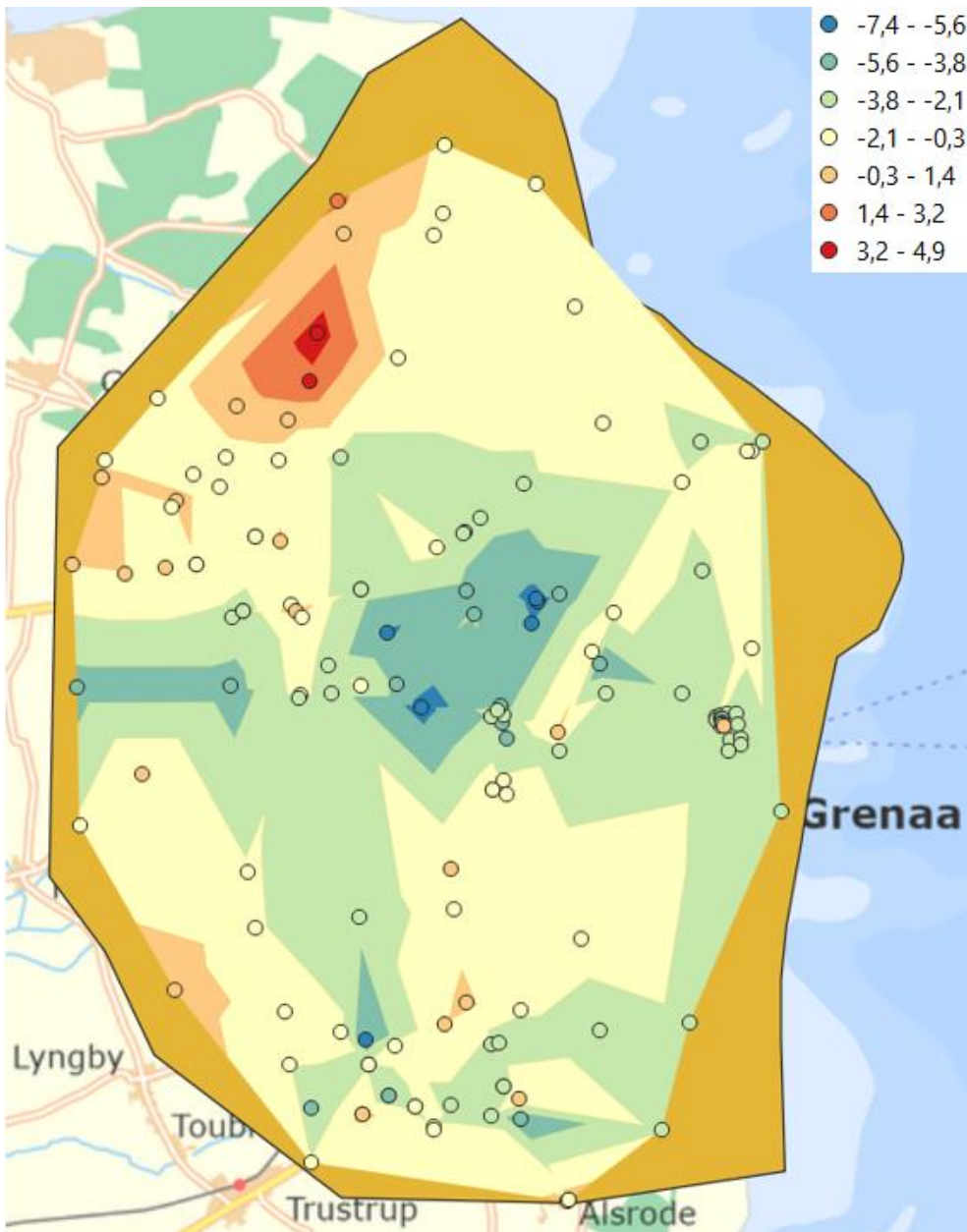


Figure 64 Map of the mean error for each well in the area. The map is for the wells screened in the chalk layers.

For the chalk layers does the model for most areas simulate a head that are too high. In most area is this error fluctuates from a couple of centimeters up to two meters. The middle part of the area is mostly simulated with a head at least five meters too high. In the north western part of the model the well simulates too low of a hydraulic head.

Statistic

To better understand the overall fit of the model the root mean square errors were collected. The method to show the RMSE values are box and whisker plot.

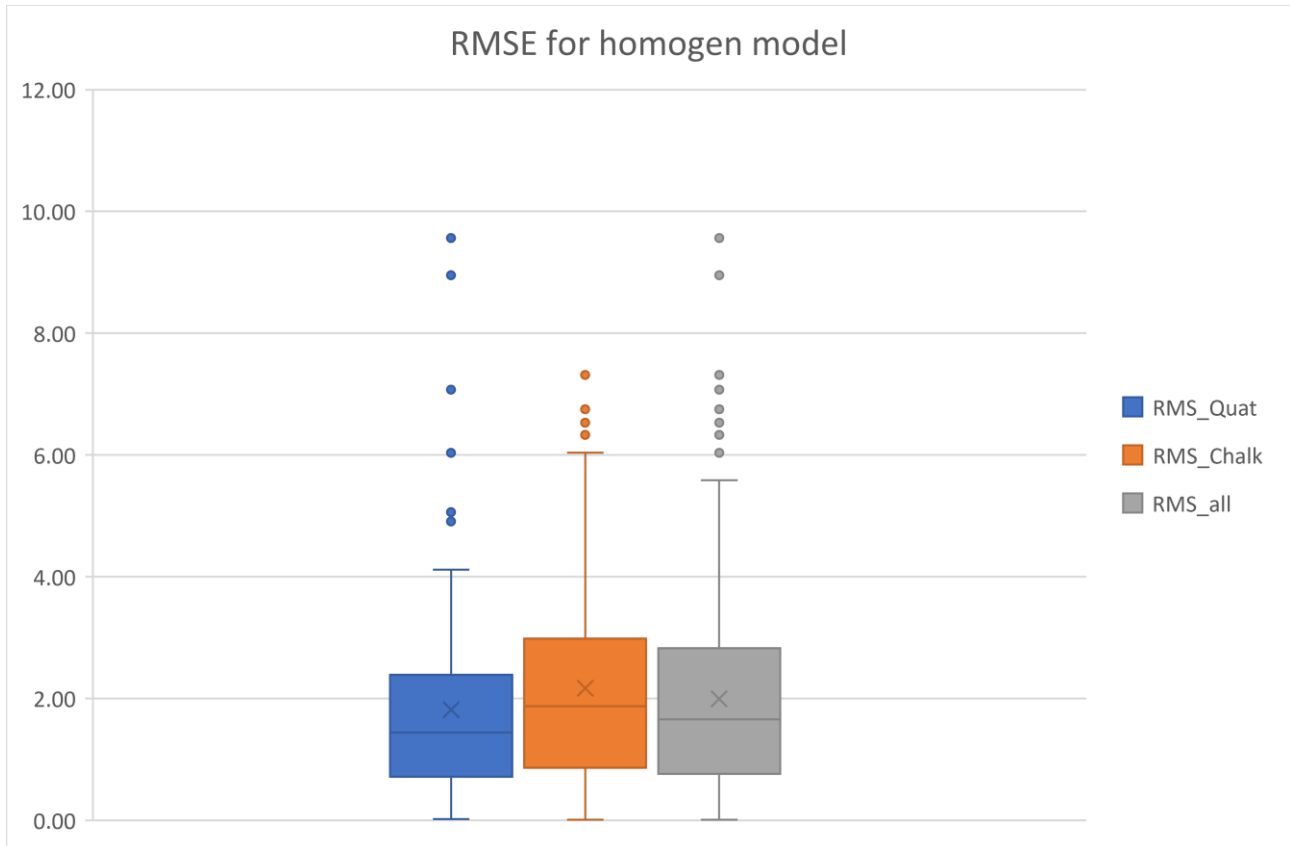


Figure 65 Box and whisker plot with the RMSE values for the model. The values are split into quaternary layers, chalk layers and all the layers.

The box and whisker plot shows the first quartile (line with a bar end), second quartile (lowest part of the box), the median (the line in the box), the average (the x), the third quartile (the upper part of the box), the fourth quartile (line with a bar end) and the outliers defined by the third quartile + 1.5 * the inter quartile range.

This shows that the model is best at simulating the hydraulic head in the quaternary layers. But the quaternary layers have the highest outliers.

The chalk layers have a wider spread. But the outliers lie close to the fourth quartile.

New geological model

In this model the new geological model based on TEM data were incorporated into MIKE SHE. This were done because of the field results obtained by WSP Denmark. This work included tTEM that led to the drilling of a knew well with a high capacity located in chalk with a relatively high resistivity. The idea was that the second chalk layer was important to conducting the groundwater flow in the area.

This model is the same as the two other models for all parameters except for the geological model and the hydrological parameters for the units in the model. The unsaturated zone,

climate, river and timesteps are the same. The evolution period was 1st of January 2010 to 31st of December 2018.

Sensitivity analysis

To get a better understanding of which parameters the model is most sensitive to, a sensitive analysis was made using the MIKE tool autocal. Since the only thing changed in the models was the geological units, the only thing analyzed in the sensitivity analysis was the hydraulic conductivity. This was done for both the vertical hydraulic conductivity and the horizontal hydraulic conductivity.

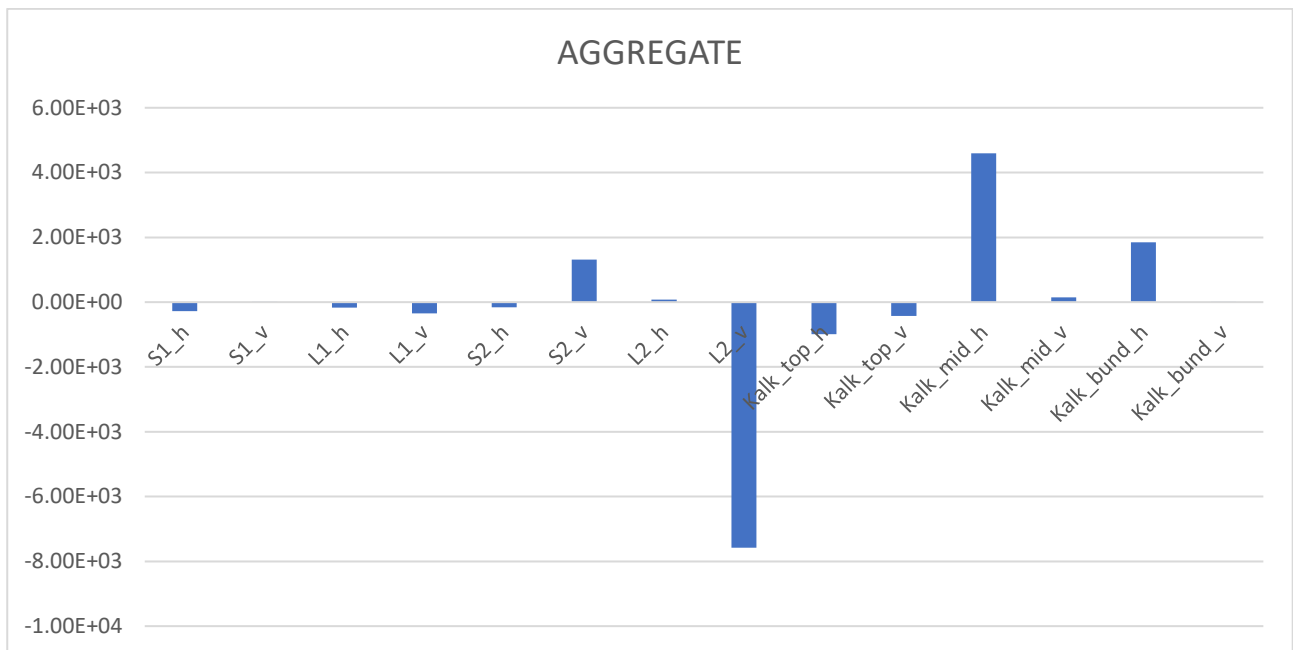


Figure 66 The sensitivity analysis for the model cut out based on the regional model.

The sensitivity analysis shows that the two upper quaternary layers is not sensitive to changes to the hydraulic conductivity in both the horizontal and vertical direction.

S2 is sensitive to changes in the vertical hydraulic conductivity. This is the same for C2. C2 vertical is also one of the most sensitive parameters in the model.

For the chalk units is it the horizontal hydraulic conductivity that is the most sensitive parameters. Of the three it is the mid chalk horizontal that is the most sensitive and is the most sensitive for the whole model.

Correlation matrix

To see if any of the layers are correlated a correlation matrix were calculated. If any of the layers has a correlation value that is close to one, they cannot be separated from each other.

If they had a correlation value close to one, they would be taken out of the calibration and a table value for the material would be used.

	S1_h	S1_v	L1_h	L1_v	S2_h	S2_v	L2_h	L2_v	Kalk_top_h	Kalk_top_v	Kalk_mid_h	Kalk_mid_v	Kalk_bund_h	Kalk_bund_v
S1_h	1.00E+00	6.04E-02	-1.74E-01	3.84E-02	8.66E-02	4.00E-01	-1.13E-03	-9.02E-03	-3.92E-02	8.41E-03	7.29E-02	-2.86E-02	9.60E-02	-1.10E-02
S1_v	6.04E-02	1.00E+00	-3.14E-01	-3.85E-01	6.98E-02	-1.49E-01	-8.22E-02	1.87E-01	-4.28E-02	-8.96E-02	1.33E-01	-6.98E-02	-1.11E-01	6.33E-02
L1_h	-1.74E-01	-3.14E-01	1.00E+00	5.26E-01	-9.48E-02	-3.29E-02	4.92E-02	-9.71E-02	-3.77E-02	5.16E-02	-1.05E-01	8.92E-02	1.56E-01	-2.83E-02
L1_v	3.84E-02	-3.85E-01	5.26E-01	1.00E+00	7.53E-03	3.71E-01	-1.52E-02	1.80E-01	1.51E-02	3.05E-02	-8.20E-02	1.93E-01	3.38E-01	-3.58E-02
S2_h	8.66E-02	6.98E-02	-9.48E-02	7.53E-03	1.00E+00	1.35E-01	-7.81E-01	-3.16E-01	3.13E-02	2.36E-03	1.05E-02	2.20E-02	1.47E-02	9.97E-03
S2_v	4.00E-01	-1.49E-01	-3.29E-02	3.71E-01	1.35E-01	1.00E+00	-1.59E-01	6.67E-02	1.56E-01	9.80E-02	2.70E-01	-4.05E-02	2.02E-02	7.78E-02
L2_h	-1.13E-03	-8.22E-02	4.92E-02	-1.52E-02	-7.81E-01	-1.59E-01	1.00E+00	2.83E-01	-4.07E-02	-1.27E-02	-5.66E-02	6.41E-03	1.85E-02	-2.27E-02
L2_v	-9.02E-03	1.87E-01	-9.71E-02	1.80E-01	-3.16E-01	6.67E-02	2.83E-01	1.00E+00	1.16E-03	-9.44E-02	-3.81E-02	5.57E-02	1.26E-01	-9.01E-02
Kalk_top_h	-3.92E-02	-4.28E-02	-3.77E-02	1.51E-02	3.13E-02	1.56E-01	-4.07E-02	1.16E-03	1.00E+00	-6.83E-01	-3.40E-01	3.36E-01	-2.63E-01	-1.43E-01
Kalk_top_v	8.41E-03	-8.96E-02	5.16E-02	3.05E-02	2.36E-03	9.80E-02	-1.27E-02	-9.44E-02	-6.83E-01	1.00E+00	3.70E-01	-5.39E-01	1.08E-01	5.81E-02
Kalk_mid_h	7.29E-02	1.33E-01	-1.05E-01	-8.20E-02	1.05E-02	2.70E-01	-5.66E-02	-3.81E-02	-3.40E-01	3.70E-01	1.00E+00	-4.06E-01	-6.54E-01	4.26E-01
Kalk_mid_v	-2.86E-02	-6.98E-02	8.92E-02	1.93E-01	2.20E-02	-4.05E-02	6.41E-03	5.57E-02	3.36E-01	-5.39E-01	-4.06E-01	1.00E+00	8.00E-03	-9.86E-02
Kalk_bund_h	9.60E-02	-1.11E-01	1.56E-01	3.38E-01	1.47E-02	2.02E-02	1.85E-02	1.26E-01	-2.63E-01	1.08E-01	-6.54E-01	8.00E-03	1.00E+00	-4.89E-01
Kalk_bund_v	-1.10E-02	6.33E-02	-2.83E-02	-3.58E-02	9.97E-03	7.78E-02	-2.27E-02	-9.01E-02	-1.43E-01	5.81E-02	4.26E-01	-9.86E-02	-4.89E-01	1.00E+00

Table 6 Covariance matrix for the new cut out model based on the regional model.

The correlation matrix shows that the different parameters are not correlated. This means that a calibration of all parameters is possible.

New geological model results

The results of the auto calculation were found and is showed below (see table 7). The optimized parameters are shown in green. The quaternary layers were optimized at the horizontal hydraulic conductivity. The anisotropy factor between the horizontal and vertical hydraulic conductivity were set to be 0.1. The two upper chalk layers were optimized for both the horizontal and vertical hydraulic conductivity. The bottom chalk was optimized with an anisotropy factor set at 0.1 between the horizontal and vertical hydraulic conductivity.

	S1	L1	S2	L2	Chalk Top	Chalk Mid	Chalk bottom
Horizontal K	3.77E-06	1.25E-05	4.77E-05	6.83E-07	9.53E-05	2.38E-06	5.08E-06
Vertical K	3.77E-07	1.25E-06	4.77E-06	6.83E-08	4.45E-05	2.38E-07	5.08E-07

Table 7 The table shows the hydraulic conductivities for the model. The green values are the optimized values obtained in the autocalculation. The unit is meters per second.

Comparing the calibrated parameters to table values gives: S1 is optimized to be within table values fir silt and glacial till. This is lower than the table values for sand. L1 is within table values for silt and silty sand which is higher than what would be expected for clay. S2 is within the table values for silty sand and clean sand. L2 is within table values for glacial till. Chalk top is within the table values for limestone and fractured basalt. Note that the hydraulic conductivity for the vertical is only half the conductivity than that for the horizontal. Chalk mid is within the table values for limestone, fractured basalt, and glacial till. Chalk bottom is within the table

values for limestone, fractured basalt, and glacial till. All table values are from “Groundwater science (Fitts, 2013). (Korkman, 1980)

Before calculating the statistics for the model and collecting the results the model was runed one more time using the new optimized parameters and with a new hot start file. The hot start file used is the one from the final run of the parameter optimization. The date used for the hot start is 31st of December 2018.

Mean hydraulic head.

To see how the model is on an average basis, the mean head where calculated. The mean head for the uppermost chalk layer is displayed in figure 67. This layer where chosen because the top of the chalk is nearly the same across the model except in Kolindsund.

The model has three hydraulic head mounts. These hydraulic head mounts follow the topography of the area. Kolindsund can be seen with the lowest hydraulic head in the area. Here the head is below the sea level.

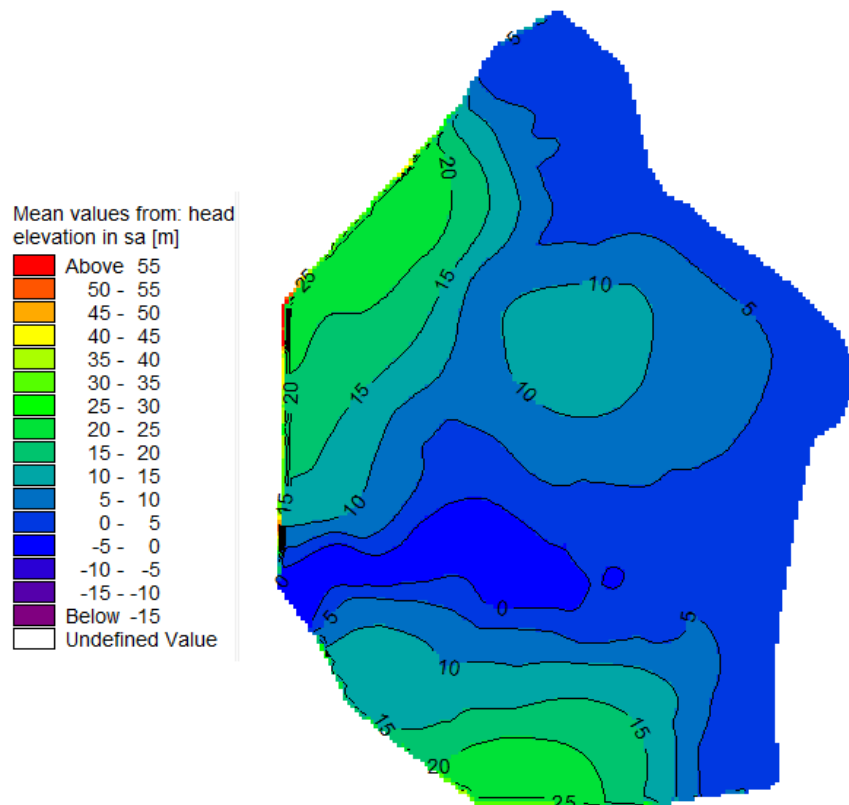


Figure 67 Shows the mean head for 2005 to 2018.

Well timelines

The fluctuation in hydraulic head is easier to view as a timeline.

Four different wells have been selected to show the different functions through the years. These wells are 71.483, 71.522, 71.757 and 71.770.



Figure 68 The maps show the position of the four wells that are chosen to show timelines for the hydraulic head.

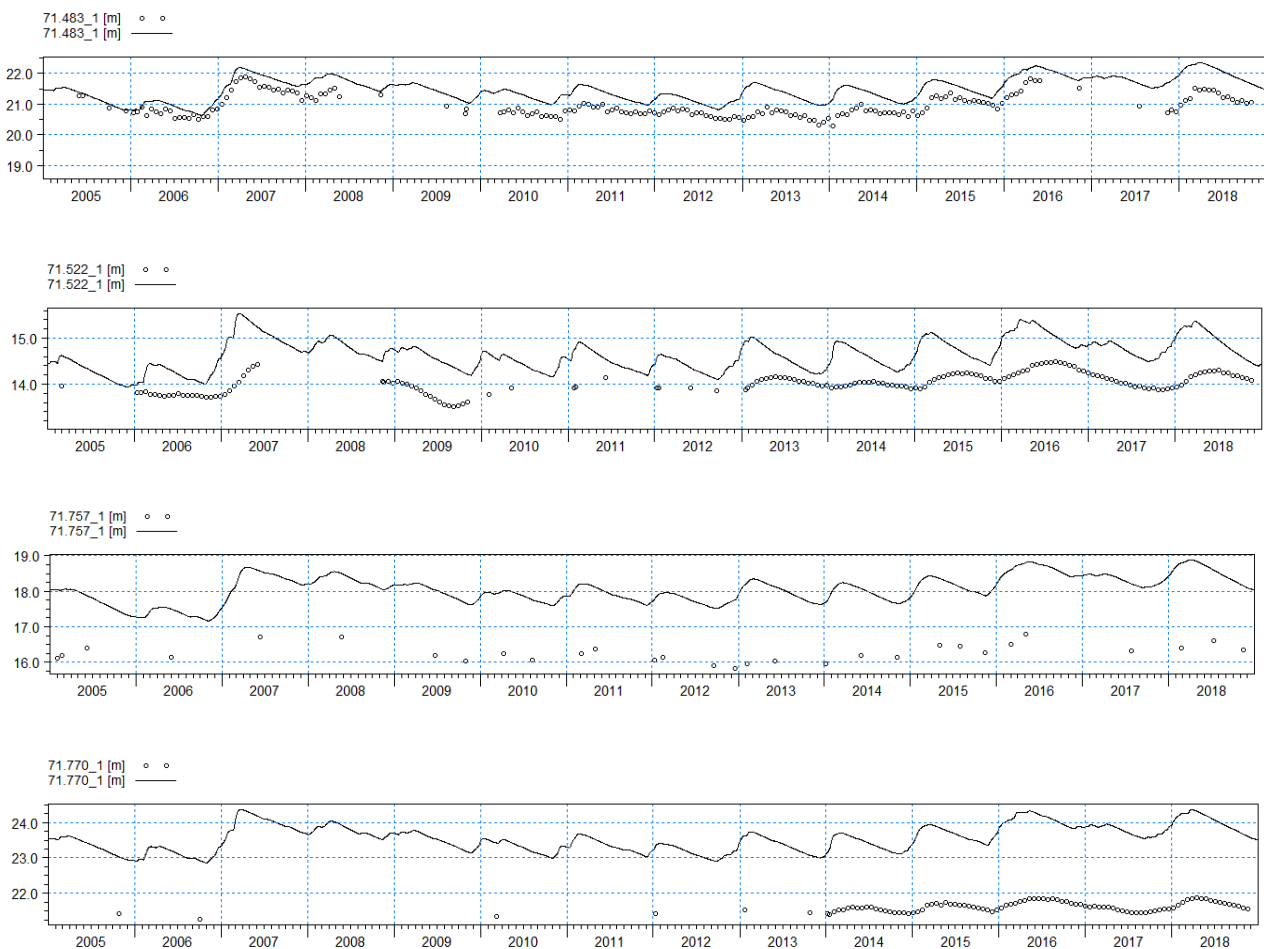


Figure 69 The four timelines show the hydraulic head in each well. The black line is the simulated head, and the dots are the observed hydraulic head.

The four timelines shows that the model in general simulates a too high of a hydraulic head. For well 71.483 the simulation hits the observed hydraulic head close to perfect.

For 71.522 the model is also close to the observed hydraulic head. The model does simulate the head too low. The time for the highest head is also simulated to be too early and spikier than

what is observed.

71.757 and 71.770 The model simulates around 2 meters too high of a hydraulic head. The time for the highest head is also simulated to be too early and spikier than what is observed.

Enslev Pumpstation

From the analysis of the spring at Enslev pumpstation it is known that the pump turns on at around a two-hour interval. In the summer there is a little more time between the pumping.

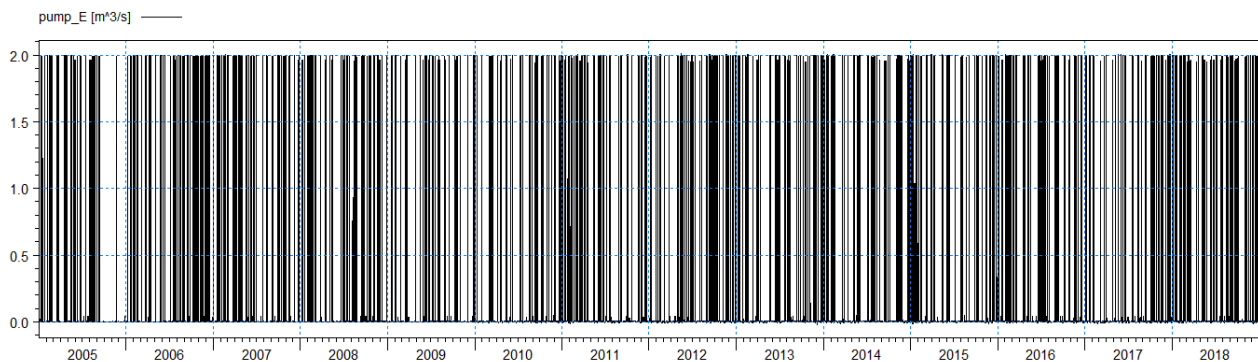


Figure 70 the volume of pumped water per second at Enslev pumpstation for the period May 2017 to December 2018.

The plot shows when the pump is turned on. Many times, through the year. But there are parts of the year where the pumps at Enslev pumpstation where they are completely shut off.

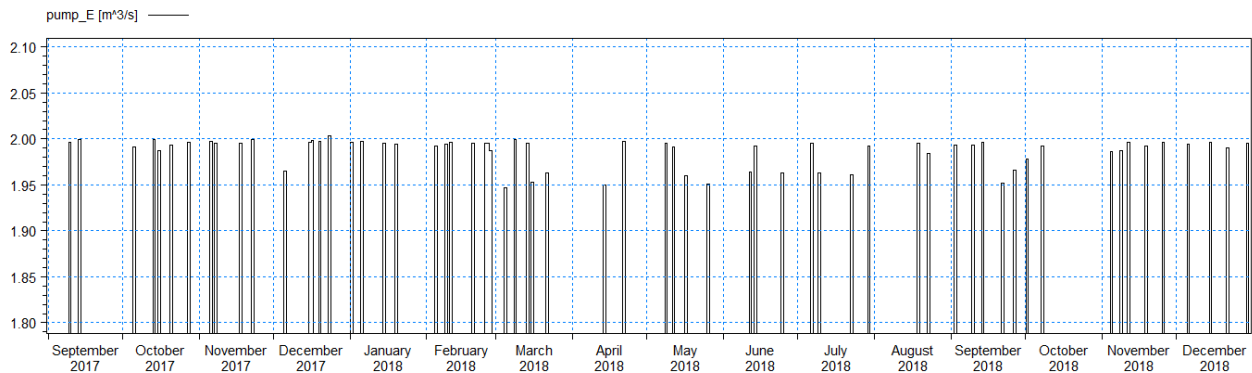


Figure 71 the volume of pumped water per second at Enslev pumpstation for the period May 2017 to December 2018.

Zoomed in to look at a monthly basis, it can be seen that the pumps only pump water for a short period of time a couple of times a month.

Skærvad stream

The only stream in the area that is not cut in any point by the new boundaries are Skærvad stream. This stream is situated north of Kolindsund and connects to Nordkanal at Enslev.

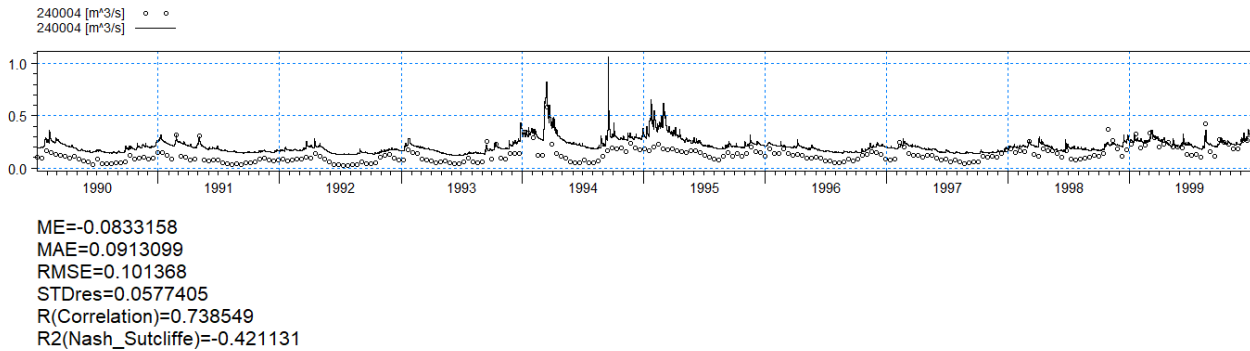


Figure 72 The discharge for Skærvad stream and the calculated statistics.

The plot of the discharge shows that the model is capable at simulating the discharge precisely. The model simulates a little too much discharge.

Map statistic

To better view where the model has the biggest deviations three maps were produced using the mean error for the different observation wells. The mean error is calculated using $ME = Obs - Sim$. This means if the model simulates too much water the mean error is negative. If the model simulates too little water the mean error is positive.

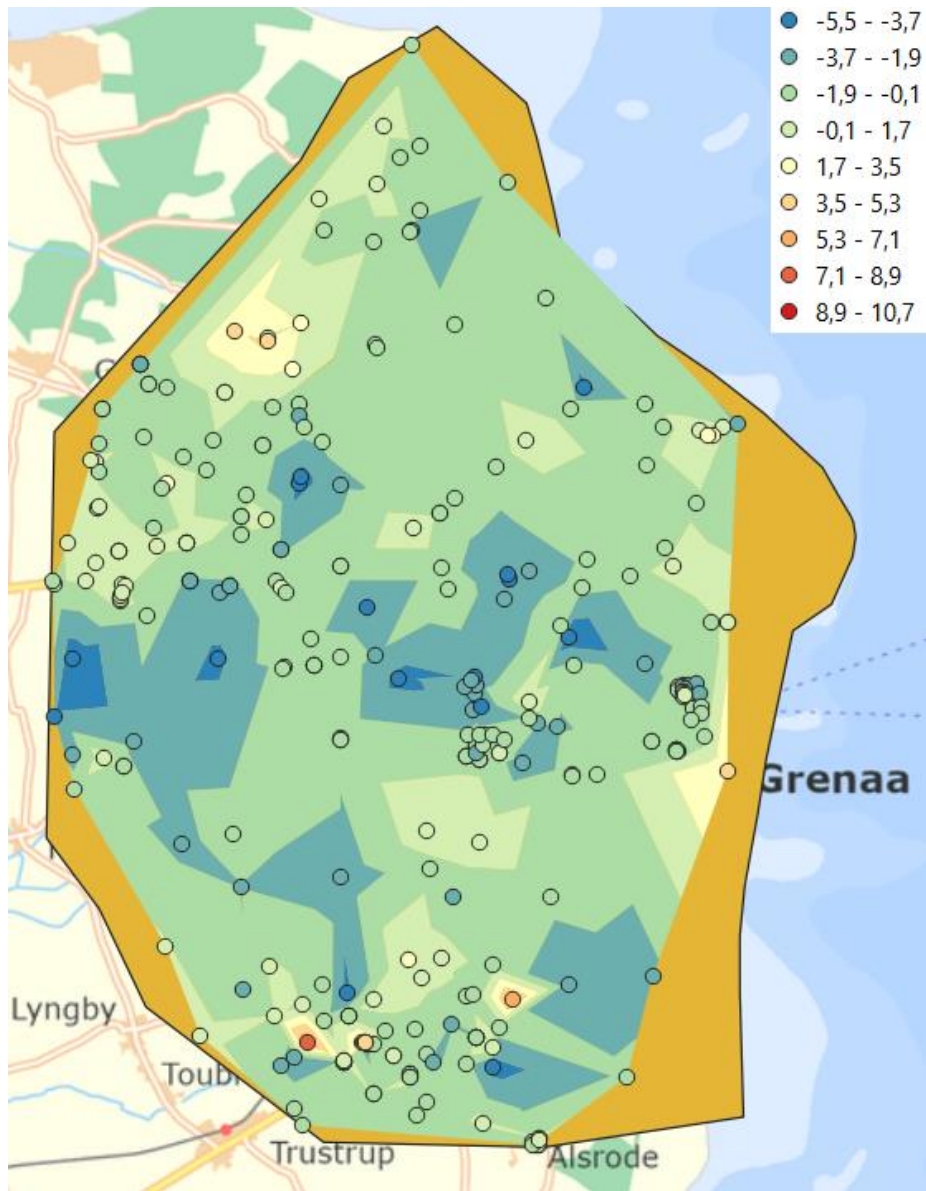


Figure 73 Map of the mean error for each well in the area. The map is for all the wells.

The map show that the model in general simulates too high of a head based on mean error. The spread in mean error is 10.7 to -5.5.

There are small areas where the model simulates too low of a hydraulic head.

The differences between wells in the same areas are high. This can be due to complex geology that the model does not consider. The differences between wells near each other can also be because of bad measurements or heterogeneity geology.

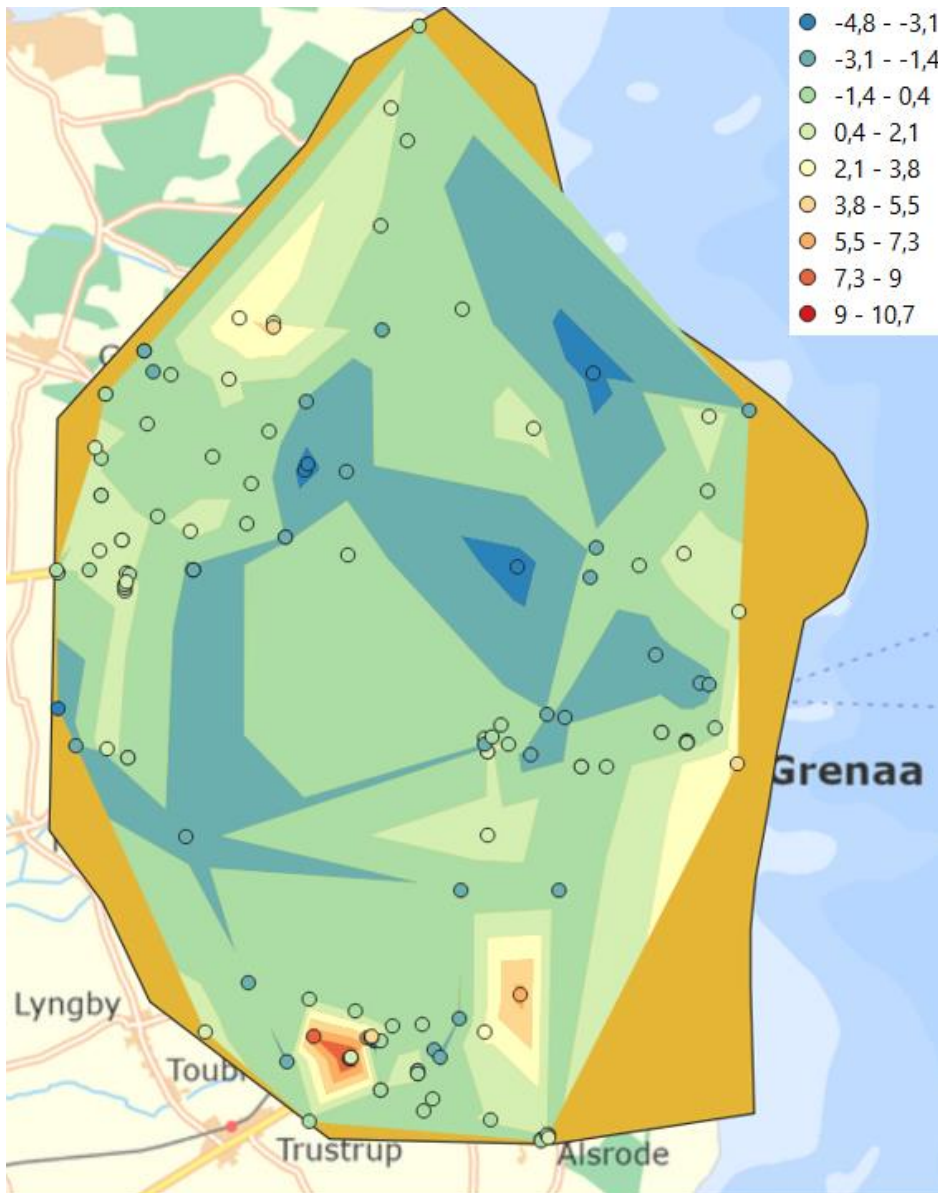


Figure 74 Map of the mean error for each well in the area. The map is for the wells screened in the quaternary layers.

For the quaternary layers, the model mostly simulates too high of a hydraulic head (the mean error is negative). But this is mostly in the range of 1.4 meters to 0.4 meters. Where the model has the thickest quaternary layers (to the south and north west, the model has a wide range of mean errors. This ranges from up to 10 meters in mean error to -4,8 meters.

This can be due to complex geology that the model does not consider for example that there is a perched aquifer in the real world. The differences between wells near each other can also be because of bad measurements or heterogeneity geology.

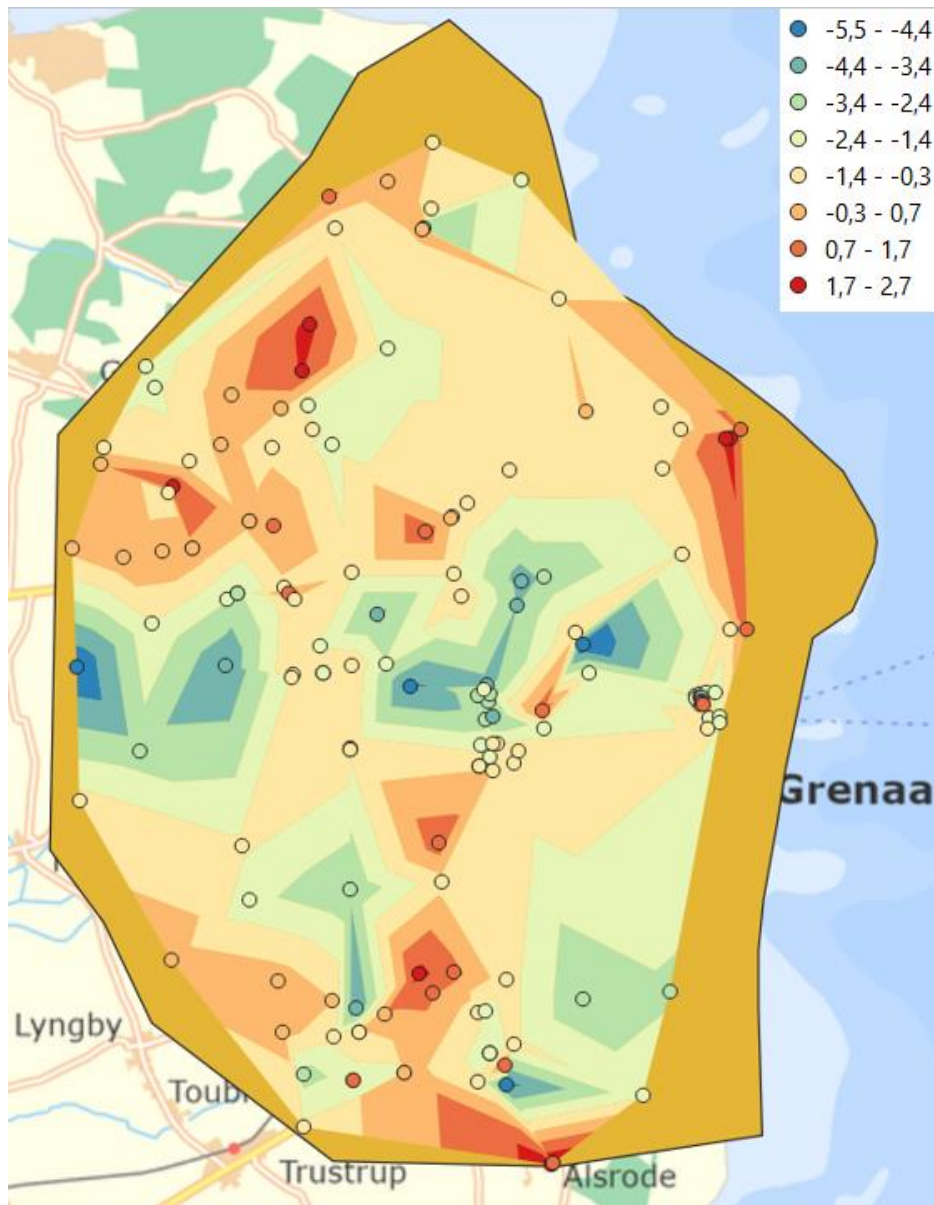


Figure 75 Map of the mean error for each well in the area. The map is for the wells screened in the chalk layers.

For the chalk layers the mean error is tight. The highest positive mean error is 2.7 and the lowest is -5.5 meters. Most of the model is simulated with a mean error of around one meter. There are still areas where the model has a widespread in mean error between wells. This can be due to heterogeneity in the chalk layers. The heterogeneity is not modeled into these layers and are assumed homogenic.

Statistic

To better understand the overall fit of the model the root mean square errors were collected. The method to show the RMSE values are box and whisker plot.

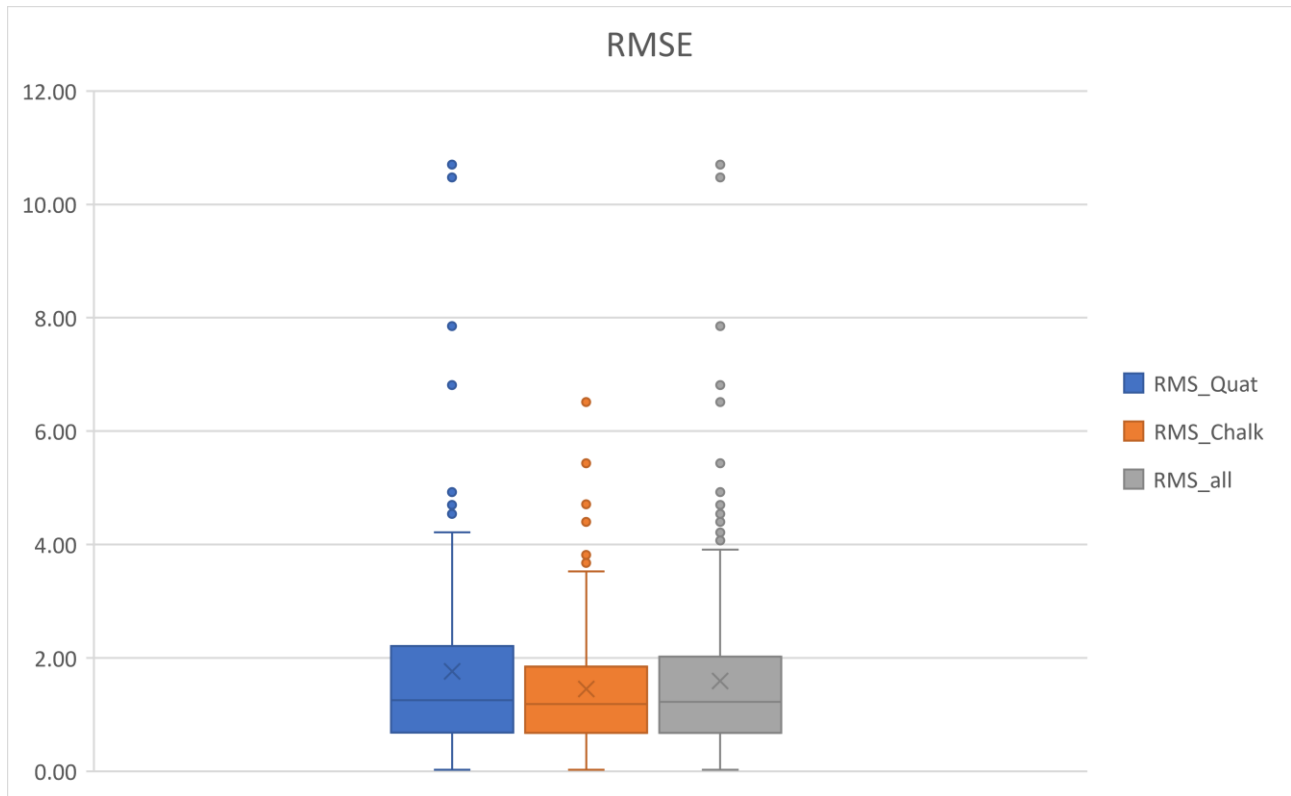


Figure 76 Box and whisker plot with the RMSE values for the model. The values are split into quaternary layers, chalk layers and all the layers.

The box and whisker plot shows the first quantile (line with a bar end), second quantile (lowest part of the box), the median (the line in the box), the average (the x), the third quantile (the upper part of the box), the fourth quantile (line with a bar end) and the outliers defined by the third quantile + 1.5 * the inter quantile range.

Overall does the model simulates the chalk layers better than the quaternary layers. The quaternary layers do also have outliers with a higher RMSE value compared with the chalk layers. This can be because of complicated geology that is not build into the model. The outliers in the chalk can be due to heterogeneity in the chalk that is not build into the model.

Discussion

Dolines

Dolines is a landform that is highly combined with developed karst. But the thickness of the quaternary layers could suggest that many of the observed dolines are not due to sinkholes but more likely could be remnants of dead ice caught in the glacial moraine. But glaciation can speed up dissolution of carbonates by focusing infiltration through the carbonate rock (Ford & Williams, 2007). It is also possible that the ice tectonics have created pull-apart cavities. These cavities could then be major conduits. The dissolution of the carbonate would continue. This could then later lead to the collapse of the roof that would form a sinkhole or a doline. Furthermore, can the saline-freshwater interface cause dissolution of the chalk. Other work suggests that a fluctuation in where this interface is causing even more dissolution (Ford & Williams, 2007). This could be an important driver in the creation of karts in the area due to the history of seawater fluctuation and later a freshening of the groundwater due to the creation of Kolindsund lake. And yet again a possible change in this saline-freshwater interface when the drainage of Kolindsund were begun and still goes on. These changes could drive further dissolution of the chalk.

And taking into the account that the saltwater-freshwater interface still is laying high in parts of the area this could then be a driver for dissolution of the carbonates.

But the direct linkage of these dolines to dissolution of the carbonate is not yet made for this area. To do this more work should be done. This should consist of more geophysical investigation to investigate the top of the chalk for depressions and infill of quaternary sediments into these depressions. The infill and creation of the doline would possibly create faults that could be viewable. This should be backed with drilling of the dolines to see if the dolines once upon a time were a lake, created by dead ice, that later were closed and filled by surrounding sediments (Götz, et al., 2018).

The sizes of the dolines are comparable to what is seen in Thisted area (Sørensen, et al., 2017). This could be because of the use of the area around Grenaa. Most of the area is used as farmland like what is also found in Thisted (Sørensen, et al., 2017).

Enslev pumpstation spring

The calculations at Enslev pumpstation strongly suggest that a large part of the water most likely is leakage from the outer channel 'Nordkanal'. This is the same result that is described by Korkman (Korkman, 1980). In the hydrological model that Korkman set up nearly half of the water pumped out of Kolindsund came from water that later returned to Kolindsund from the outer drain channels 'Nordkanal' and 'Sydkanal'. But the return of water is happening other

places in this part of Kolindsund. The springs and areas are described for Kolindsund (Korkman, 1980). And there are made other temperature analyses and chemical analyses' that show that this problem of return water throughout Kolindsund. But the problem is no near as big as in the area that is drained through the Enslev pumpstation (Korkman, 1980). To get an even better understanding of where the water comes from the well, used for groundwater temperature should be placed outside of Kolindsund. This should be done to minimize the risk that the well is influenced by water coming from the outer channel.

Another thing that could be done to back up the calculations could be a tracer experiment. This experiment could be carried out be to put color or use another tracer in 'Nordkanal' a different color and observe the spring.

Flow logs

The flow logs do show that there are at least two different flow patterns in the focus area. The two areas are also at opposite site of Kolindsund. The northern area has a flow pattern that has most of the inflow of water in the upper 15- 20 meters of the wells. This consist with the traditional way the flow in chalk is understood in Denmark. This is due to the fractures made in the chalk by ice tectonics during the last ice age. The TEM measurements for the area around the wells shows a resistivity that are more constant through the layers.

The southern area is dominated by in flow of water to the well at very narrow intervals. Many of the wells has near to no inflow at the top of the well and more than 30 % of the inflow deep in the wells. This deep inflow matches the depth of chalk with high resistivity at the nearby tTEM site.

These differences in flow for the two area on opposite site of Kolindsund strongly suggest that the chalk units have undergone different processes that created these different flow patterns. To make a more precise model these difference in flow could be an area of focus to try to model into the model. Also, the lithology should be tried to be correlated to the different flow patterns.

Geological model based on resistivity patterns in the chalk.

The new geological model was based on TEM data. This TEM data consists of TTEM and SKYTEM data that are publicly available on GEUS' Gerda database. This were done because of work started by WSP Denmark. Their work showed an area north of Grenaa that had a layer of chalk that have high resistivity chalk below a layer of less resistivity chalk. A new well drilled into the high resistivity chalk yielded a high yield well.

This high yield well together with the resistivity pattern in the chalk led to look for this throughout the area. This led to an investigation to uncover if this pattern was present in the

whole area.

The high resistivity layer in the chalk were present in most of the area and this led to a new geological model were created. This model consisted of four quaternary layers and three chalk layers.

The new geological model is based on the results found by WSP Denmark north of Grenaa. This was based on that this high resistivity layer could be a layer with a high conductivity and it is that that gave the high yield in the test well and therefore also could be a sign of karst in the area.

But other work does suggest that high resistivity in chalk is common in different limestone. This is also the pattern seen in dry karstified limestone. And the resistivity for waterlogged karstified is lower than the other two examples stated before (Ford & Williams, 2007).

This differences in resistivity can be explained by the water in the pore spaces. Water is a bad conductor. It is the dissolved ions in groundwater that makes it a better conductor. This means that the groundwater in the pore space will lower the resistivity that is measured in the unit. And the more porous the chalk becomes, the lower its resistivity will become because of the amount of water that takes up the volume (Matsui, et al., 2016).

But work done in France shows that the karstified chalk can have a high resistivity even with a larger cave system present (Reninger, et al., 2014).

These relations between the resistivity and the porous media are hard to establish. This is due to the large differences in the sedimentary rocks and the groundwater present in the area (Matsui, et al., 2016). Also, the scale of the TEM investigation plays a role. This is due to the way the TEM data is processed. This process is making an average of the resistivity in a certain depth over a certain area. This can then mask smaller karst structures that otherwise would be visible because of the low resistivity groundwater. And furthermore, the interpolation made to make the data cover larger areas. This could also hide more of the structures due to the averaging of the resistivity.

The differences and the broad range of resistivity materials can have makes it hard to make a conclusion if the material is karstified and sometimes which material is which. Several places in the area are there, clays that has a higher resistivity than the one seen for the upper chalk measured by the tTEM north of Grenaa.

Weakness of the new geological model

Kolindsund

Kolindsund is most likely a buried valley or a semi buried valley. But to quantify this there must be made a lot more data than what is available. There are no deep wells located inside of Kolindsund to show how deep the valley possible is. In this geological model there are not interpreted in Kolindsund due to the lack of data. But the only data available (SKYTEM) shows

that the resistivity in Kolindsund is low (see figure 77). It also shows that the saltwater freshwater interface lies relatively high. And it shows that the resistivity of the area is low that implies that the ion content throughout Kolindsund is high. This could interfere with the flow of groundwater in the area due to the difference in density. This problem could be minimized using a model that could count this in like the GMS package SEAWARD.

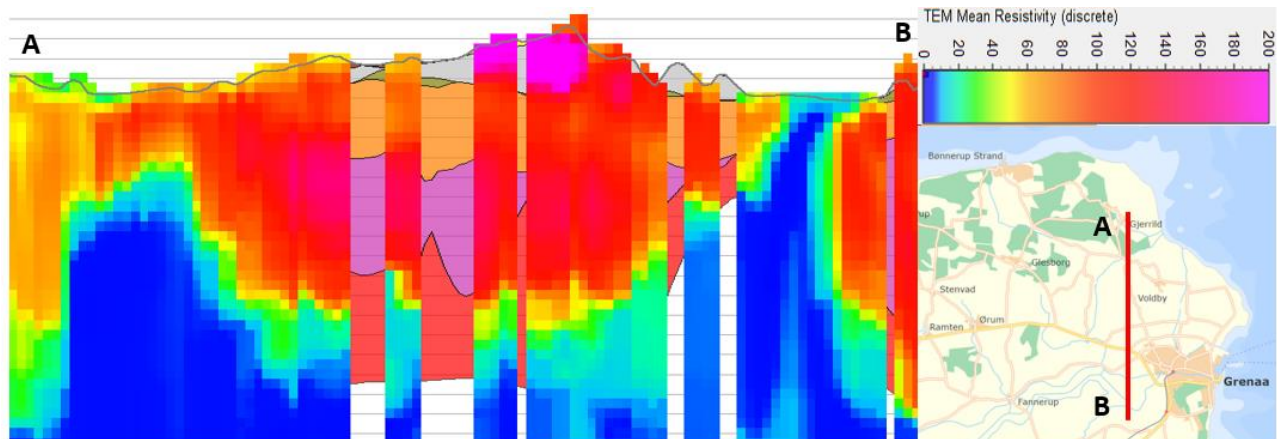


Figure 77 The cross section shows that there is large area where the saline water is near to the ground and that the saline water reaches the surface in outer part of Kolindsund.

There are also no geological units that are specific to Kolindsund in the model. Kolindsund is dominated by marine sediments and lake sediments like gyttja.

Also, the leakage of water from the channels have not been correlated to the material they are built in or on. This could make it impossible to make a precise representation of the water flowing in and being pumped out of Kolindsund.

Fornæs klint and coast

A weakness in the interpolation of the chalk is that at Fornæs beach the cliff is made of chalk. But due to lack of wells in the area this were not interpreted as such. This makes the sedimentary layers in this area around 5 meters too thick.

Another weakness of the model is that SKYTEM is not available for the whole area. This makes most of the southern part of the area and the eastern part of the area one big question mark. The differences in the chalk layers comes only from interpolation made automatically by Geoscene3D. This means that the thickness of the different chalk units most likely is not correct. The same applies for the freshwater-saltwater interface at the bottom of the geological model. Here the boundary was interpreted as a wedge that gradually moves upwards towards the coast and then meets the coastal waters a couple of hundred of meters beyond the coast.

Streams

As the model is a cutout from the regional model there is large parts of the stream network that is cut off. This means that it is not a comparable amount of water that runs into the new area though some of 'Midterkanal' and the two outer channels 'Norkanal' and 'Sydkanal'. Due to this the model was not calibrated using data from Grenaa river and the leakage and other parameters connected to the streams were maintained.

Problems with wells

Going through the wells while interpolating the chalk units it was noted that the lithology of the chalk units could vary a lot. In some wells could the same lithology turn up several times interrupted by another chalk unit even though the unit has been described having a precise position in relation to the one it alternated with. This could make it hard to make a geological model of the area based on the lithology of the chalk units.

TEM France

Similar TEM investigation in France suggests that this method can be used to split a chalk unit into different subunits just like what were done at the focus area around Grenaa. The site in France has multiple faults and karst caves that are precisely described.

The work here showed that the chalk unit that has the karst features and the faults has a higher resistivity (Reninger, et al., 2014). And the low resistivity chalk in a fractured and highly weathered chalk. This second chalk would compare to the upper chalk found in Grenaa which is highly fractured by ice tectonics. The work in France also showed that the hydraulic head highs were found on top of the low resistivity chalk together with the drainage axis in the area followed the high resistivity chalk. This gives ground for modelling chalk in different units to better simulate the hydraulic head because of different properties of the chalk that is based on the petrophysical properties of the chalk.

Enslev Pumpstation

To better understand how the models simulates the influx of water to Kolindsund the best measure to look at is the pumping from the Enslev pumpstation. Even though the other two pumpstations are in the model this station is the best to look at because of most of its draining area is not cut out of the new model. The goal was to hit a pumping rate that was every two hours.

The model that was closest to hit this goal were the one with heterogeneity in the chalk layers. But this model had days and even weeks where the pumps at Enslev pumpstation never were turned on.

The second-best model is the model with the new geological model. This model had even longer periods where the pumps never turned on. The pumping was started at around every three days. And had up to three weeks where it never turned on the pumps.

The worst model to simulate the water levels in the drain in Kolindsund was the homogenic model. Here there was long periods without pumping and at best it was pumping one to twice a week.

The reasons why the pumping at Enslev pumpstation is so far off are many. The calculation at Enslev shows that the return flow from the channels into Kolindsund should be high. This parameter of leakage into Kolindsund has not been optimized to fit this new knowledge. But also, the geology within Kolindsund could be wrong. There is very limited data about how the geology is in Kolindsund. For all three models there is a lot of clay throughout Kolindsund. This could force a major part of the groundwater to run deeper and never being cached by the drains.

Skærvad stream

The three models were all close to have a mean error of zero. But all of them simulated a little too much water. The best of the three models were the heterogenic model. It has a mean error at -0.018 liters per second. The second best were the homogenic model with a mean error at -0.05. The model with the new geology had a mean error at -0.08 liters per second.

The errors are small, but the discharge of the stream is not that large either. The differences in the mean error between the models mainly comes from differences in the hydraulic conductivity of the quaternary layers. But part of the stream is on or very near to chalk. This could also make a small difference between the three models.

Comparing of results

There is a lot of differences between the different models in relation to the hydraulic conductivity. Most of the hydraulic conductivities for the quaternary layers falls within a reasonable category of table values. This is because it should be considered the layers are created under the ice age and there most certain is a much more complex geology than the geology that is modeled into the two different geology models.

For the chalk layers the homogenic model has a very high vertical hydraulic conductivity. This could be real for the top layer if the fracturing and dissolution were much larger than what is known. But looking at the sensitivity analysis it shows that the vertical hydraulic conductivity is not sensitive to changes. This makes it easy for the model to have a good fit even with this high vertical hydraulic conductivity.

The differences in hydraulic head for the three models are large. But the areas where the models struggle is similar. The homogenic model does in large areas simulate too low of a head, especially in the southern part of the model in the chalk layers. The heterogenic model does also simulate too low of a head in some of these areas but more of the area overall are

simulated with a higher head. The new geological model has some areas with a too low of a head, but these are few and the error is lower for this compared to the homogenic and heterogenic model. The differences for the homogenic and the heterogenic model comes from the differences in the quaternary layers due to the optimization. And a large part of it comes from the heterogeneity in the chalk layers. Comparing this to the new geological model, the largest differences that results in the differences in errors lays in the simplification of the quaternary layers and most important the three-layer chalk model that has much thicker layers that differs independently from each other.

To better understand how the different models compare to each other, the different statistics have been set side by side. The statistics are presented as three different charts. The three different charts consist of one with all the observation wells, one with wells screened in the quaternary layers and one chart with wells screened in the chalk layers. The charts consist of root mean square errors for the three different models. The wells used for this is the same for all three models.

Quaternary layers

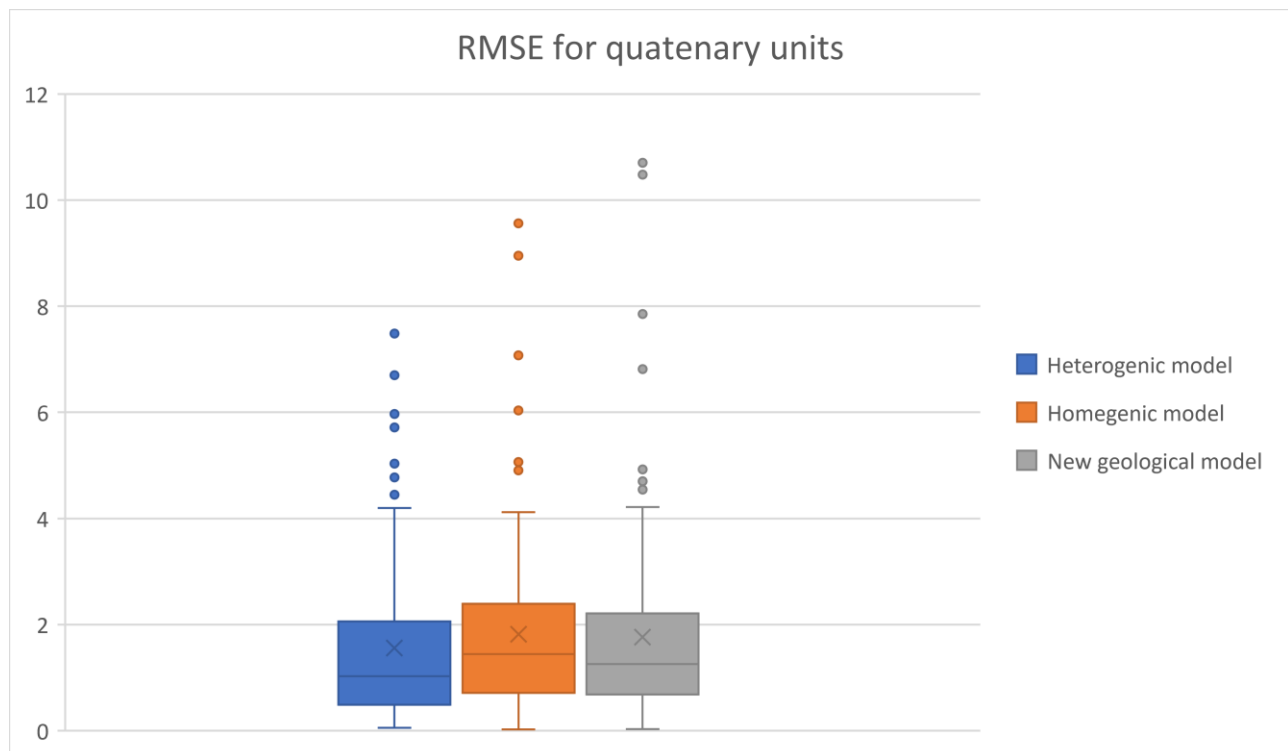


Figure 78 Box and whisker plot with the RMSE values for the quaternary layers for three different models. The x is the average.

The quaternary layers are similar in the RMSE values. The worst model is the homogeny model that has a slightly higher average (1.82) than the New geological model (1.76). The best model

is then the heterogenic model with an average RMSE at 1.55. The heterogenic model is better than the homogenic model because the calibration only was made on the quaternary layers for this model. The heterogenic model has also on this background a lower spread in the outliers than the other two models. This can be because of complicated geology that is not build into the model that the other two models hits better than the new geological model.

Chalk layers

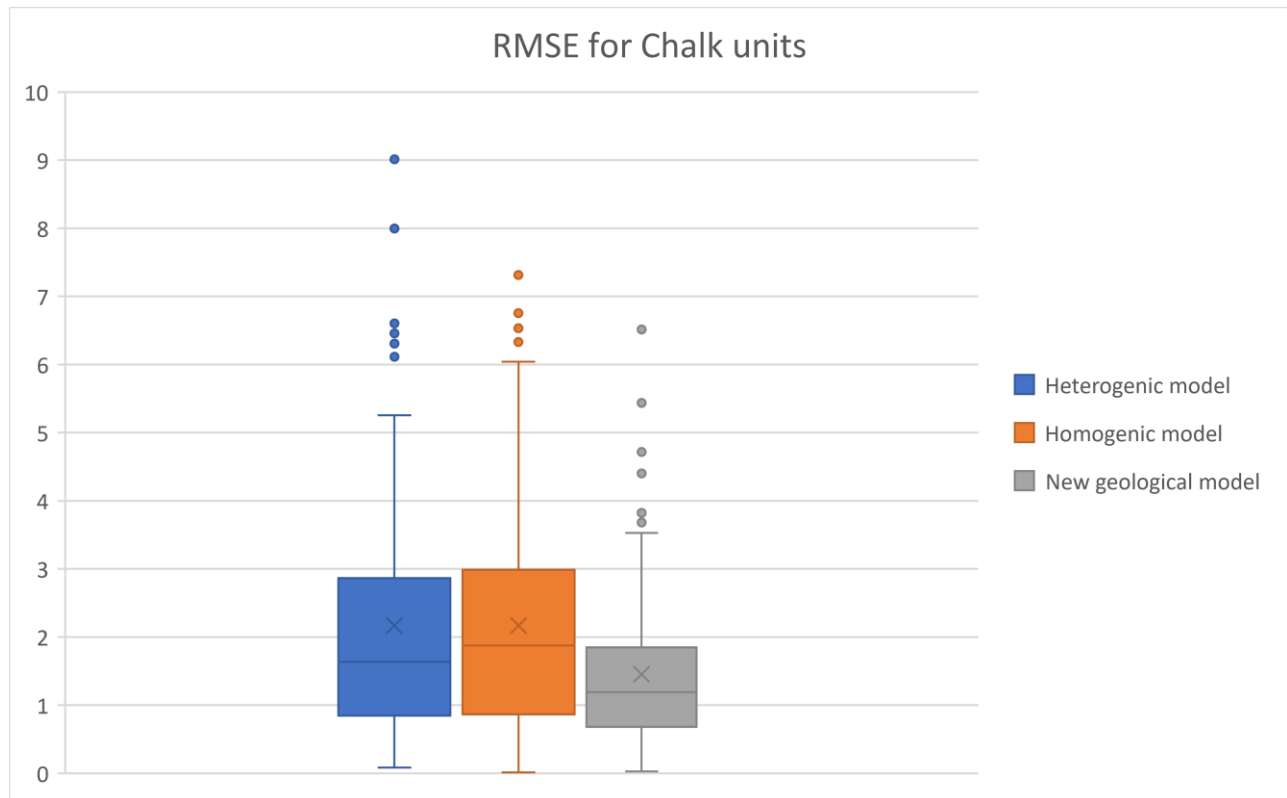


Figure 79 Box and whisker plot with the RMSE values for the chalk layers for three different models. The x is the average.

The chalk layers have a wide range between the three models. The heterogenic chalk model and the homogenic chalk model both has an average RMSE at 2.17. But the median and third quartile is better for the heterogenic model. Yet the heterogenic model has more and outliers with a higher RMSE value. This was surprising because the heterogeneity is based on interpolating data about hydraulic conductivity. But this data is also limited in the area and large areas is interpolated between them.

The new geological model has an average RMSE at 1.45 for the chalk layers. This is significantly lower than what is achieved for the two other models. The spread in RMSE for the different observation wells is also tighter than what is achieved at the other two models.

The most important change in the chalk is the thickness of the layers and the addition of a layer. This large difference in thickness of the two top layers suggest that the thickness in the old model is not representative of what it should be.

All statistics

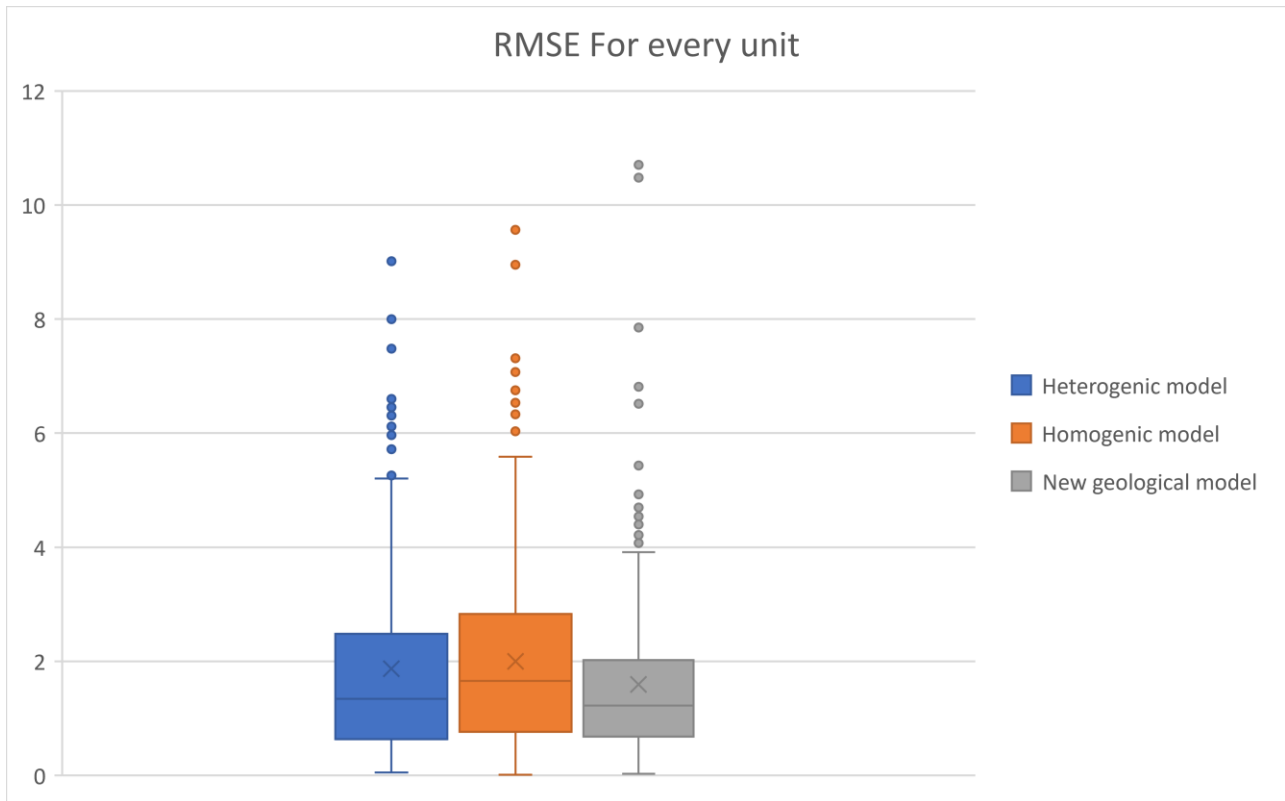


Figure 80 Box and whisker plot with the RMSE values for all the layers for three different models. The x is the average.

Comparing all the RMSE points for each model against each other it shows that the new geological model still is the best with an average RMSE at 1.6. The heterogenic model is at 1.87 and the homogenic model at 2. But the new geological model still has the highest outliers that show the quaternary layers are more complex than what is modelled into this model.

Comparing the two other models that shares geology the heterogenic model is a little better than what is achieved with the homogenic model. Some of this comes from the heterogeneity in the chalk. But most of it comes from the calibration of the quaternary layers where the calibration tool only had to optimize four quaternary layers.

This modeling does not show any signs of karstic flow. This could be because of the nature of such flow that it is locally and confined to small pipes. To investigate this more fieldwork should be carried out.

Conclusion

For a long time there have been talked about that the chalk in the Grenaa river catchment has karst features. But the documentation of this has either been lost or not properly documented. Systematic mapping of dolines in the area using shadow maps yielded 136 dolines. These dolines could be a remanence of sinkholes created by dissolution of the chalk.

The sizes of the dolines are between 22.3 and 91.8 meters with an average of 42 meters. The depth of the dolines is between 0.2 and 3.9 meters. This range of size and depth matches what is found in Thisted (Sørensen, et al., 2017). Both Thisted and the Grenaa area is dominated by agricultural use that over time is leveling the dolines and makes them shallower.

The depth from the dolines bottom to the top of the chalk were also measured using the top surface of the chalk created for the new geological model. These yielded depths between 5.9 and 69.1 meters with an average at 29.5 meters. The thinnest quaternary layer was found north of Grenaa and the thickest north west of Grenaa. With the average thickness of the quaternary layers being so high it questions if all the dolines are created by sinkholes. Especially with the quaternary layers being deposited by ice. This ice is known to have left blocks of ice within the moraine. These blocks later left kettle holes. But to know if the dolines is a remnant of ice or karst, further studies need to be carried out.

Calculation of the backflow in the drain channel feeding Enslev pumpstation showed that a significant amount of water comes from the outer channel. For the calculated day it was around 46% of the water that came from the outer channel and 54% came from the groundwater. This matches the water budget that was calculated by Korkman for the Enslev area (Korkman, 1980).

This also shows that to get the water balance right and to match the pumping rate that is observed, a future model should let more water drain from the outer drain channels back into Kolindsund.

TEM was brought into the investigation based on a resistivity pattern discovered by WSP Denmark north of Grenaa. This together with a high yield well screened in chalk with high resistivity. This led to an investigation throughout the whole area. The TEM investigation showed that most of the area has a pattern with a high resistivity chalk in the interval between 40 meters below sea level and 80 meters below sea level. This led to the creation of a geological model with three different chalk layers and four quaternary layers. The three chalk layers were defined by one relatively low resistivity, one with relative high resistivity and one with low resistivity with its bottom defined as the saltwater-freshwater inface that was defined

on resistivity at around 5 to 0 ohms. The pattern of resistivity is not widely linked to karstification.

Analyzing flow logs in the area showed two different inflow patterns. One that is very sporadic and have a large inflow deep in the well. And one that have an evenly inflow with most of the inflow at the top of the chalk. The first pattern could be a sign of conduits, but it is also a sign of fractures. The latter pattern consists with chalk that is fractured at the top 10 to 20 meters by ice during the last ice age.

Three models were made for a smaller area of The Grenaa river catchment. All the models shared the parameters that calculated recharge, unsaturated flow, river, and the overland flow. Two of the models shared the same geological model but differed from each other by one had differentiated hydraulic conductivity in the chalk layers. The last model had the new geological model with three chalk layers modelled into it. The three models were all calibrated using the MIKE Autocal tool. The same observation wells and period were used for all three models. The same was true for the statistic.

The homogenic model reached an average RMSE of 2 meters. The heterogenic model reached an average RMSE of 1.87 meters and the model with the new geological model reached an average RMSE of 1.6 meters.

For the quaternary layers was the RMSE for the models different. The homogenic model reached an average RMSE of 1.82 meters. The heterogenic model reached an average RMSE of 1.56 meters and the model with the new geological model reached an average RMSE of 1.76 meters.

For the chalk layers was the RMSE for the models different again. The homogenic model reached an average RMSE of 2.17 meters. The heterogenic model reached an average RMSE of 2.17 meters and the model with the new geological model reached an average RMSE of 1.45 meters.

This shows that the optimization of only the four quaternary layers in the heterogenic model made this model better based on the RMSE values. The heterogeneity did not make the RMSE for the chalk layers better on average. The RMSE for the quaternary layers for the new geological model were not better than the one for the two with the geology from the DK model. But with the much lower value for the RMSE for the chalk layers this came out the best. The modelling also showed that the influx of water to Kolindsund could not be modelled precisely. This is shown through the analysis of the pumping at Enslev pumpstation.

All this have shown that this area of Grenaa river catchment can be modelled with a low RMSE value if three chalk layers defined by its petrophysical properties. The chalk clearly show that it also differs in how thick its different units is and that there is a difference in how the chalk conduct water through its matrix.

To see if this pattern is present at a regional scale and if this method of modeling the chalk is a

sustainable method, more of the area should be included and larger areas should be mapped using Skytem so that large areas not anymore are defined by data far away.

References

- Appelo, C. & Postma, D., 2005. *Geochemistry, groundwater and pollution, second edition*. 2. ed. Amsterdam: CRC Press.
- Auken, E., Pedersen, J. B. & Maurya, P. K., 2018. A new towed geophysical transient electromagnetic system for. *Environmental geophysics*.
- Fitts, C. R., 2013. *Groundwater Science*. 2 ed. Oxford: Elsevier Inc.
- Ford, D. & Williams, P., 2007. *Karst hydrogeology and geomorphology*. 1 ed. Chichester: John Wiley & Sons Ltd.
- Götz, J., Salcher, B., Starnberger, R. & Krisai, R., 2018. Geophysical, topographic and stratigraphic analyses of perialpine kettles and implications for postglacial mire formation. *Geografiska Annaler: Series A, Physical Geography*, Issue 100:3, pp. 254-271.
- Korkman, T.-E., 1980. *Beskrivelser af kilder og væld i Kolindsund*, Aarhus: Aarhus Universitet.
- Korkman, T.-E., 1980. *En hydrologisk-hydrokemisk undersøgelse af det kunstigt afvandede Kolindsund*, Aarhus: Aarhus Universitet.
- MacDonald, A. M., Brewerton, L. J. & Allen, D. J., 1998. Evidence for rapid groundwater flow and karst-type behaviour in the Chalk of southern England. *Groundwater Pollution, Aquifer Recharge and Vulnerability. Geological Society, London, Special Publications*, Issue 138, pp. 95-106.
- Matsui, T., Park, S. G., Park, M. K. & Matsuura, S., 2016. Relationship between electrical resistivity and physical properties of rock. *Conference: Near Surface Geoscience 2016 - First Conference on Geophysics for Mineral Exploration and Mining*, September.
- Mussett, A. E. & Khan, M. A., 2000. *Looking into the earth, an introduction to geological geophysics*. s.l.:s.n.
- Nilsson, B. & Gravesen, P., 2018. Karst Geology and Regional Hydrogeology. In: W. W. e. al., ed. *Karst Groundwater Contamination and Public Health, Advances in Karst Science*. Copenhagen: Springer International Publishing AG, pp. 289-298.
- NIRAS, 2017. *www.Gerda.geus.dk*. [Online]
Available at: <https://gerda.geus.dk/Gerda/dataset/show/737761>
[Accessed 19 05 2021].
- Niras, 2018. *www.gerda.geus.dk*. [Online]
Available at: <https://gerda.geus.dk/Gerda/dataset/show/737762>
[Accessed 19 05 2021].
- Niras, 2018. *www.gerda.geus.dk*. [Online]
Available at: <https://gerda.geus.dk/Gerda/dataset/show/737773>
[Accessed 19 05 2021].
- Orbicon, 2011. *www.Gerda.geus.dk*. [Online]
Available at: <https://gerda.geus.dk/Gerda/projects/read/1770>
[Accessed 19 05 2021].

Reninger, P.-A. et al., 2014. Geological environment of karst within chalk using airborne time domain electromagnetic data cross-interpreted with boreholes. *Journal of Applied Geophysics*, Issue 106, pp. 173-186.

Siemon, B., Christiansen, A. V. & Auken, E., 2009. A review of helicopter-borne electromagnetic methods for groundwater exploration. *Near Surface Geophysics*, pp. 629-646.

Sørensen, P. B., Lykke-Andersen, H., Gravesen, P. & Nilsson, B., 2017. Karst sinkhole mapping using GIS and. *Geological Survey of Denmark and Greenland Bulletin*, Issue 38, p. 25–28.

Taylor, C. J. & Greene, E. A., n.d. Hydrogeologic Characterization and Methods Used in the Investigation of Karst Hydrology. In: D. O. R. a. J. W. LaBaugh, ed. *Field Techniques for Estimating Water Fluxes Between Surface Water and Ground Water*. s.l.:U.S. Department of the Interior & U.S. Geological Survey, pp. 75-107.

Wang, X. et al., 2016. Characterisation of the transmissivity field of a fractured and karstic aquifer, Southern France. *Advances in Water Resources*, Issue 87, pp. 106-121.

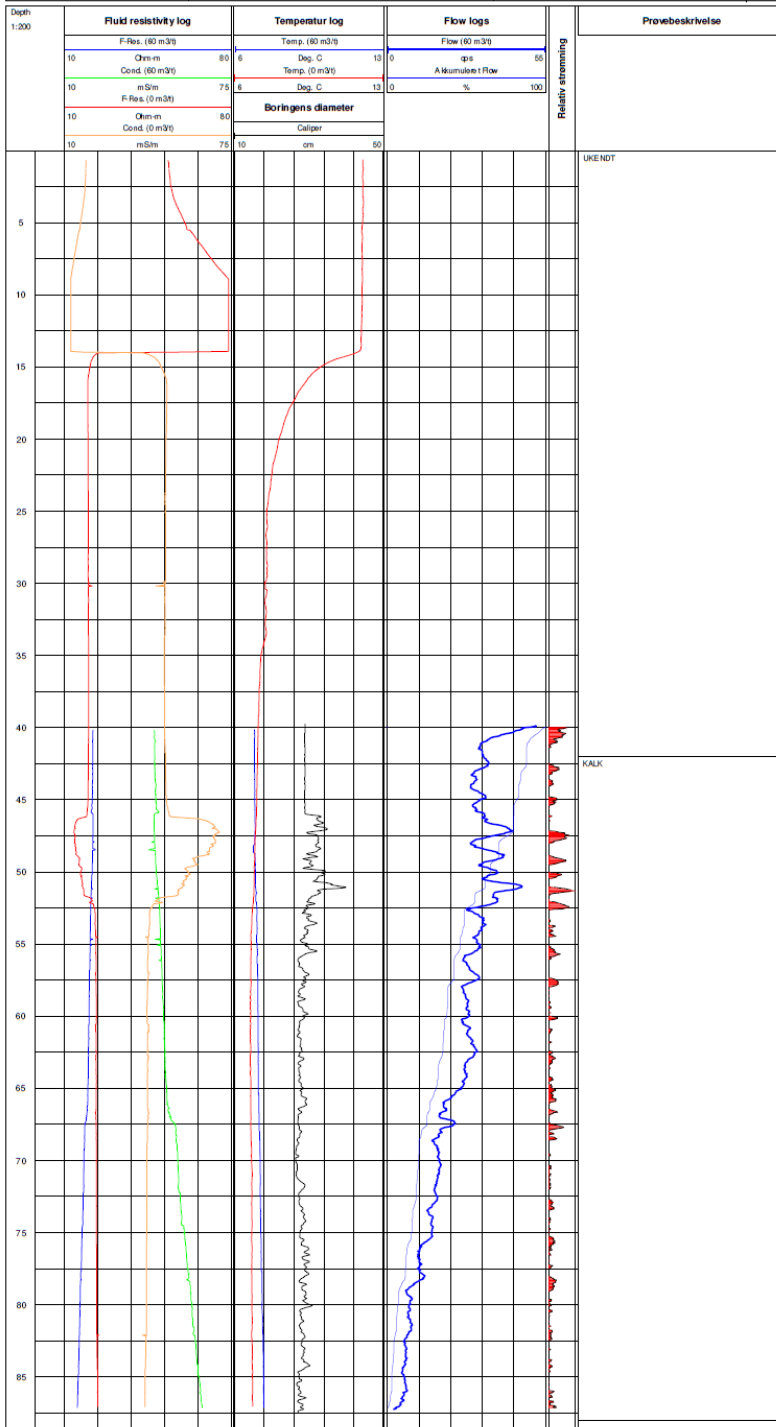
Worthington, S. R. & Soley, R. W., 2017. Identifying turbulent flow in carbonate aquifers. *Journal of Hydrology*, Issue 552, pp. 70-80.

Appendices

Appendix A

NIRAS		Boringslogging DGU-nr. 61.149																													
Sag: 226704 Rekvirent: NIRAS Filnavn: 61_149.wcl		Databehandling: SBJ Date: 3. november 2017 Kvalitetssikring: KIAG																													
Boringsoplysninger Boretdorert: SP-Boretdorert Boremetode: Lufthave Boringdiameter: Se calliperlog Borehulvæske: Vand Casingsinterval: 0-46 m u.l. (PVC) Udbygning: - Tarrænkote: 35,58 meter (DVR90) Dybde: 88 meter Vandtæppe: - Boringnr.: DGU-nr. 61.149 Koordinater: 609.313, 6.262.891 m Kilde 14 koord.: GEUS Projektion, datum: EUREF89, UTM zone 32N		Loggingoplysninger Udført dato: 30. oktober 2017 Operatør: ABPE, Oleksion Logging udført i: Åben boring Referencopunkt: Tarsen																													
Anvendte sonder <table border="1"> <thead> <tr> <th>Sonde</th> <th>Logtype</th> <th>Enhed</th> <th>Skala</th> </tr> </thead> <tbody> <tr> <td>2PGA-1000 Gamma/SPI/SFR</td> <td>Gamma</td> <td>cpm</td> <td>0-100</td> </tr> <tr> <td>2PEA-1000 8/16/32/64 Nonmat/res.</td> <td>Resistivitet</td> <td>ohm-m</td> <td>0-80</td> </tr> <tr> <td>2FA-1000 Electromagnetic Conductivity</td> <td>Conductivitet</td> <td>ohm-m</td> <td>0-80</td> </tr> <tr> <td>2PCA-1000 Three-Arm Caliper</td> <td>Calliper</td> <td>cm</td> <td>3-8</td> </tr> <tr> <td>RLP-2492 Spinner Flow meter</td> <td>Flow</td> <td>ml/min</td> <td>0-100</td> </tr> <tr> <td>2PFA-1000 Temperature/Fluid Resistivity</td> <td>Temperatur</td> <td>°C</td> <td>0-100</td> </tr> </tbody> </table>		Sonde	Logtype	Enhed	Skala	2PGA-1000 Gamma/SPI/SFR	Gamma	cpm	0-100	2PEA-1000 8/16/32/64 Nonmat/res.	Resistivitet	ohm-m	0-80	2FA-1000 Electromagnetic Conductivity	Conductivitet	ohm-m	0-80	2PCA-1000 Three-Arm Caliper	Calliper	cm	3-8	RLP-2492 Spinner Flow meter	Flow	ml/min	0-100	2PFA-1000 Temperature/Fluid Resistivity	Temperatur	°C	0-100		
Sonde	Logtype	Enhed	Skala																												
2PGA-1000 Gamma/SPI/SFR	Gamma	cpm	0-100																												
2PEA-1000 8/16/32/64 Nonmat/res.	Resistivitet	ohm-m	0-80																												
2FA-1000 Electromagnetic Conductivity	Conductivitet	ohm-m	0-80																												
2PCA-1000 Three-Arm Caliper	Calliper	cm	3-8																												
RLP-2492 Spinner Flow meter	Flow	ml/min	0-100																												
2PFA-1000 Temperature/Fluid Resistivity	Temperatur	°C	0-100																												

Bilag 1: Boringslogging DGU-nr. 61.149

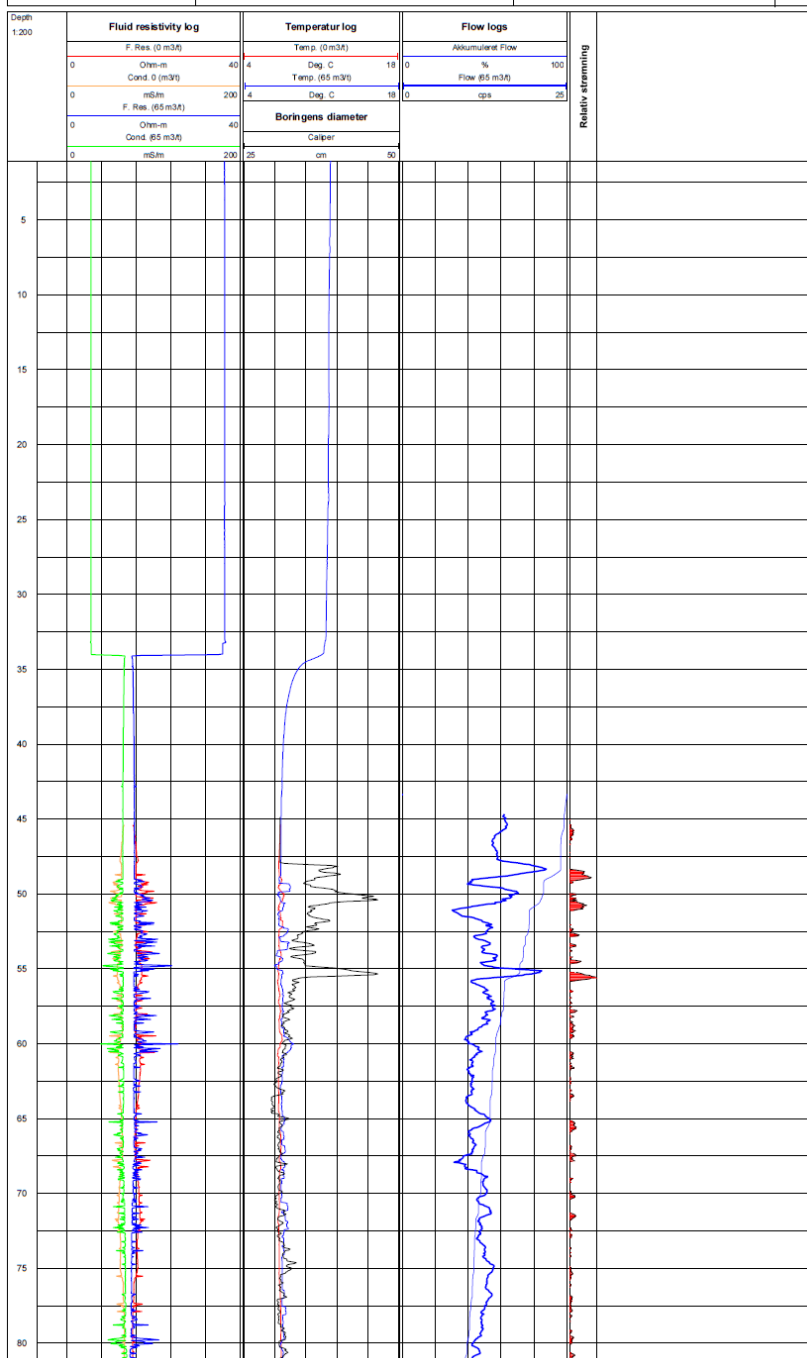


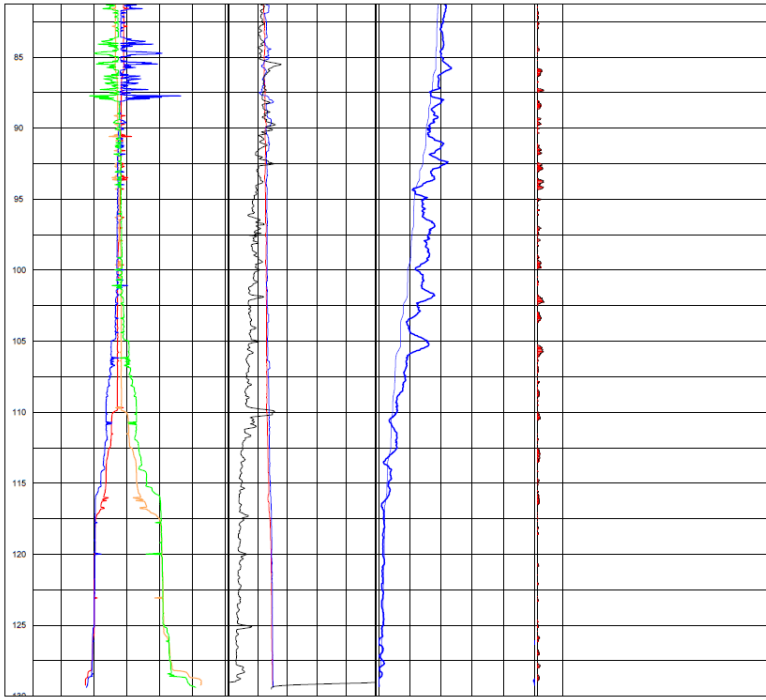
(NIRAS, 2017)

Appendix B

NIRAS		Borehullogning DGU-nr. 61.219																													
Sag: 1031134-004 Rekvirent: NIRAS Fileavn: 61_219.WCL		Databehandling: SBJ Dato: 18. maj 2018 Kvalitetsikring: KIAG																													
Boringsoplysninger Boreborer: Poul Christiansen Boremetode: Luftåreboring Boringdiameter: - Borehulvæske: Boremasse Casinginterval: 0-48 meter Udbyrning: - Terrænkote: 28,77 meter (DVR90) Dybde: 130 meter (ifølge boreborer) Vandspejl: - Boringnr.: DGU-nr. 61.219 Koordinater: 611 032, 6 263 911 m Kilde til koordin.: GEUS Projektion, datum: EUREF89, UTM zone 32N		Loggingsoplysninger Udført dato: 18. maj 2018 Operatør: ABPE, Ortoion Logging udført i: Eksisterende boring Referencepunkt: Terrain																													
Anvendte sonder																															
		<table border="1"> <thead> <tr> <th>Sonde</th> <th>Logningsdybde (m)</th> <th>Max. dybde (m)</th> <th>Notering</th> </tr> </thead> <tbody> <tr> <td>2PGA-1000 Gamma/SP/SPR</td> <td>-</td> <td>-</td> <td>op</td> </tr> <tr> <td>2PEA-1000 B/6/23/6/ Normal res.</td> <td>-</td> <td>-</td> <td>op</td> </tr> <tr> <td>2PA-1000 Electromagnetic Conductivity</td> <td>-</td> <td>-</td> <td>op</td> </tr> <tr> <td>2PCA-1000 Three-Arm Caliper</td> <td>3</td> <td>5</td> <td>op</td> </tr> <tr> <td>FLP-2462 Spinner Flow meter</td> <td>3</td> <td>5</td> <td>ned</td> </tr> <tr> <td>2PFA-1000 Temperature/Fluid Resistivity</td> <td>8</td> <td>5</td> <td>ned</td> </tr> </tbody> </table>		Sonde	Logningsdybde (m)	Max. dybde (m)	Notering	2PGA-1000 Gamma/SP/SPR	-	-	op	2PEA-1000 B/6/23/6/ Normal res.	-	-	op	2PA-1000 Electromagnetic Conductivity	-	-	op	2PCA-1000 Three-Arm Caliper	3	5	op	FLP-2462 Spinner Flow meter	3	5	ned	2PFA-1000 Temperature/Fluid Resistivity	8	5	ned
Sonde	Logningsdybde (m)	Max. dybde (m)	Notering																												
2PGA-1000 Gamma/SP/SPR	-	-	op																												
2PEA-1000 B/6/23/6/ Normal res.	-	-	op																												
2PA-1000 Electromagnetic Conductivity	-	-	op																												
2PCA-1000 Three-Arm Caliper	3	5	op																												
FLP-2462 Spinner Flow meter	3	5	ned																												
2PFA-1000 Temperature/Fluid Resistivity	8	5	ned																												

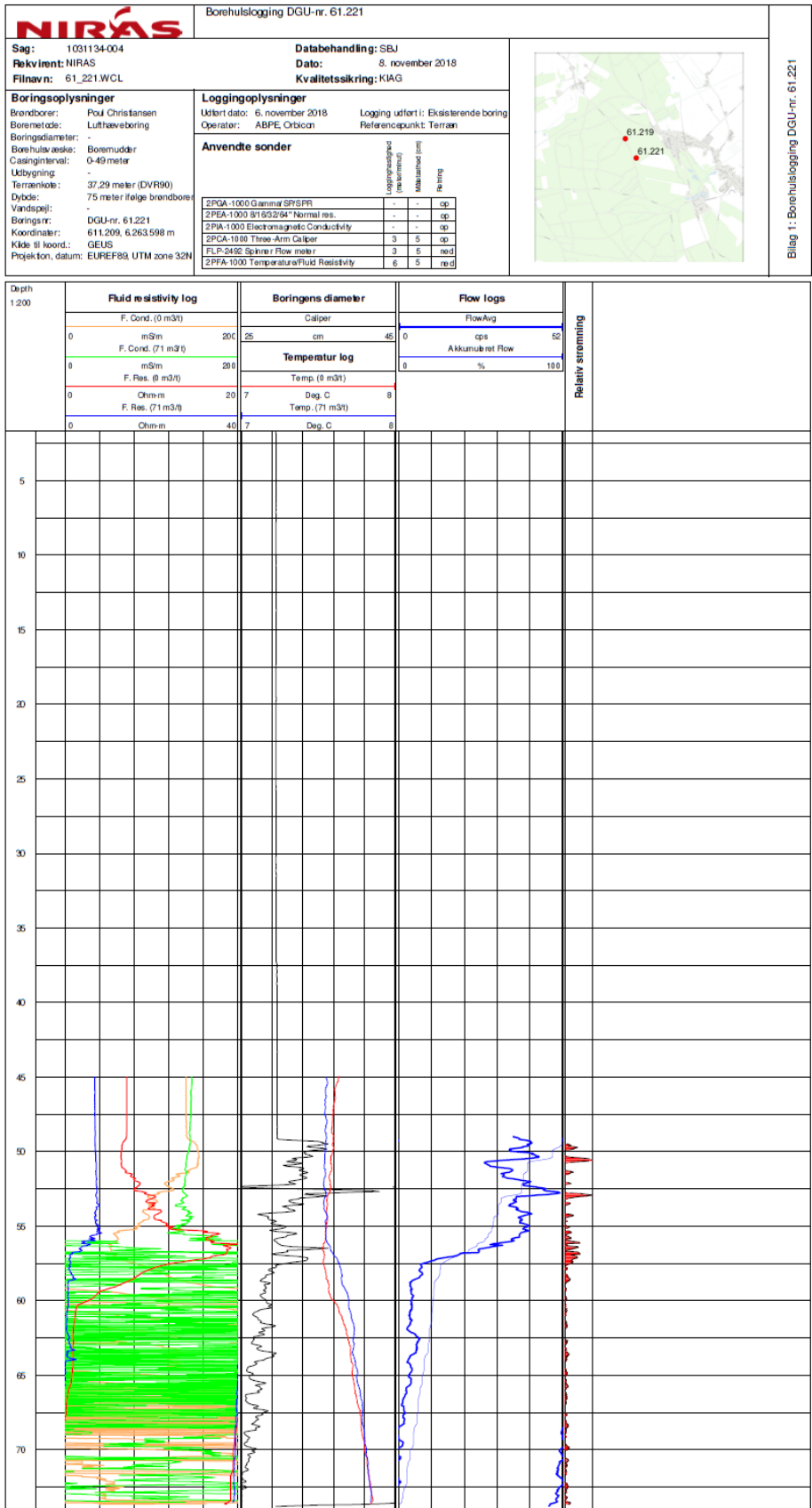
Bilag 1: Borehullogning DGU-nr. 61.219





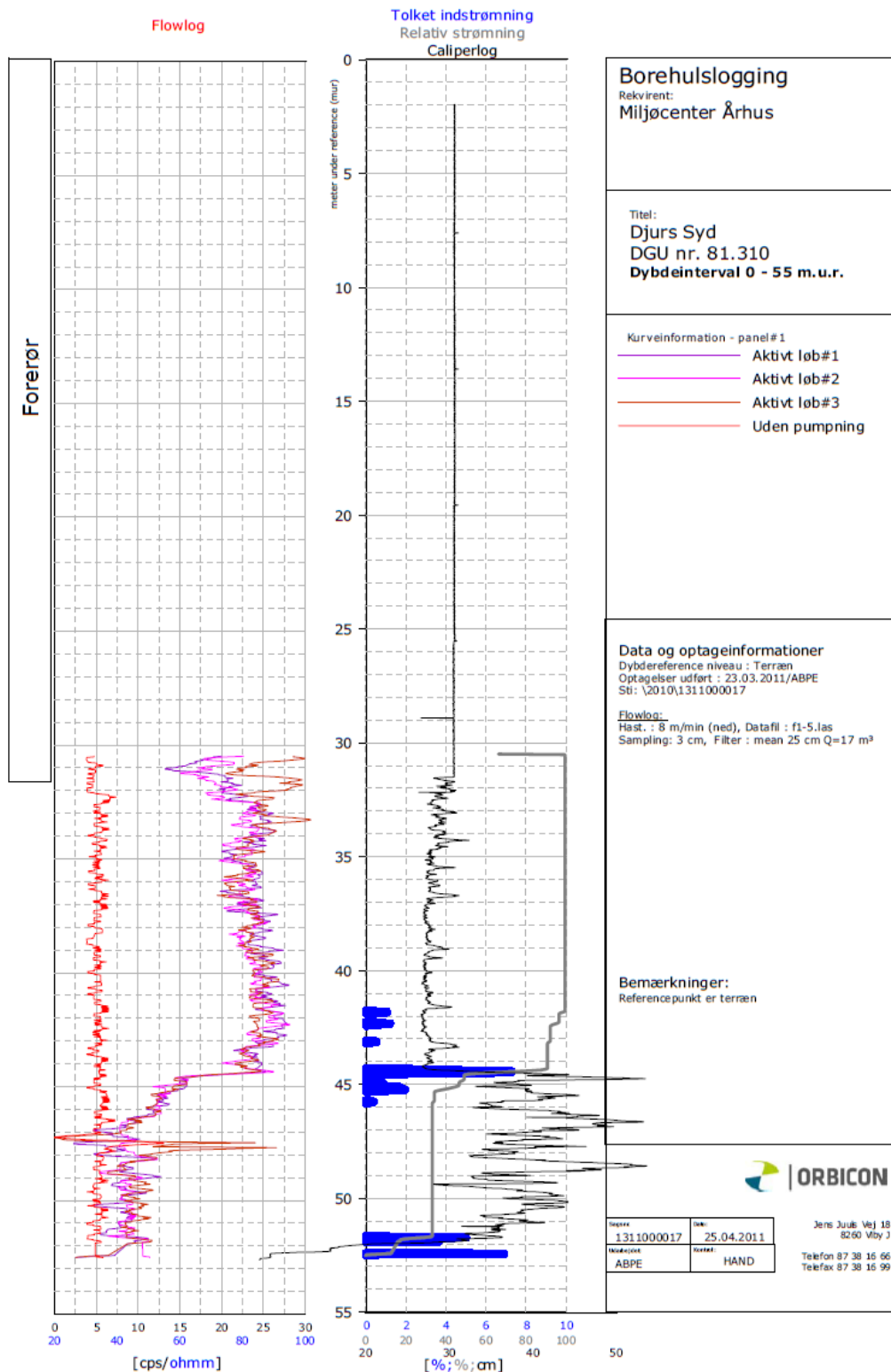
(Niras, 2018)

Appendix C



(Niras, 2018)

Appendix G



(Orbicon, 2011)